



APPLICATION OF TIAB'S DIRECT SYNTHESIS TECHNIQUE TO INJECTIVITY AND FALL-OFF PRESSURE TRANSIENT TEST UNDER NON-ISOTHERMAL CONDITION

A thesis presented to the Department of Petroleum Engineering

African University of Science and Technology, Abuja

In partial fulfillment of the requirements for the degree of

MASTER OF SCIENCE

By

Oluogun Mojeed Olawale

Supervised by

Professor Djebbar Tiab

June, 2016

APPLICATION OF TIAB'S DIRECT SYNTHESIS TECHNIQUE TO INJECTIVITY AND FALL-OFF PRESSURE TRANSIENT TEST UNDER NON-ISOTHERMAL CONDITION

By

Oluogun Mojeed Olawale

A THESIS APPROVED BY THE PETROLEUM ENGINEERING DEPARTMENT

RECOMMENDED

Supervisor, Professor Djebbar Tiab

.....

Committee Member, Professor David O. Ogbe

.....

Committee Member, Dr. Mukhtar Abdulkadir

.....

Head, Department of Petroleum Engineering

APPROVED:

Chief Academic Officer

.....

Date

ABSTRACT

In this study, we present a new analytical solution method that accurately corrects the non-isothermal effects from injection and fall-off tests. The derivative of these solutions is applied to develop the Tiab's Direct Synthesis (TDS) technique. New equations have been developed to determine the different reservoir parameters from pressure injection/fall-off test data. The flow regimes that can occur during an injection test or fall-off test are obtained by separating the different pressure transient time sequences from the analytical solutions. These various flow regimes are also confirmed by analysis of simulated cases for injectivity tests and field examples of pressure fall-off tests.

The TDS technique is a method which uses the characteristics of intersection points and slopes of various straight lines from a log-log plot of pressure and pressure derivative data. Field and simulated data are interpreted with the conventional methods (Semilog analysis) and TDS technique. There exists a close agreement between the two methods. The result shows that to analyze correctly the pressure transients governed by a moving thermal front, the effects of temperature- and saturation-gradient must be considered. If the fall-off test is not run long enough, the semilog straight line or the second radial line of the derivative plot corresponding to the uninvaded region will not be attained.

Keywords: Pressure Derivative, TDS technique, Permeability, Skin factor, Wellbore storage and Non-Isothermal condition.

ACKNOWLEDGMENT

Firstly, my appreciation goes to God Almighty who bestowed upon me knowledge and understanding, good health and abundant blessings. I also extend my appreciation to my supervisor, Professor Djebbar Tiab for the knowledge he imparted and time spent on this work; without your contribution, this research work would not have been possible. I would also like to thank other members of the committee: the head of department, Professor David O. Ogbe, and Dr. Mukhtar Abdulkadir for their support towards the success of this work.

Thanks to the support from Professor Djebbar Tiab and the Nelson Mandela Institute (NMI) for the financial support, without which I would not have been able to undergo the intensive training at the African University of Science and Technology (AUST). Appreciation also goes to my mentor, Dr. Arinkoola O. Akeem for his contribution towards my life and academic performance, you are indeed a mentor. Also, my appreciation for all the support given to me from Mrs. Aborishade Opeyemi, Mrs. Aladeitan Yetunde and my classmates, Precious, Chuks, Obed, Sandra, Belinda and others., God bless you all and thanks for the support rendered.

To all non-teaching staff and faculties at AUST, I thank you. My sincere gratitude goes to my blood brother, Dr. Oluogun A. Waheed for the fatherly support rendered towards my success in life, you are wonderful.

Lastly, I thank my parents, Mr. and Mrs. Oluogun and my wife, Fatimoh, for the love, support, understanding and tolerance showed throughout my study.

DEDICATION

To the three most wonderful females in my life, my dearest mom, Mrs. Oluogun, S., for her immeasurable support, my wife, Fatimoh Adeola for her care and love, and finally to my daughter, Khadiijah Ololade for her tolerance and understanding.

TABLE OF CONTENT

| | |
|---|-----|
| ABSTRACT | iii |
| ACKNOWLEDGMENT | iv |
| DEDICATION | v |
| TABLE OF CONTENT | vi |
| LIST OF FIGURES | ix |
| LIST OF TABLES | x |
| CHAPTER 1 | 1 |
| INTRODUCTION | 1 |
| 1.0 Introduction | 1 |
| 1.1 Problem Statement | 2 |
| 1.2 Study Objectives | 3 |
| 1.3 Study Organization | 3 |
| CHAPTER 2 | 4 |
| LITERATURE REVIEW | 4 |
| 2.0 Literature Survey | 4 |
| 2.1 Basic Flow Equations | 6 |
| 2.2 Dimensionless Groups | 7 |
| 2.4 Continuous Line Source Solution | 8 |
| 2.4 Wellbore Storage and Skin | 9 |
| 2.5 Derivative of the Line Source Solution | 10 |
| 2.6 Basic Injection Concepts | 12 |
| CHAPTER 3 | 14 |
| METHODOLOGY | 14 |
| 3.0 ANALYTICAL SOLUTIONS TO PRESSURE INJECTIVITY AND FALL-OFF TESTS USING TIAB'S DIRECT SYNTHESIS (TDS) TECHNIQUES DURING ISOTHERMAL CONDITION | 14 |

| | |
|--|----|
| 3.1 Mathematical Model | 14 |
| 3.2 Injection Solution | 14 |
| 3.3 Fall-off Solution | 18 |
| 3.4 Skin Factor | 20 |
| 3.5 Pressure Derivative Calculations | 21 |
| 3.5.1 During injection period | 21 |
| 3.5.2 During fall-off period | 22 |
| 3.6 Application of the Derivative Equations to Tiab's Direct Synthesis (TDS) Techniques | 22 |
| 3.6.1 Pressure injection period | 24 |
| 3.6.1.1 First radial flow | 24 |
| 3.6.1.2 Second radial flow | 28 |
| 3.6.2 During fall-off period | 29 |
| 3.6.2.1 During first radial flow | 29 |
| 3.6.2.2 During second radial flow | 30 |
| 3.7 Application of Tiab's Direct Synthesis (TDS) Techniques to Pressure Injectivity and Fall-Off Test Under Non-Isothermal Condition | 31 |
| 3.8 Mathematical Model | 31 |
| 3.9 Injection Solution | 32 |
| 3.10 Fall-Off Solution | 35 |
| 3.11 Skin Factor | 37 |
| 3.12 Pressure Derivative Calculations | 38 |
| 3.12.1 During injection period | 38 |
| 3.12.2 During fall-off period | 38 |
| 3.13 Application of the Derivative Equations to Tiab's Direct Synthesis (TDS) Techniques | 39 |
| 3.13.1 Pressure injection period | 40 |
| 3.13.1.1 First radial flow | 41 |
| 3.13.1.2 Second radial flow | 43 |
| 3.13.2 During fall-off period | 44 |
| 3.13.2.1 During first radial flow | 44 |
| 3.13.2.2 During second radial flow | 45 |
| 3.14 Summary of Equations | 47 |

| | |
|--|----|
| CHAPTER 4 | 49 |
| RESULTS AND DISCUSSIONS | 49 |
| 4.0 Simulated Pressure Injection Tests | 49 |
| 4.1 System Description | 49 |
| 4.2 Simulated Injection Test (Case-1) | 49 |
| 4.2.1. Conventional Semilog Analysis | 51 |
| 4.2.2 Tiab's Direct Synthesis Techniques: Isothermal Condition | 51 |
| 4.2.3 Tiab's Direct Synthesis Techniques: Non-Isothermal Condition | 52 |
| 4.3 Simulated Pressure Injection Test (Case-2) | 55 |
| 4.3.1 Conventional Semilog Analysis | 56 |
| 4.3.2 Tiab's Direct Synthesis Techniques: Isothermal Condition | 57 |
| 4.3.3 Tiab's Direct Synthesis Techniques: Non-Isothermal Condition | 58 |
| 4.4 Numerical Examples of Pressure Fall-off Tests in Water Injection Wells | 60 |
| 4.4.1 Conventional method (Field Case-1) | 60 |
| 4.4.2 Tiab's Direct Synthesis Techniques: Isothermal Condition | 64 |
| 4.4.3 Tiab's Direct Synthesis Techniques: Non-Isothermal Condition | 66 |
| 4.5 Field Example-2 | 70 |
| 4.5.1 Conventional Analysis | 71 |
| 4.5.2 Tiab's Direct Synthesis Techniques: Isothermal Condition | 73 |
| 4.5.3 Tiab's Direct Synthesis Techniques: Non-Isothermal Condition | 75 |
| CHAPTER 5 | 79 |
| CONCLUSION AND SUMMARY | 79 |
| 5.1 Summary | 79 |
| 5.2 Conclusion | 79 |
| Nomenclature | 80 |
| References | 83 |
| Appendix | 86 |

LIST OF FIGURES

| | |
|--|----|
| Figure 2. 1: Pressure transient data for injection of 95°C water into 250°C reservoir | 5 |
| Figure 2. 2: Dimensionless Pressure Function at Various dimensionless Distances from a Well Located in an Infinite System. | 9 |
| Figure 2. 3: Log-Log Plot of the Dimensionless Pressure and Pressure Derivative versus (t_D/r_D^2) ratio. (Tiab, 1993) | 11 |
| Figure 2. 4: Saturation distribution (Buckley, and Leverett, 1942) | 12 |
| Figure 2. 5: Plane view of saturation distribution around injection well | 12 |
| | |
| Figure 3. 1: Injection Model | 14 |
| Figure 3. 2: Semilog Plot of Injection Data Using Eqs. (3.19) and (3.20) | 18 |
| Figure 3. 3: Log-log Plots of Pressure and Pressure Derivative Injection Data | 18 |
| Figure 3. 4: Semilog Plot of Fall-off Data Using Eqs. (3.27) and (3.28) | 20 |
| Figure 3. 5: Pressure and Pressure Derivative Type Curves for Fall-off Tests | 27 |
| Figure 3. 6: Pressure and Pressure Derivative Type Curves for Pressure Fall-off Tests | 28 |
| | |
| Figure 3.7: Injection Model | 32 |
| Figure 4.1: Relative Permeability Curves (Case-1) | 53 |
| Figure 4.2: Fractional Flow Curve (Case-1) | 54 |
| Figure 4. 3: Semilog Plot of Pressure vs. Time (Pressure Injection Test Case-1) | 54 |
| Figure 4.4: Log-log Plots of Simulated Pressure and Pressure Derivative Data | 55 |
| Figure 4. 5: Relative Permeability Curves (Case-2) | 59 |
| Figure 4. 6: Fractional-Flow Curve (Case-2) | 59 |
| Figure 4.7: Semilog Plot of Simulated Pressure Injection Test (Case-2) | 60 |
| Figure 4. 8: Log-log Plots of Simulated Pressure Injection Test Data (Case-2) | 60 |
| Figure 4.9: Semilog Plot of Pressure Fall-off Data (Example1) | 68 |
| Figure 4.10: Pressure and Pressure Derivative Plot Pressure Fall-off Data (Example-1) | 69 |
| Figure 4.11: Plot of Pressure Vs Horner time-Semilog Fall-off Data (Example-2) | 77 |
| Figure 4.12: Pressure and Pressure Derivative Plots (Example-2) | 77 |

LIST OF TABLES

| | |
|--|----|
| Table 4. 1: Rock and Fluid properties and Well Conditions for Simulated test, Case-1 | 50 |
| Table 4. 2: Rock and Fluid properties and Well Conditions for Simulated test, Case-2 | 55 |
| Table 4.3: Reservoir Rock, Fluid, and Well Data (Pressure Fall-off Test) (Example-1) | 61 |
| Table 4. 4: Pressure and Pressure Derivative Data (Example-1) | 62 |
| Table 4.5: Final Results (Example-1) | 69 |
| Table 4. 6: Comparison of Results (Example-1) | 70 |
| Table 4.7: Reservoir Rock, Fluid, and Well Data (Pressure Fall-off Test) (Example-2) | 70 |
| Table 4. 8: Pressure and Pressure Derivative Data (Example-2) | 72 |
| Table 4. 9: Final Results (Example-2) | 78 |
| Table 4.10: Comparison of Results (Example-2) | 78 |

CHAPTER 1

INTRODUCTION

1.0 Introduction

The lack of adequate natural drive in most reservoirs has led to the practice of supplementing the natural reservoir energy by introducing some form of artificial drive, the most basic method being the injection of water or gas. Secondary oil recovery refers to the supplementary recoveries that result from the conventional methods of water injection and immiscible gas injection (Ahmed T., 2006). Usually, the selected secondary recovery process follows the primary recovery but it can also be conducted alongside the primary recovery. Waterflooding is perhaps the most common method of secondary recovery.

During the planning phase of waterflooding, water injection tests of oil zones are recurrently undertaken. The analysis of the bottom-hole pressure data recorded during these tests provides similar information to that obtained from production tests concerning the well and the reservoir characteristics and also allows the mobility ratio between the injected and in-situ fluids to be determined (Tiab, and Abdesselam, 2001). The economic feasibility of numerous fields depends upon the successful implementation of water injection at an early stage. Injection tests are, therefore, performed on appraisal wells drilled prior to the decision to develop the field. These tests are designed to assess equally the efficiency of the filtration equipment and the injection characteristics of the formation.

Generally, in a water-injection well test, the temperature of the injected fluid is different from that of the in-situ reservoir fluid. For the period of the injection, both saturation and temperature front propagate into the reservoir. Also, because of the differences in oil and water properties, a saturation gradient is established in the reservoir. The water saturation ceiling is close to the well and incessantly decreases with distance from the well. Ahead of this invaded region is the unflooded oil bank at initial water saturation. The effect of temperature strongly influences the fluid mobility, the saturation gradient and the transient pressure response with a continuous change in the total mobility.

In an injectivity test, the well is shut-in until the pressure is stabilized and then injection is begun at a constant rate while recording the bottom-hole pressure. But in a pressure fall-off test, fluid is injected into a well at a constant rate for a period of time, followed by shut-in of the well and monitoring of the pressure decline.

Injection well testing has its applications in waterflooding, pressure maintenance by water or gas injection, gas recycling, and enhanced oil recovery (EOR) operations. Injection and fall-off tests can provide important information about the parameters of an injection system; and these tests are usually run to detect near-wellbore damage, estimate the average reservoir pressure and determine formation permeability.

Appropriate analysis of fall-off tests can lead to the determination of saturation distribution around the wellbore, monitoring the movement of fluid banks, evaluation of well injectivity and reservoir pressure with respect to time. These tests can also be used to detect reservoir heterogeneity and flood front movement; i.e., the determination of the locations of the fluid interfaces that form in the reservoir due to the injection of a fluid that differs in physical properties from the in-situ reservoir fluid.

Many different models have been introduced for the analysis of water injection and fall-off tests in reservoirs with radial discontinuities. The pressure buildup during injection period, though, has received relatively little attention. The main reason being that the falloff part matches with the pressure buildup test in production wells, which has ease of analysis with it. Also, the injectivity test is mathematically difficult to handle due to the moving boundary.

1.1 Problem Statement

During the non-isothermal injection, viscosity, which is the most important temperature dependent fluid property, it must be accounted for in the interpretation of well testing; and there is usually a radial thermal discontinuity which is formed around the well. With increased injection, the distance to the discontinuity increases. Both the effect of this radial discontinuity and that of the moving thermal front on the pressure transient response must be considered.

O'Sullivan, and Pruess, (1980), and Garg, and Pritchett, (1981), studied the problem of cold-water injection into a two-phase geothermal reservoir. They all established that the permeability/ thickness of the reservoir can be estimated from pressure buildup data using conventional analysis methods. Satman et al., (1980), also worked on pressure transient behavior in system with radial discontinuities. They compared their studies with the previous work and later summarized their derivatives. Tsang, and Tsang, (1978) give an approximate analytical method and demonstrated the previous numerical studies, for predicting the behavior of a pressure transient system in an idealized well reservoir system for estimating the pressure buildup during non-isothermal injection.

Tiab, (1993), developed the TDS technique to analyze pressure and pressure derivative curves for pressure tests which do not require type curves. TDS is very useful in conditions of short tests and early time data missing tests. It also allows for the verification of results of the test data analysis since it uses more than one equation for estimation of permeability, wellbore storage, and skin factor. TDS has been applied to pressure injectivity and fall-off tests considering isothermal condition. However, the effect of temperature-and saturation-gradient (Non-isothermal) is neglected. The aim of this study is to apply TDS to account for the Non-isothermal effects during injection and fall-off test.

1.2 Study Objectives

The main objectives of this study are to:

- i. Develop analytical solutions to the Non-isothermal effect during injection and fall-off test analysis in water injection wells
- ii. Introduce the pressure derivative to these solutions for both injection and fall-off tests
- iii. Apply the pressure derivative equations to Tiab's Direct Synthesis (TDS) in order to obtain new equations for determining the different reservoir parameters from the injection and fall-off tests.

1.3 Study Organization

Chapter one gives some background to the subject matter. Chapter two is literature review.

In chapter three, past work on the application of pressure injectivity and fall-off test under isothermal condition using Tiab's Direct Synthesis techniques is presented. It also discusses the application of pressure injectivity and fall-off test under Non-isothermal conditions using Tiab's Direct Synthesis techniques. The derived derivative equations are applied to Tiab's Direct Synthesis to interpret pressure injection and fall-off tests data.

In chapter four, several field and simulated examples that involved both injection and fall-off tests are analyzed and the results obtained using Tiab's Direct Synthesis is compared with the application of other techniques.

Chapter five gives the summary and conclusion of the study.

CHAPTER 2

LITERATURE REVIEW

2.0 Literature Survey

Several papers have been published that discuss the interpretation of injection well test data in a reservoir with radial discontinuities created by waterflooding, steam injection or in-situ combustion. The frontal advance equation specified by Wedge, (1952), and the Buckley-Leverett (1942) displacement model, are the most fundamental theories in which injection well test is based on. Sosa et al., (1981), formulated a numerical simulation model that is based on the Buckley-Leverett displacement model, and considered different mobility ratios to examine the effect of saturation gradients on pressure fall-off tests but limited the analysis to fall-off tests in liquid-liquid displacements.

Bodvarsson, and Tsang, (1980), studied the pressure transient response during cold-water injection into a hot water reservoir using a numerical simulator. They show how viscosity, density and the influence of a moving thermal boundary affect the pressure transient response. O'Sullivan and Pruess, (1980), and Garg and Pritchett, (1981), studied the problem of cold-water injection into a two-phase geothermal reservoir. They all established that the permeability/ thickness of the reservoir can be estimated from pressure buildup data using conventional analysis methods. Satman et al., (1980), also worked on pressure transient behavior in a system with radial discontinuities. They compared their studies with previous work and later summarized their derivatives.

Tsang and Tsang, (1978), presented a semi-analytical solution that accounts for the temperature and differences in the viscosity between the injected fluid and formation waters for the pressure response during injection tests of geothermal reservoirs. They also gave an approximate analytical method for predicting behaviors of a pressure transient system in an idealized well reservoir system and demonstrated the previous numerical studies for estimating the pressure buildup during non-isothermal injection.

Bixel and van Pollen, (1967), and Kazemi, et al., (1972), gave a principle to circumvent misinterpretation of pressure buildup and fall-off tests that may be affected by different mobility ratios, after flow, storage capacity and the presence of reservoir boundaries on the pressure transient data.

Other studies have presented on the development of analytic solutions or approximate analytic solutions for calculating different reservoir parameters in composite reservoir systems with a stationary boundary separating the reservoir regions of different fluid or rock properties (Larkin, 1963, Van Pollen, 1965, Kazemi, 1966, Odeh, 1969, and Ramey, 1970). These studies show that two semilog straight lines are observed, the first semilog corresponding to the rock or fluid properties of the inner region and the second line corresponding to the properties of the outer region. The permeability/thickness of the two reservoir regions can be calculated from the slopes of the two semilog straight lines. The mechanical skin factor for the well can be calculated using the conventional methods from the first semilog straight line. The radial

distance to the discontinuity can be evaluated when the two semilog straight lines intersect. Hazebroek, et al., (1958), presented a method for analyzing pressure fall-off tests in water-injection wells. This method is based on a trial-and-error method where the accurate average reservoir pressure, skin factor and the permeability/ thickness of the reservoir can be estimated. However, the late time pressure transient data will have to be adjusted linearly on pressure Vs log (time) plot. Woodward and Thambynayagam, (1983), obtained an analytical solution for non-unit mobility ratio conditions not including wellbore storage and skin effects. Their explanation was based on the use of a semilog analysis for pressure injection and fall-off tests.

Benson and Bodvarsson, (1986), considered the effects of diffuse and moving thermal front, pre-existing cold spots around the wells, and wellbore storage to develop analytical methods for evaluating the permeability/thickness of the reservoir and the skin factor of the well considering the non-isothermal effect during injection and fall-off test. They illustrate the pressure transient behavior during the non-isothermal (cold-water) injection as shown in Fig 2.1.

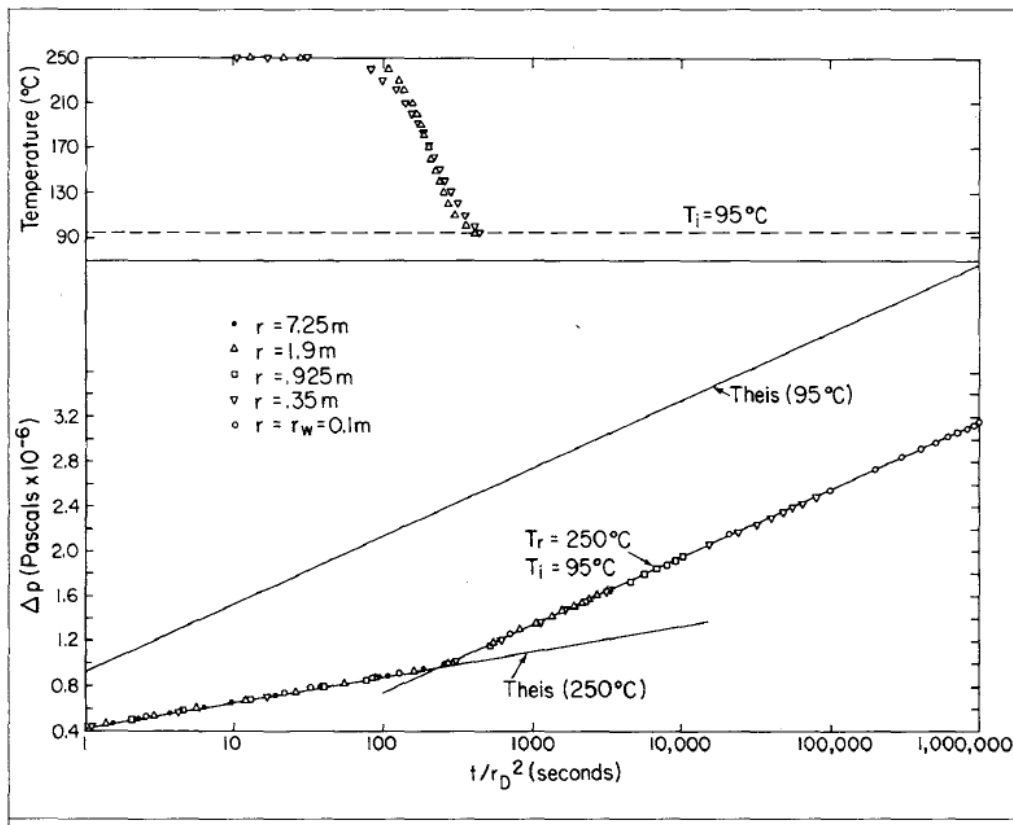


Figure 2.1: Pressure transient data for injection of 95°C water into 250°C reservoir

(Benson and Bodvarsson, 1986)

Reldar and Roland, (1990), derived analytical solutions that account for both the saturation gradient and temperature effects in non-isothermal water –injection and fall-off test. Micheal, (2002), presented a new

solution method for the analytical solution of two-phase pressure transient problem associated with water injection and fall-off test.

Abbaszadeh and Kamal, (1989), provided a solution to fall-off test problem in a composite reservoir in terms of the Laplace transform. They extended their study to the case with a region of variable saturation around the injection well and also included the effect of the saturation gradient in the invaded region; although non-isothermal effects were not considered. Yeh and Agarwal, (1989), presented another approach to the fall-off test problem in reservoirs with multiple fluid banks, through the use of a reservoir simulator; their method does not require the availability of relative permeability data. Kong, Xiang-Yan, and De-Tang, (1991), developed type curves to analyze pressure fall-off test which includes wellbore storage effect and skin factor. They solved the two-bank system model numerically.

Tiab, (1993), developed the TDS technique to analyze pressure and pressure derivative curves for pressure tests which do not require type curves. TDS is very useful in conditions of short tests and early time data missing tests. It also verifies the results since it uses more than one equation for the estimation of permeability, wellbore storage, and skin factor. Tiab and Abdesselam, (2001), gave an analytical solution to injection and fall-off test during an isothermal condition using the TDS techniques. Escobar et al., (2013), extended the TDS techniques to injection and fall-off test of Non-Newtonian pseudo plastic fluids. So far, TDS techniques have been applied to several well conditions including hydraulically fractured reservoirs and naturally fractured reservoirs.

2.1 Basic Flow Equations

The pressure transient analysis techniques are based on the diffusivity equation describing the flow of fluids through porous media. According to John L., (1982), in cylindrical coordinates, the diffusivity equation is written as follows:

$$\frac{\partial^2 p}{\partial r^2} + \frac{1}{r} \frac{\partial p}{\partial r} = \frac{\phi \mu c_i}{0.0002637k} \frac{\partial p}{\partial t} \quad (2.1)$$

Where

p = pressure, psia

r = radius of flow, ft

ϕ = formation porosity, fraction

μ = viscosity, cp

k = formation permeability, md

Eq. (2.1) is obtained by the combination of the material balance equation and Darcy's flow equation.

The derivation of Eq. (2.1) assumes:

1. Negligible gravity effects.

2. The porous medium is isotropic, homogeneous, uniform in thickness and has constant permeability and porosity.
3. Single-phase fluid is present and occupies the entire pore volume.
4. Viscosity and compressibility of the fluid remain constant at all pressures.
5. Radial flow into the well over the net pay thickness.
6. Small pressure gradients ($\frac{\partial p}{\partial r}$) within the reservoir.
7. Fluid density is governed by the following equation.

$$\rho = \rho_0 e^{[c(p-p_0)]} \quad (2.2)$$

Where

ρ_0 = fluid density at some reference pressure, p_0

c = fluid compressibility.

Assuming a constant rate during the infinite acting flow period, the initial and boundary conditions needed to find a solution to Eq. (2.1) are:

- $p = p_i$ at $t = 0$ for all r
- $r\left(\frac{\partial p}{\partial r}\right)_{r_w} = \frac{q\mu B}{2\pi kh}$ for $t > 0$
- $P \rightarrow P_i$ as $r \rightarrow \infty$ for all t .

2.2 Dimensionless Groups

To obtain a dimensionless form of Eq. (2.1), Van Everdingen and Hurst made the following transformations:

$$r_D = \frac{r}{r_w} \quad (2.3)$$

$$t_D = \frac{0.0002637kt}{\phi\mu c_t r_w^2} \quad (2.4)$$

$$p_D(r_D, t_D) = \frac{kh}{141.2q\mu B}(p_i - p(r, t)) \quad (2.5)$$

Where

r_D = dimensionless radius

r_w = wellbore radius, ft

t_D = dimensionless time

t = duration of flow, hrs

q = flow rate. STB/D for oil and MSCF/D for gas

h = formation thickness, ft

c_t = formation compressibility, psi-1

p_i = initial pressure, psi

$p_{(r,t)}$ = pressure at distance r from the wellbore after time t , psi

Eq. (2.1) is then written in dimensionless form as:

$$\frac{\partial^2 p_D}{\partial r_D^2} + \frac{1}{r_D} \frac{\partial p_D}{\partial r_D} = \frac{\partial p_D}{\partial t_D} \quad (2.6)$$

For the case of flow into a well at a constant volumetric rate and during infinite acting radial flow period, the solution to Eq. (2.6) is referred to as the *Ei* solution and the continuous line source solution.

2.4 Continuous Line Source Solution

For a constant rate and a small well radius ($r_w \rightarrow 0$) in an infinite system, the continuous line source solution to the diffusivity equation in dimensionless form is:

$$p_D(r_D, t_D) = -\frac{1}{2} Ei \left[-\frac{r_D^2}{4t_D} \right] \quad (2.7)$$

Where *Ei* denotes the exponential integral and is defined as:

$$-Ei(-x) = \int_x^\infty \frac{e^{-u}}{u} du \quad (2.8)$$

Muller and Witherspoon investigated the validity of this solution in the case of a finite wellbore radius. They concluded that the line source solution is an excellent approximation within 1% for all values of $r_D \geq 20$ and $\frac{t_D}{r_D^2} \geq 0.5$. Thus for most r_D and t_D values encountered during a well test, Eq. (2.6) can be used

to determine dimensionless pressures in an infinite radial system, as shown in Figure (2.2). For small values of arguments, the exponential integral function may be approximated within less than 1% error for $\left(\frac{t_D}{r_D^2}\right) \geq 70$ by a logarithmic function as follows:

$$-Ei\left(-\frac{r_D^2}{4t_D}\right) = -Ln\left[\frac{r_D^2}{4t_D}\right] - 0.5772 = Ln\left[\frac{t_D}{r_D^2}\right] + 0.80907 \quad (2.9)$$

The number 0.5772 is the Euler's constant.

Eq. (2.7) can be written as:

$$p_D(r_D, t_D) = -\frac{1}{2} \left[Ln\left(\frac{r_D^2}{4t_D}\right) + 0.5772 \right] = \frac{1}{2} \left[Ln\left(\frac{t_D}{r_D^2}\right) + 0.80907 \right] \quad (2.10a)$$

At the well ($r_D = 1$), Eq. (2.10) becomes,

$$p_D(t_D) = \frac{1}{2} [Ln(t_D) + 0.80907] \quad (2.10b)$$

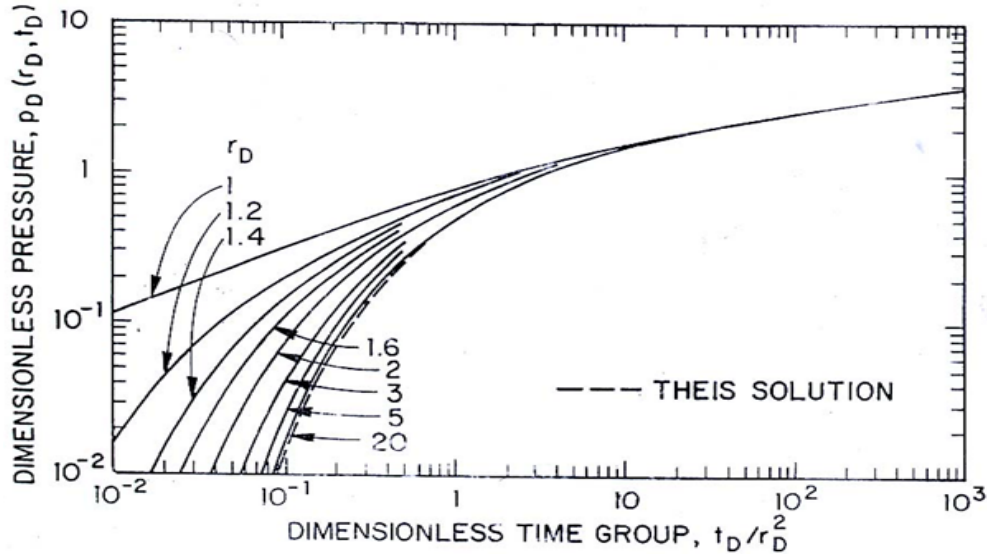


Figure 2.2: Dimensionless Pressure Function at Various dimensionless Distances from a Well Located in an Infinite System.

(Mueller and Witherspoon, 1965)

2.4 Wellbore Storage and Skin

Wellbore storage also called after flow, after production, or after injection has long been recognized as affecting short time transient pressure behavior. The wellbore storage constant (coefficient factor) is defined by:

$$C = \frac{\Delta V}{\Delta p} \quad (2.11)$$

Where

C = wellbore storage constant, *bbl/ psi*

ΔV = change in volume of fluid in the wellbore at wellbore conditions, *bbl*.

Δp = change in bottom-hole pressure, *psi*

The dimensionless wellbore storage coefficient C_D is defined as:

$$C_D = \frac{5.615C}{2\pi\phi c_t h r_w^2} \quad (2.12)$$

Where

c_t = total reservoir compressibility, *psi*⁻¹

From material balance, the pressure in the wellbore is directly proportional to time during the wellbore storage dominated period of the test:

$$p_D = \frac{1}{C_D} t_D \quad (2.13)$$

Van Everdingen and Hurst defined the skin effect as an impediment to flow that is caused by an infinitesimally thin damaged region around the wellbore. This damage causes an additional pressure drop. This thin zone is called “skin”. The damage of this zone is caused by mud filtrate or cement during drilling or completion, partial penetration, partial completion, and plugging of perforations.

The skin factor S is a variable used to quantify the magnitude of the skin effect, and is defined (in oil field units) by:

$$S = \frac{kh}{141.2q\mu B} \Delta p_s \quad (2.14)$$

Where

Δp_s = additional pressure drop due to skin effect, *psi*

If the skin effect is due to a damaged zone of radius r_s and reduced permeability k_s , the skin factor S can be calculated from the following equation:

$$S = \left(\frac{k}{k_s} - 1 \right) \ln \frac{r_s}{r_w} \quad (2.15)$$

When the skin factor is considered not equal to zero, Eq. (2.10) becomes:

$$p_D = -\frac{1}{2} \left[\ln \left(\frac{1}{4t_D} \right) + 0.5772 \right] + S = \frac{1}{2} \left[\ln t_D + 0.80907 + 2S \right] \quad (2.16)$$

In term of real parameters and oil field units, the pressure drop at the wellbore is:

$$\Delta p = p_i - p_{wf} = \frac{162.6qB\mu}{kh} \left[\log(t) + \bar{S} \right] \quad (2.17)$$

Where

$$\bar{S} = \left[\log \left(\frac{k}{\phi\mu c_i r_w^2} \right) - 3.227 + 0.8686S \right] \quad (2.18)$$

2.5 Derivative of the Line Source Solution

Tiab showed that the first derivative of the p_D -function is:

$$p'_D = \frac{\partial p_D}{\partial t_D} = \frac{1}{2t_D} e^{\left(\frac{-r_D^2}{4t_D} \right)} \quad (2.19)$$

Tiab demonstrated that the above relation is a good approximation to that calculated from finite-radius wellbore under the following conditions:

- (1) for all t_D when $r_D \geq 30$ and

(2) for all $r_D > 2$ when $\left(\frac{t_D}{r_D^2}\right) \geq 0.5$.

Equation (2.19) may be rearranged in the following form:

$$p'_D \times r_D^2 = \frac{1}{2(t_D/r_D^2)} \exp\left(-\frac{1}{4t_D/r_D^2}\right) \quad (2.20)$$

The rate of change with time of the dimensionless well pressure, i.e, $r_D = 1$, is given by :

$$p'_{wD} = \frac{1}{2t_D} \exp\left(-\frac{1}{4t_D}\right) \quad (2.21)$$

For $t_D \geq 250$, the exponential term is closer to unity, and then Eq. (2.21) is approximated to:

$$p'_{wD} = \frac{1}{2t_D} \quad (2.22)$$

In term of real parameters, the rate of change of pressure with time is given by:

$$p'(r,t) = \frac{\partial p}{\partial t} = \frac{1}{t} \left(\frac{q\mu}{4\pi kh} \right) \exp\left(-\frac{\phi\mu c_t r^2}{4kt}\right) \quad (2.23)$$

$$\text{For } \frac{kt}{\phi\mu c_t r^2} \geq 250, \quad p'(r,t) = \frac{1}{t} \left(\frac{q\mu}{4\pi kh} \right) \quad (2.24)$$

Figure (2.3) is a log-log plot of p_D and $(p'_D \times r_D^2)$ versus (t_D/r_D^2) for a line-source solution well in an infinite reservoir.

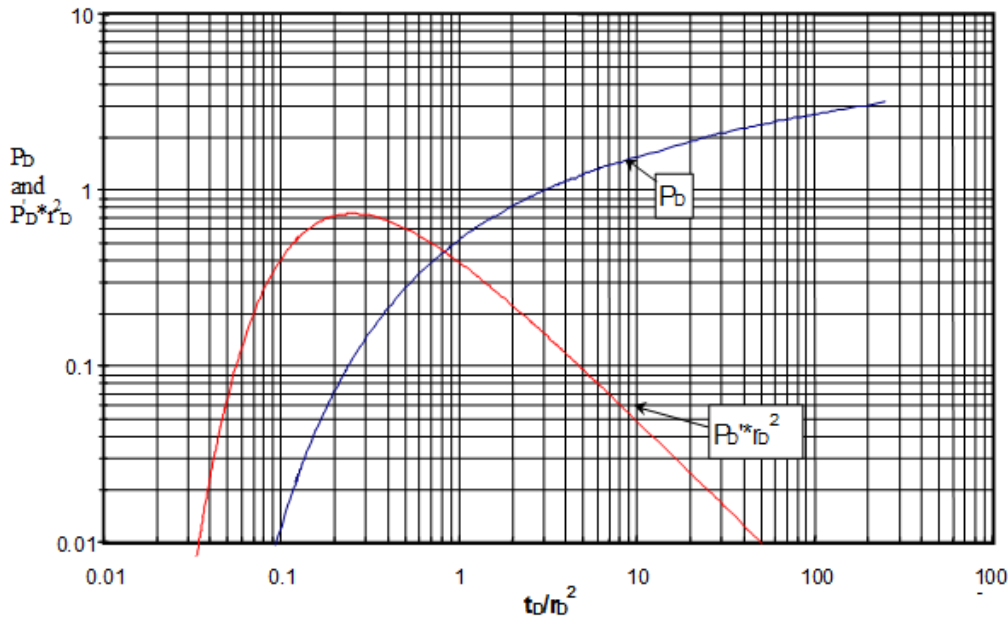


Figure 2.3: Log-Log Plot of the Dimensionless Pressure and Pressure Derivative versus (t_D/r_D^2) ratio. (Tiab, 1993)

2.6 Basic Injection Concepts

Injection well testing models are largely based on the Buckley-Leverett, (1942), displacement model and the frontal advance solution given by Wedge, (1952). Figure 2.4 shows the saturation profile which develop in the reservoir according to the Buckley-Leverett model as a result of injecting water into an oil-bearing reservoir. Figure 2.5 shows a plan view of the saturation distribution in the vicinity of the injection well.

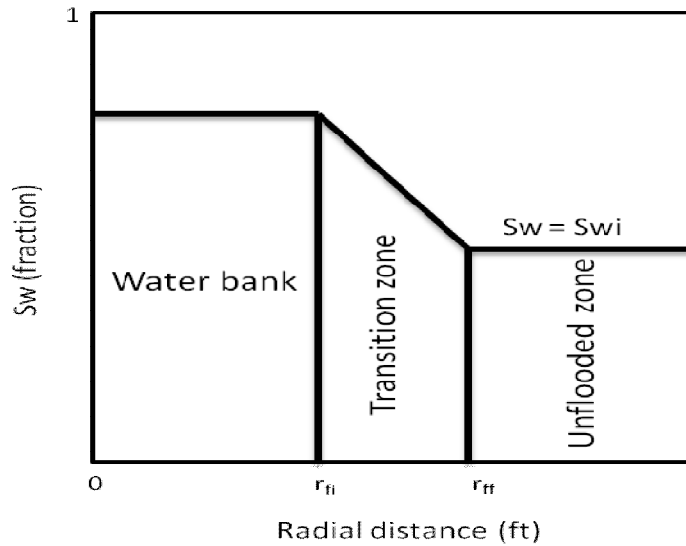


Figure 2.4: Saturation distribution (Buckley, and Leverett, 1942)

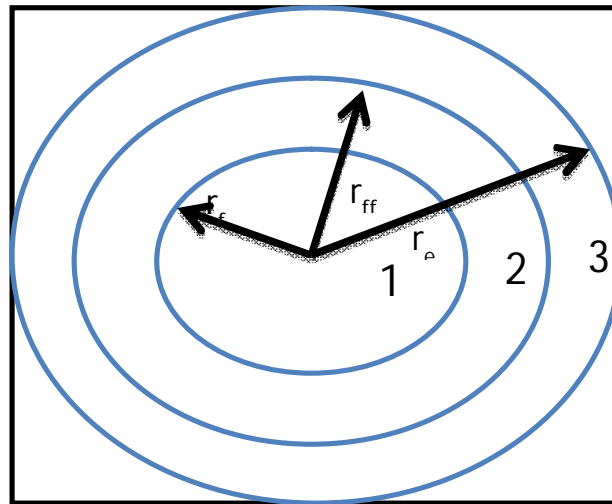


Figure 2.5: Plane view of saturation distribution around injection well

1-flooded zone, 2-transition zone and 3-unflooded zone

(Merrill et al., 1974)

The two figures show three distinct zones, water bank, transition zone and unflooded zone. Oil saturation in the water bank is S_{or} and in the transition zone, it varies from S_{or} to S_{oi} existed before the injection begun. The front is located at the beginning of the uninvaded zone and is marked by the abrupt change in saturation as indicated by the vertical saturation profile.

The average water saturation behind the front \bar{S}_w can be determined on the basis of the Buckley-Leverett model. The corresponding relative permeability to water k_{rw} can be determined from the representative relative permeability curves of the reservoir. The same relative permeability data provides the relative permeability to oil k_{ro} at S_{wi} .

The effective permeability to oil is $k_{ro} \times k$ and to water is $k_{rw} \times k$.

For given oil and water viscosities μ_o and μ_w , the mobility ratio M is defined by Ahmed T., (2006), as follows,

$$M = \frac{k_w(\bar{S}_w)}{\mu_w} \times \frac{\mu_o}{k_o(S_{wi})} = \frac{\lambda_w(\bar{S}_w)}{\lambda_o(S_{wi})} \quad (2.25)$$

Based on the value of M ; the displacement can be characterized as follows (Tiab, and Abdesselam, 2001);

$M < 1$: Piston-like displacement, high recovery efficiency and small transition zone

$M = 1$: Weak piston-like displacement, moderate recovery efficiency, and moderate transition zone width.

$M > 1$: Low recovery efficiency, a small water zone, and a large transition zone.

According to Ahmed T., (2006), we can use the relative permeability curve to plot the total mobility λ_t versus S_w as indicated in the following equation,

$$\lambda_t = k \left(\frac{k_{ro}(S_w)}{\mu_o} + \frac{k_{rw}(S_w)}{\mu_w} \right) \quad (2.26)$$

In case of oil displacement by gas, only two zones exist; the invaded and un-invaded zones. The water saturation in each zone is S_{wi} . The gas saturation S_g of the invaded zone is $(1 - S_o - S_{wi})$. Because the gas compressibility is high, the specific storage (ϕc_t) in the invaded zone would be higher than that of the un-invaded zone

CHAPTER 3

METHODOLOGY

3.0 ANALYTICAL SOLUTIONS TO PRESSURE INJECTIVITY AND FALL-OFF TESTS USING TIAB'S DIRECT SYNTHESIS (TDS) TECHNIQUES DURING ISOTHERMAL CONDITION

3.1 Mathematical Model

Tiab and Abdesselam, (2001), presented the physical model that consists of a well located in an infinite, homogeneous, and isotropic medium of uniform thickness. The formation and fluid properties are independent of pressure. The fluid is assumed to have small compressibility and gravity effects are negligible. Water injection occupies the entire thickness of the reservoir and a piston-like displacement of oil by water is assumed, such that uniform immobile oil saturation exists behind the flood front. The model and corresponding parameters are illustrated in Figure 3.1

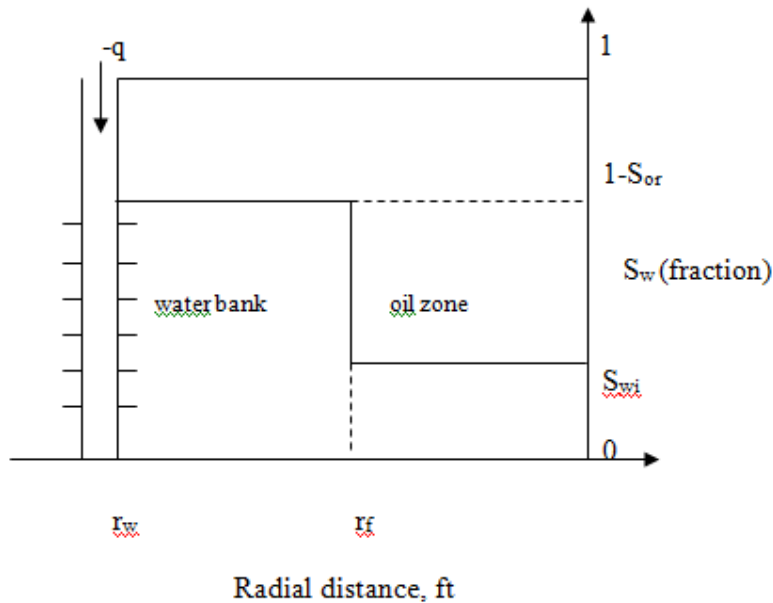


Figure 3.1: Injection Model

(Tiab and Abdesselam, 2001)

3.2 Injection Solution

According to Tiab, and Abdesselam, (2001); the governing equations for an infinite system with a line source well for both the invaded and un-invaded zones are,

- For the invaded zone:

$$\frac{\partial^2 p_{D1}}{\partial r_D^2} + \frac{1}{r_D} \frac{\partial p_{D1}}{\partial r_D} = \frac{\partial p_{D1}}{\partial t_D}, \quad 0 < r_D < r_{Df} \quad (3.1)$$

- For the uninverted zone:

$$\frac{\partial^2 p_{D2}}{\partial r_D^2} + \frac{1}{r_D} \frac{\partial p_{D2}}{\partial r_D} = \frac{\eta_1}{\eta_2} \frac{\partial p_{D2}}{\partial t_D}, \quad r_{Df} < r_D < \infty \quad (3.2)$$

Where η_1, η_2 are the hydraulic diffusivities of the invaded and un-invaded zones, respectively. They are defined as follows

$$\eta_1 = \frac{k_w}{\phi \mu_w c_{t1}}$$

and

$$\eta_2 = \frac{k_o}{\phi \mu_o c_{t2}}.$$

Initial conditions

$$p_{D1} = p_{D2} = 0, \quad t_D = 0 \quad (3.3)$$

$$r_{Df} = 0, \quad t_D = 0 \quad (3.4)$$

Boundary conditions

$$\lim_{r_D \rightarrow 0} r_D \left(\frac{\partial p_{D1}}{\partial r_D} \right) = -1 \quad (3.5)$$

$$\lim_{r_D \rightarrow \infty} p_{D2} = 0 \quad (3.6)$$

Moving-boundary conditions

$$p_{D1} = p_{D2}, \quad r_D = r_{Df} \quad (3.7)$$

$$M \cdot \frac{\partial p_{D1}}{\partial r_D} = \frac{\partial p_{D2}}{\partial r_D}, \quad r_D = r_{Df} \quad (3.8)$$

All variables and parameters are dimensionless, p_{D1} and p_{D2} are the pressures in the invaded and un-invaded regions, respectively. The term r_{Df} is the position of the moving interface between the two regions. From the Buckley-Leverett theory, the saturation profile is defined by the frontal advance equation given as,

$$\left[r_D \left(\frac{dr_D}{dt_D} \right) \right]_{s_w} = \mathcal{E}f' \quad (3.9)$$

Where, $\varepsilon = \frac{qBc_{11}\mu_w}{2\pi hk_w}$ and $f' = \frac{df}{ds_w}$ denotes the slope of the fractional-flow curve.

If Eq. (3.9) is integrated, we will have:

$$r_D^2 = 2\varepsilon f' t_D \quad (3.10)$$

Hence, by transforming the problem from the independent variables r_D and t_D to the Boltzmann variable

$y = \frac{r_D^2}{4t_D}$, we fix the moving interface and transform the moving-boundary problem into a composite

problem in one variable; if we substitute y into Eq. (3.1) and (3.2), we have

$$y \frac{d^2 P_{D1}}{dy^2} + (y+1) \frac{dP_{D1}}{dy} = 0 \quad (3.11) \quad :$$

$$y \frac{d^2 P_{D2}}{dy^2} + \left(1 + \frac{\eta_1}{\eta_2} y\right) \frac{dP_{D2}}{dy} = 0 \quad (3.12)$$

With

$$\lim_{y \rightarrow 0} y \left(\frac{dP_{D1}}{dy} \right) = -\frac{1}{2} \quad (3.13)$$

$$\lim_{y \rightarrow \infty} p_{D2} = 0 \quad (3.14)$$

$$P_{D1} = P_{D2}, \quad y = y_f \quad (3.15)$$

$$M \cdot \frac{dp_{D1}}{dy} = \frac{dp_{D2}}{dy}, \quad y = y_f \quad (3.16)$$

Where

$$y_f = \frac{r_{Df}^2}{4t_D}$$

Applying the above initial and boundary conditions to the differential Equations (3.11) and (3.12), the following solutions is obtained at the wellbore ($r_D = 1$).

$$P_{wD} = 1/2 \left[Ei(-y) - Ei(-y_f) + M \exp(-y_f (1 - \frac{\eta_1}{\eta_2})) Ei(-\frac{\eta_1}{\eta_2} y_f) \right],$$

$$y_f \leq \frac{1}{4t_D} \quad (3.17)$$

$$P_{wD} = \frac{M}{2} \exp\left\{-y_f \left(1 - \frac{\eta_1}{\eta_2}\right)\right\} Ei\left(-\frac{\eta_1}{\eta_2} y\right), \quad y_f \geq \frac{1}{4t_D} \quad (3.18)$$

For typical water injection test, y_f is small because of small water compressibility, this makes the exponential terms in the solution to be close to one after a short time of injection.

Equation (3.17) and (3.18) can be written as a function of time as follows:

$$P_{wD} = \frac{M}{2} Ei\left(-\frac{\eta_1}{\eta_2} \frac{1}{4t_D}\right), \quad t_D \leq \frac{1}{4y_f} \quad (3.19)$$

$$P_{wD} = \frac{1}{2} \left[Ei\left(-\frac{1}{4t_D}\right) - Ei(-y_f) + MEi\left(-\frac{\eta_1}{\eta_2} y_f\right) \right], \quad t_D \geq \frac{1}{4y_f} \quad (3.20)$$

Thus, for injection period, the semilog plot of the wellbore dimensionless pressure P_{wD} versus the dimensionless time t_D should exhibit two straight lines. The first straight line corresponds to the mobility of the uninvaded reservoir fluid with a slope of $\frac{M}{2}$. The second line has a slope of $\frac{1}{2}$ and corresponds to the mobility in the completely flooded region; where $S_w = 1 - S_{or}$ as shown in Figures 3.2 and 3.3.

If the logarithmic approximation is used, Equation (3.19) and (3.20) can be written as,

$$p_{wf} - p_i = \frac{162.6qB\mu_w}{k_w h} M \left[\log \frac{k_o t}{\phi \mu_o c_{i2} r_w^2} - 3.23 \right] \quad (3.21)$$

and

$$p_{wf} - p_i = \frac{162.6qB\mu_w}{k_w h} \left[\log \frac{\alpha t}{r_w^2} + M \log \frac{k_o}{\phi \mu_o c_{i2} \alpha} - 3.23M \right] \quad (3.22)$$

Where

$$\alpha = \frac{5.615qB}{\pi h \phi \Delta S_w}$$

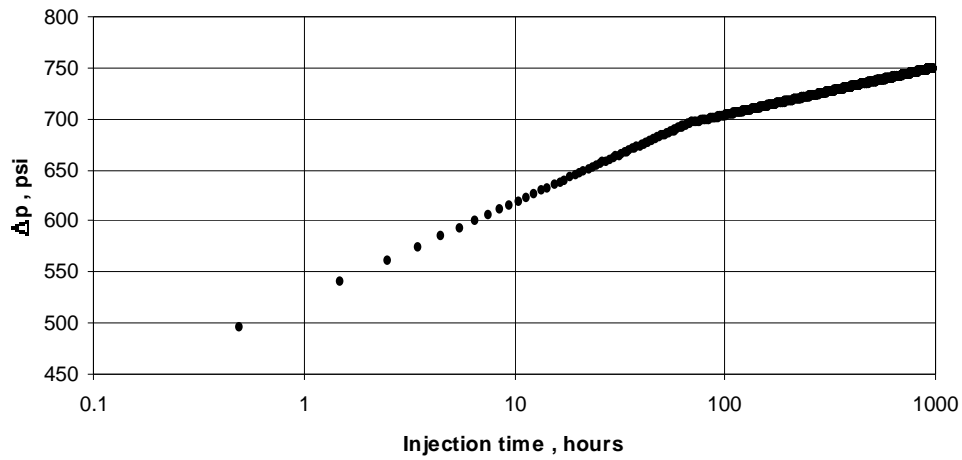


Figure 3.2: Semilog Plot of Injection Data Using Eqs. (3.19) and (3.20)

(Tiab and Abdesselam, 2001)

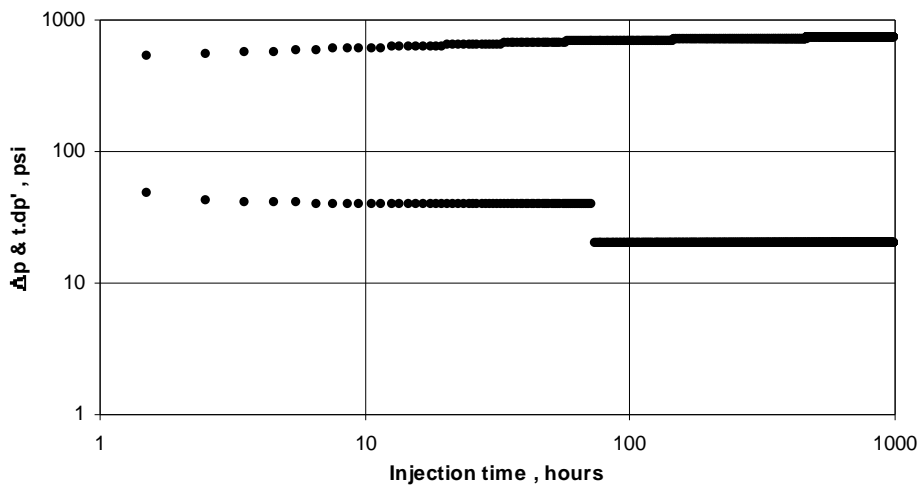


Figure 3.3: Log-log Plots of Pressure and Pressure Derivative Injection Data

(Tiab and Abdesselam, 2001)

3.3 Fall-off Solution

The assumption of stationary interface is generally acceptable due to the fact that the compressibility's of fluids are small. Hence, any volumetric expansion or compression of the fluids is negligible. The first bank is often large at the time of shut-in; therefore any volume change expressed in terms of radial distance produces a negligible change in the location of the interface. In addition to the small duration of fall-off test

compared to injection time, one can generate a fall-off solution by superimposing the injection solution assuming that the fall-off period corresponds to pressure decay in the radially composite reservoir that is formed at the end of the injection period.

According to Tiab and Abdesselam, (2001), the fall-off solution is given as:

$$P_{D(falloff)} = P_D(t_{iD} + \Delta t_D) - P_D(\Delta t_D) \quad (3.23)$$

The p_D terms on the right side of the above equation represent the injectivity solutions satisfying the governing partial-differential equations and boundary conditions of the fall-off problem.

$$P_{D(falloff)} = \frac{1}{2} \left[\begin{aligned} & Ei\left(-\frac{1}{4(t_{iD} + \Delta t_D)}\right) - Ei\left(-\frac{r_{Df}^2}{4(t_{iD} + \Delta t_D)}\right) + Me^{-\frac{r_{Df}^2}{4(t_{iD} + \Delta t_D)}\left(1 - \frac{\eta_1}{\eta_2}\right)} \\ & Ei\left(-\frac{\eta_1}{\eta_2} \frac{r_{Df}^2}{4(t_{iD} + \Delta t_D)}\right) \end{aligned} \right] \\ - \frac{1}{2} \left[\begin{aligned} & Ei\left(-\frac{1}{4\Delta t_D}\right) - Ei\left(-\frac{r_{Df}^2}{4\Delta t_D}\right) + Me^{-\frac{r_{Df}^2}{4\Delta t_D}\left(1 - \frac{\eta_1}{\eta_2}\right)} \\ & Ei\left(-\frac{\eta_1}{\eta_2} \frac{r_{Df}^2}{4\Delta t_D}\right) \end{aligned} \right] \quad (3.24)$$

When the radius of investigation is within the water bank and the injection time is generally larger than the fall-off period, Eq. (3.24) is simplified to,

$$P_{wD} = -\frac{1}{2} \left[\begin{aligned} & Ei\left(-\frac{1}{4\Delta t_D}\right) - Ei\left(-\frac{1}{4(t_{iD} + \Delta t_D)}\right) + Ei\left(-\frac{r_{Df}^2}{4t_{iD}}\right) - MEi\left(-\frac{\eta_1}{\eta_2} \frac{r_{Df}^2}{4t_{iD}}\right) \end{aligned} \right] \quad (3.25)$$

At later times when the radius of investigation exceeds r_{Df} , Eq. (3.24) becomes,

$$P_{wD} = -\frac{M}{2} \left[\begin{aligned} & Ei\left(-\frac{\eta_1}{\eta_2} \frac{1}{4\Delta t_D}\right) - Ei\left(-\frac{\eta_1}{\eta_2} \frac{1}{4(t_{iD} + \Delta t_{iD})}\right) \end{aligned} \right] \quad (3.26)$$

Thus the semilog plot of the dimensionless bottom-hole pressure P_{wD} versus the dimensionless time $\frac{t_{iD} + \Delta t_D}{\Delta t_D}$ should exhibit two straight lines. The first straight line has a slope $-\frac{1}{2}$, which defines the mobility

of the water bank and the second straight line has a slope $-\frac{M}{2}$ which corresponds to the mobility of the native reservoir fluid as shown in Figure. 3.4.

If the logarithmic approximation is used, Equations (3.25) and (3.26) can be written as

$$p_i - p_{ws} = m \left[\log\left(\frac{t_i + \Delta t}{\Delta t}\right) + M \log\left(\frac{k_o}{\phi \mu_o c_{i2} \alpha}\right) - 3.23M - \log\left(\frac{k_w}{\phi \mu_w c_{i1} \alpha}\right) + 3.23 \right] \quad (3.27)$$

And

$$P_i - P_{ws} = m.M \log\left(\frac{t_i + \Delta t}{\Delta t}\right) \quad (3.28)$$

Where

$$m = -\frac{162.6qB\mu}{k_w h}$$

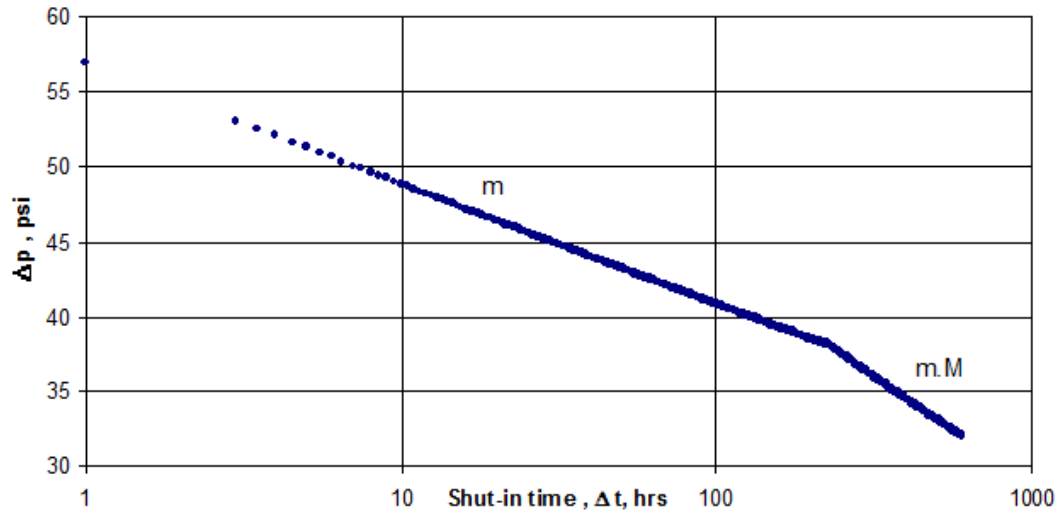


Figure 3.4: Semilog Plot of Fall-off Data Using Eqs. (3.27) and (3.28)

(Tiab and Abdesselam, 2001)

3.4 Skin Factor

By considering the late time section of the injection pressure plot, the skin factor S can be determined by using Equation (3.22) which can be written as follows

$$P_{wf} - P_i = m \left[\log \frac{\alpha t}{r_w^2} + M \cdot \log \frac{k_o}{\phi \mu_o c_{t2} \alpha} - 3.23M + 0.87S \right] \quad (3.29)$$

Thus, from equation (3.29), the skin factor S can be written as:

$$S = 1.1513 \left\{ \frac{\Delta P_{1hr}}{m} - \log\left(\frac{\alpha}{r_w^2}\right) - M \left[\log \frac{k_o}{\mu_o \phi c_{t2} \alpha} - 3.23 \right] \right\} \quad (3.30a)$$

Equation (3.30a) can also be given as:

$$S = 1.1513 \left[\frac{\Delta p_{1hr}}{m} - \log \frac{\lambda}{\phi c_{t1} r_w^2} + 3.23 \right] \quad (3.30b)$$

Where

$$m = \frac{162.6qB_w\mu_w}{k_w h}$$

For the fall-off period, the mechanical skin factor is obtained from the conventional semilog plot if the first semilog straight line corresponding to the water bank is present. If only the semilog straight line corresponding to the oil bank is developed, the skin factor can be computed from this line.

Thus, by combining Equations (3.22) and (3.28), we have:

$$S = 1.1513 \left[M \left(\frac{\Delta P_{1hr}}{m \times M} - \log \frac{k_o}{\phi \mu_o c_{t2} r_w^2} + 3.23 \right) + (M - 1) \log \frac{\alpha t}{r_w^2} \right] \quad (3.31)$$

Eq. (3.31) can be written as

$$S = MS' + 1.1513(M - 1) \log \frac{\alpha t}{r_w^2} \quad (3.32)$$

Where $S' = 1.1513 \left[\frac{\Delta P_{1hr}}{m \times M} - \log \frac{k_o}{\phi \mu_o c_{t2} r_w^2} + 3.23 \right]$ and $\alpha = \frac{5.615q_{inj} B_w}{\pi h \phi \Delta S_w}$

S' is an apparent skin factor which neglects the presence of the water bank

3.5 Pressure Derivative Calculations

Since pressure derivative is very sensitive to small variation in the pressure, it therefore provides valuable qualitative information about the reservoir heterogeneity, which otherwise may be missed in semilog analysis.

3.5.1 During injection period

The derivative of Equations (3.21) and (3.22) with respect to the natural logarithm of the dimensionless time t_D yields:

$$\frac{dP_D}{d \ln t_D} = \frac{M}{2} \quad (3.33)$$

and

$$\frac{dP_D}{d \ln t_D} = \frac{1}{2} \quad (3.34)$$

In real parameters, Equations (3.33) and (3.34) can be written as,

$$\frac{dP}{dLnt} = t \cdot \frac{dP}{dt} = \frac{70.6q_{inj}B_w\mu_w M}{k_w h} \quad (3.35)$$

and

$$\frac{dP}{dLnt} = t \cdot \frac{dP}{dt} = \frac{70.6q_{inj}B_w\mu_w}{k_w h} \quad (3.36)$$

Equations (3.35) and (3.36) state that during the infinite acting radial flow periods, the slopes of the plot of $\frac{dp}{dLnt}$ versus t on log-log scale are constant and are equal to $\frac{70.6qB\mu_w M}{k_w h}$ and $\frac{70.6qB\mu_w}{k_w h}$ respectively.

3.5.2 During fall-off period

Taking the derivative of Equation (3.27) and (3.28) with respect to the natural logarithm of the dimensionless shut-in time Δt_D when $\Delta t_D \ll t_{iD}$ will yield,

$$\frac{dP_D}{dLn(\Delta t_D)} = \frac{1}{2} \quad (3.37)$$

And

$$\frac{dP_D}{dLn(\Delta t_D)} = \frac{M}{2} \quad (3.38)$$

In real parameters, the above equations become,

$$\frac{dP}{dLn(\Delta t)} = t \cdot \frac{dP}{d(\Delta t)} = \frac{70.6q_{inj}B_w\mu_w}{k_w h} \quad (3.39)$$

And

$$\frac{dP}{dLn(\Delta t)} = t \cdot \frac{dP}{d(\Delta t)} = \frac{70.6q_{inj}B_w\mu_w M}{k_w h} \quad (3.40)$$

The infinite acting radial flow periods are characterized by constant slopes of $\frac{70.6qB\mu_w}{k_w h}$ and $\frac{70.6qB\mu_w M}{k_w h}$ on a log-log plot of $\frac{dp}{dLn(\Delta t)}$ versus Δt respectively.

3.6 Application of the Derivative Equations to Tiab's Direct Synthesis (TDS) Techniques

The dimensionless pressure p_{wD} , time t_D , and wellbore storage coefficient can be expressed according to John L., (1982) as follows:

$$p_D = \left(\frac{kh}{141.2qB\mu} \right) \Delta p \quad (3.41)$$

$$t_D = \left(\frac{0.0002637k}{\phi\mu c_i r_w^2} \right) t \quad (3.42)$$

$$c_D = \left(\frac{0.8935}{\phi c_i h r_w^2} \right) c \quad (3.43)$$

During early time, the pressure curve is characterized by a unit slope line which corresponds to pure wellbore storage effects. This unit slope line is a unique feature of early time for injection and fall-off tests. During these periods, fluid is dumped into the wellbore. In case of constant wellbore storage, Van Everdingen, and Agarwal et al., studied this early period and developed equations governing the sand face flow rate.

According to Tiab, (1993), during pure wellbore storage period, the pressure in the wellbore is directly proportional to the time, i.e.,

$$p_D = \frac{t_D}{c_D} \quad (3.44)$$

The derivative of Eq. (3.44) with respect to (t_D / c_D) is

$$\left(\frac{t_D}{c_D} \right) p_D' = \frac{t_D}{c_D} \quad (3.45)$$

Combining Eq. (3.42) and Eq. (3.43) results (for the water zone),

$$\frac{t_D}{c_D} = \frac{2.95 \times 10^{-4} k_w h t}{\mu_w c} \quad (3.46)$$

Substituting Eq. (3.41) and (3.46) into Eq. (3.44) and solving for the wellbore storage coefficient, this will give

$$c = \frac{qB}{24} \frac{t}{\Delta p} \quad (3.47)$$

The infinite acting radial flow portion of the pressure derivative is a horizontal line. The equation of this line for a homogeneous reservoir is,

$$(p_D)_r = \frac{1}{2} \left\{ \text{Ln} \left(\frac{t_D}{c_D} \right)_r + 0.80907 + \text{Ln}(c_D e^{2S}) \right\} \quad (3.48)$$

The derivative of Eq. (3.48) with respect to (t_D / c_D) is given as follows

$$\left[\left(\frac{t_D}{c_D} \right) p_D' \right]_r = 0.5 \quad (3.49)$$

Taking the derivative of Eq. (3.41) with respect to (t_D / c_D) , yields

$$p_D' = \frac{\partial p_D}{\partial (t_D / c_D)} = \frac{kh}{141.2qB\mu} \frac{\partial \Delta p}{\partial t} \frac{\partial t}{\partial (t_D / c_D)} = \frac{kh}{141.2qB\mu} \cdot \frac{c\mu}{2.95 \times 10^{-4} kh} \Delta p'$$

Or

$$p_D' = \frac{24c}{qB} \Delta p' \quad (3.50)$$

Substituting Eq. (3.46) into Eq. (3.50) gives

$$\frac{t_D}{c_D} p_D' = \frac{k_w h}{141.2qB\mu_w} (t \Delta p') \quad (3.51)$$

3.6.1 Pressure injection period

The wellbore storage coefficient that is given by Eq. (3.47) can also be written as

$$c = \frac{q_{inj} B_w}{24} \frac{t}{\Delta p} \quad (3.52)$$

Where t and Δp are obtained from the unit slope line of the pressure and pressure derivative curve.

3.6.1.1 First radial flow

From the pressure derivative curve during the first infinite acting radial flow period, the derivative of Eq. (3.21) yields,

$$(t \Delta p')_{r1} = \frac{70.6qB\mu_w}{k_w h} M \quad (3.53)$$

Eq. (3.53) provides permeability corresponding to the oil zone.

$$k_o = \frac{70.6qB\mu_o}{(t \Delta p')_{r1} h} \quad (3.54)$$

Where $(t \Delta p')_{r1}$ is the value of pressure derivative corresponding to the first infinite acting flow. The early-time unit slope line and the early-time infinite acting line of the pressure derivative i.e. the horizontal line intersect at

$$\left[\left(\frac{t_D}{c_D} \right) p_D' \right]_{il} = 0.5M \quad (3.55)$$

$$(p_D)_i = \left(\frac{t_D}{c_D} \right)_{il} = 0.5M \quad (3.56)$$

Where the subscript i stands for

intersection; since the unit slope line is the same for pressure and pressure derivative curves at the intersection point, we have,

$$(\Delta p)_{i1} = (t\Delta p')_{i1} = (t \cdot \Delta p')_{r1} \quad (3.57)$$

In real units, the coordinates of this intersection point are,

$$(t \cdot \Delta p')_{i1} = \frac{70.6qB\mu_w}{k_w h} M \quad (3.58)$$

And

$$t_{i1} = \frac{1695\mu_w c}{k_w h} M \quad (3.59)$$

Then, we can determine from Eq. (3.59), k_o and c as:

$$k_o = \frac{1695\mu_o c}{t_{i1} h} \quad (3.59a)$$

$$c = \frac{k_o h t_{i1}}{1695\mu_o} \quad (3.59b)$$

From Figures 3.5 and 3.6, one can see that the shape of the wellbore storage and skin regions on the pressure derivative curves is preserved. The coordinates of the ‘peaks’ for $c_D e^{2S} > 10^2$ were obtained from the second derivative and plotted on a Cartesian graph. The equation of this line is given by Tiab for single phase production wells as:

$$\left[\left(\frac{t_D}{c_D} \right) p_D' \right]_x = 0.36 \left(\frac{t_D}{c_D} \right)_x - 0.42 \quad (3.60)$$

Combining Equations (3.46), (3.51) and (3.60), yields,

$$(t\Delta p')_x = (0.015 \frac{qB}{c}) t_x - \frac{59.30q\mu_w B}{k_w h} \quad (3.61)$$

Where $(t.\Delta p')_x$ and t_x are the coordinates of the maximum point (peak) of the pressure derivative curve.

Also, combining Equations (3.61), (3.59) and (3.53), yields the mobility ratio,

$$M = \frac{0.84}{0.36 \frac{t_x}{t_{i1}} - \frac{(t.\Delta p')_x}{(t.\Delta p')_{r1}}} \quad (3.62)$$

A log-log plot of $\log(c_D e^{2S})$ versus the coordinates of the peaks yielded the following,

$$\log(c_D e^{2S}) = 0.35 \left(\frac{t_D}{c_D} \right)_x^{1.24} \quad (3.63)$$

$$\log(c_D e^{2S}) = 1.71 \left(\frac{t_D}{c_D} p_D' \right)_x^{1.10} \quad (3.64)$$

Substituting Equations (3.46) and (3.51) into Equations (3.63) and (3.64) and combining with Equations (3.53) and (3.59), gives

$$\log(c_D e^{2S}) = 0.1485 \left(\frac{t_x}{t_{i1}} M \right)^{1.24} \quad (3.65)$$

And

$$\log(c_D e^{2S}) = 0.80 \left[\frac{(t.\Delta p')_x}{(t.\Delta p')_{r1}} M \right]^{1.10} \quad (3.66)$$

Replacing C_D by its expression in Eq. (3.43) and solving for skin in Equations (3.65) and (3.66), gives respectively:

$$S = 0.171 \left(\frac{t_x}{t_{i1}} M \right)^{1.24} - 0.5 \text{Ln} \left(\frac{0.8935c}{\phi h c_{i1} r_w^2} \right) \quad (3.67)$$

And

$$S = 0.921 \left[\frac{(t.\Delta p')_x}{(t.\Delta p')_{i1}} M \right]^{1.10} - 0.5 \text{Ln} \left(\frac{0.8935c}{\phi h c_{i1} r_w^2} \right) \quad (3.68)$$

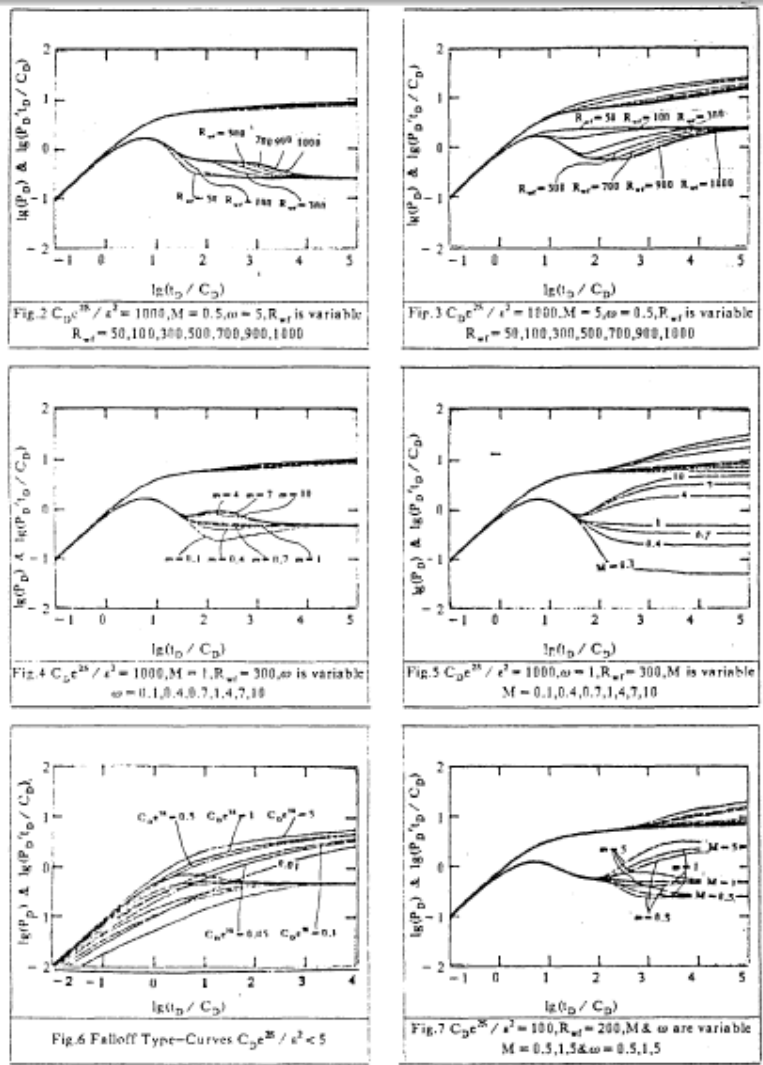


Figure 3.5: Pressure and Pressure Derivative Type Curves for Fall-off Tests

(Kong and Lu, 1991)

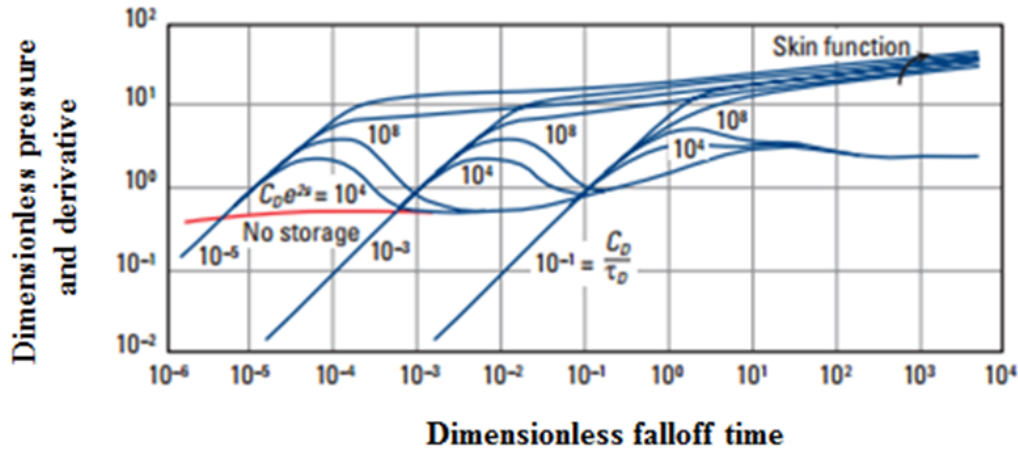


Figure 3.6: Pressure and Pressure Derivative Type Curves for Pressure Fall-off Tests

(Abbaszadeh and Kamal, 1989)

3.6.1.2 Second radial flow

The equation of the second infinite acting radial flow line can be written as,

$$\left[\left(\frac{t_D}{c_D} \right) p_D' \right]_{r_2} = 0.5 \quad (3.69)$$

Combining Equations (3.51) and (3.69) and solving for the effective water permeability, we have:

$$k_w = \frac{70.6 q_{inj} B_w \mu_w}{h(t \cdot \Delta p')_{r_2}} M \quad (3.70)$$

The early time unit slope line and the later time infinite acting line of the pressure derivative intersect at,

$$\left[\left(\frac{t_D}{c_D} \right) p_D' \right]_{i_2} = 0.5 \quad (3.71)$$

and

$$p_{Di_2} = \left(\frac{t_D}{c_D} \right)_{i_2} = 0.5 \quad (3.72)$$

In real units, Equations (3.71) and (3.72) can be written as:

$$k_w = \frac{70.6 q B \mu_w}{(t \cdot \Delta p')_{i_2} h} \quad (3.73)$$

$$t_{i2} = \frac{1695\mu_w c}{k_w h} \quad (3.74)$$

Another expression is derived for the mobility ratio, M , by dividing Eq. (3.61) by Eq. (3.53) and combining with Eq. (3.74) yields:

$$M = \frac{(t.\Delta p')_{r1}}{(t.\Delta p')_x} (0.36 \frac{t_x}{t_{i2}} - 0.84) \quad (3.75)$$

The later infinite acting radial flow line equation is given by,

$$p_{Dr2} = 0.5 \left[Ln \frac{\alpha t_{r2}}{r_w^2} + M \left(Ln \frac{5.9 \times 10^{-4} k_o}{\phi \mu_o c_{t2} \alpha} \right) + 2S \right] \quad (3.76)$$

By dividing Eq. (3.76) by Eq. (3.69), using the real units and solving for skin factor, gives

$$S = 0.5 \left[\frac{\Delta p_{r2}}{(t.\Delta p')_{r2}} - M Ln \frac{k_o}{\phi \mu_o c_{t2} \alpha} + 7.43M - Ln \frac{\alpha t_{r2}}{r_w^2} \right] \quad (3.77)$$

Where t_{r2} is any convenient time during the second infinite acting radial flow period and (Δp_{r2}) is the corresponding pressure value.

When t is expressed in hours, α can be written as $\alpha = \frac{5.615 q_{inj} B_w}{24\pi h \phi \Delta s_w}$

3.6.2 During fall-off period

During the pressure fall-off response, the pressure wave passes through the water invaded zone. Thus, pressure response during this flow regime is a representative of the invaded zone properties.

3.6.2.1 During first radial flow

The Equation of this flow period can be written as

$$\left[\left(\frac{t_D}{c_D} \right) p_D \right]_{r1} = 0.5 \quad (3.78)$$

Expressing Eq. (3.69) in oilfield variables and solving for permeability at 100% water saturation during the first radial flow gives

$$k_w = \frac{70.6 q_{inj} B_w \mu_w}{h(t.\Delta p')_{r2}} \quad (3.78a)$$

By dividing the first infinite acting line equation by the equation of the peaks, we have,

$$\frac{(t.\Delta p')_x}{(t.\Delta p')_{r1}} = 2 \left[1.062 \times 10^{-4} \left(\frac{k_w h}{\mu_w} \right) \frac{\Delta t_x}{c} - 0.42 \right] \quad (3.79)$$

The above equation is used to calculate k_w or c . Equations (3.63) and (3.64) are used to compute the skin factor and if combined with Equations (3.73) and (3.74), they yield

$$S = 0.171 \left(\frac{\Delta t_x}{\Delta t_{i1}} \right)^{1.24} - 0.5 \text{Ln} \left(\frac{0.8935c}{\phi h c_{i1} r_w^2} \right) \quad (3.80)$$

and

$$S = 0.921 \left[\frac{(t.\Delta p')_x}{(t.\Delta p')_{r1}} \right]^{1.1} - 0.5 \text{Ln} \left(\frac{0.8935c}{\phi h c_{i1} r_w^2} \right) \quad (3.81)$$

3.6.2.2 During second radial flow

At a later time during pressure fall-off, the pressure wave is dominated by the un-invaded (Oil) zone properties. The representative equation of this time period in oil field units is

$$P_i - P_{ws} = \frac{162.6qB_w \mu_o}{k_o h} \log \left(\frac{t + \Delta t}{\Delta t} \right) \quad (3.81a)$$

The derivative of the above equation is

$$\frac{d\Delta P}{dt} \times t = \frac{d\Delta P}{d(\ln t)} = \frac{70.6qB_w \mu_o}{k_o h} \quad (3.81b)$$

For the second infinite acting radial flow, the effective oil permeability is then calculated using Equation (3.81b)

$$k_o = \frac{70.6qB_w \mu_o}{(t.\Delta p')_{rf2} h} \quad (3.81c)$$

Where pressure derivative $(t.\Delta p')_{rf2}$ refers to second radial (Infinite acting) of the fall-off period. The wellbore storage co-efficient is estimated from the intersection point of the second infinite acting line with the early time unit slope line.

$$t_{i,2rf} = \frac{1695\mu_o C}{k_o h} \quad (3.81d)$$

$$k_o = \frac{1695\mu_o C}{t_{i,2fo} h} \quad (3.81e)$$

Thus k_o or C can be estimated using Eq. (3.81e)

An expression for the mobility ratio M can be derived using Eq. (3.59b) and Eq. (3.79) for fall-off, to obtain:

$$M = 5.55 \frac{\Delta t_{i2}}{\Delta t_x} \left[0.5 \frac{(t.\Delta p')_x}{(t.\Delta p')_{rf1}} + 0.42 \right] \quad (3.82)$$

M can also be obtained by dividing Eq.(3.59b) by Eq.(3.53):

$$M = 133.4 \cdot \frac{c}{qB} \frac{(t.\Delta p')_{rf2}}{\Delta t_x} \left[0.5 \frac{(t.\Delta p')_x}{(t.\Delta p')_{rf1}} + 0.42 \right] \quad (3.83)$$

Eq. (3.62) can also be used to compute, M , which will give for the pressure fall-off test as:

$$M = \frac{0.84}{0.36 \frac{\Delta t_x}{\Delta t_{if2}} - \frac{(t.\Delta p')_x}{(t.\Delta p')_{rf2}}} \quad (3.84)$$

The skin factor can also be computed using Equations (3.67) and (3.68); where t_{i1} for injection is replaced by Δt_{i2} for fall-off and can be written as:

$$S = 0.17 \left[\left(\frac{\Delta t_x}{\Delta t_{i2,fo}} \right) \cdot M \right]^{1.24} - 0.5 \text{Ln} \left(\frac{0.8935c}{\phi h c_{i1} r_w^2} \right) \quad (3.85)$$

$$S = 0.92 \left[\frac{(t.\Delta p')_x}{(t.\Delta p')_{r2,fo}} \cdot M \right]^{1.10} - 0.5 \text{Ln} \left(\frac{0.8935c}{\phi h c_{i1} r_w^2} \right) \quad (3.86)$$

3.7 Application of Tiab's Direct Synthesis (TDS) Techniques to Pressure Injectivity and Fall-Off Test Under Non-Isothermal Condition

3.8 Mathematical Model

The model consists of a reservoir that is assumed to be cylindrical with a well located at the center. The reservoir is assumed to have a uniform and constant porosity, permeability, heat capacity, thermal conductivity and infinite of constant thickness. The fluids have a negligible compressibility, gravity slumping of the cold-water front is neglected and the viscosities are assumed to be functions of temperature only. The well has a finite-radius and fully penetrates the entire formation thickness. Piston-like displacement of oil and water is assumed. The reservoir is completely saturated with oil and water and the fluid is injected at a constant rate. The equivalent model and parameters can be illustrated in Fig. 3.7

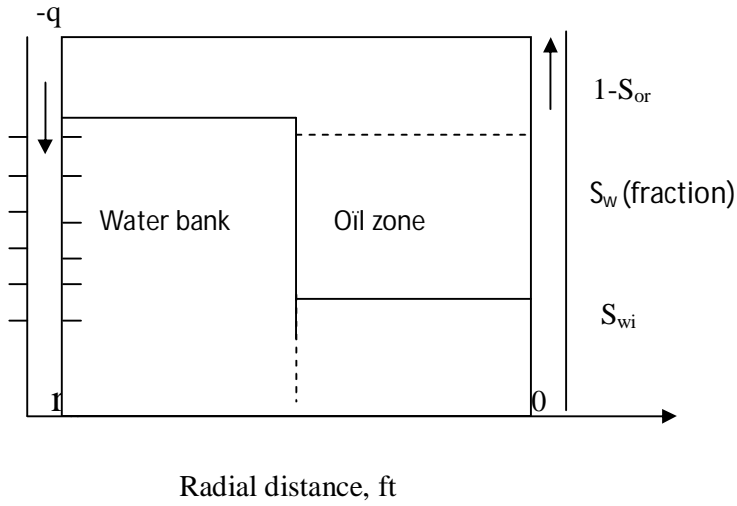


Figure 3.7: Injection Model

3.9 Injection Solution

Assuming that the reservoir consists of two different regions separated by a moving discontinuity in fluid saturation.

For an infinite system with a line source well, we have;

Governing Equations

The invaded zone

$$F_m \frac{\partial^2 P_{D1}}{\partial r_D^2} + F_m \frac{1}{r_D} \frac{\partial P_{D1}}{\partial r_D} = \frac{\partial P_{D1}}{\partial t_D}, \quad 0 < r_D < r_{Df} \quad (3.87)$$

The uninvaded zone

$$\frac{\partial^2 P_{D2}}{\partial r_D^2} + \frac{1}{r_D} \frac{\partial P_{D2}}{\partial r_D} = \frac{\eta_1}{\eta_2} \frac{\partial P_{D2}}{\partial t_D}, \quad r_{Df} < r_D < \infty \quad (3.88)$$

Where

$$F_m(S_w, T) = M_t 10^A = \frac{10^{\left(-1.6173 + \frac{247.8}{T_{inj} - 140}\right)} \left(\frac{K_{ro}}{\mu_o} + \frac{K_{rw}}{\mu_w} \right) \bar{s}_w}{K_{rw(1-s_{or})}}$$

$$P_D(t_D, r_D) = \frac{2\pi k_w h}{q\mu_w B_w} \Delta P$$

$$t_D = \frac{k_w t}{\phi\mu_w c_{t1} r_w^2}$$

$$r_D = \frac{r}{r_w}$$

$$\eta_1 = \frac{k_w}{\phi\mu_w c_{t1}}$$

$$\eta_2 = \frac{k_o}{\phi\mu_o c_{t2}}$$

Initial conditions:

$$P_{D1} = P_{D2} = 0, \quad t_D = 0 \quad (3.89)$$

$$r_{Df} = 0, \quad t_D = 0 \quad (3.90)$$

Boundary conditions:

$$\lim_{r_D \rightarrow 0} r_D \left(\frac{\partial P_{D1}}{\partial r_D} \right) = -1 \quad (3.91)$$

$$\lim_{r_D \rightarrow \infty} P_{D2} = 0 \quad (3.92)$$

Moving boundary conditions:

$$P_{D1} = P_{D2}, \quad r_D = r_{Df} \quad (3.93)$$

$$F_m \frac{\partial P_{D1}}{\partial r_D} = \frac{1}{M} \frac{\partial P_{D2}}{\partial r_D}, \quad r_D = r_{Df} \quad (3.94)$$

Where η_1, η_2 are the hydraulic diffusivities of the invaded and uninvaded zones respectively. All other variables and parameters are dimensionless, P_{D1} and P_{D2} are the pressures in the invaded and un-invaded regions respectively, r_{Df} is the position of the moving interface between the two regions and F_m represents the temperature- and saturation-dependent total mobility.

From the Buckley-Leverett theory, we know that the saturation profile is defined by the frontal advance equation as:

$$\left[r_D \left(\frac{dr_D}{dt_D} \right) \right]_{s_w} = \varepsilon f' \quad (3.95)$$

Where, $\varepsilon = \frac{qBc_{t1}\mu_w}{2\pi h k_w}$ and $f' = \frac{df}{ds_w}$ denote the slope of the fractional-flow curve.

If Eq. (3.95) is integrated, we obtain

$$r_D^2 = 2\epsilon f' t_D \quad (3.96)$$

By transforming the problem from independent variables r_D and t_D to the Boltzmann variable $y = \frac{r_D^2}{4t_D}$,

we fix the moving interface and transform the moving-boundary problem into a composite problem in one variable.

Substituting the Boltzmann variable y into Equation (3.87) and (3.88), will give

$$F_m y \frac{d^2 P_{D1}}{dy^2} + (F_m + y) \frac{dP_{D1}}{dy} = 0 \quad (3.97)$$

$$y \frac{d^2 P_{D2}}{dy^2} + \left(1 + \frac{\eta_1}{\eta_2} y\right) \frac{dP_{D2}}{dy} = 0 \quad (3.98)$$

With

$$\lim_{y \rightarrow 0} y \left(\frac{dP_{D1}}{dy} \right) = -\frac{1}{2} \quad (3.99)$$

$$\lim_{y \rightarrow \infty} P_{D2} = 0 \quad (3a.1)$$

$$P_{D1} = P_{D2}, \quad y = y_f \quad (3a.2)$$

$$F_m M \frac{dp_{D1}}{dy} = \frac{dp_{D2}}{dy}, \quad y = y_f \quad (3a.3)$$

Where

$$y_f = \frac{r_{Df}^2}{4t_D}$$

Applying the above initial and boundary conditions to the differential Equations (3.97) and (3.98), the following equation will be obtained at the wellbore (i.e. $r_D=1$)

$$P_{wD} = \frac{1}{2} \left[Ei \left(-\frac{y}{F_m} \right) - Ei \left(-\frac{y_f}{F_m} \right) + F_m M \exp \left(-y_f \left(\frac{1}{F_m} - \frac{\eta_1}{\eta_2} \right) \right) Ei \left(-\frac{\eta_1}{\eta_2} y \right) \right], t_D \geq \frac{1}{4y_f} \quad (3a.4)$$

$$P_{wD} = F_m \frac{M}{2} \exp \left[-y_f \left(\frac{1}{F_m} - \frac{\eta_1}{\eta_2} \right) \right] Ei \left(-\frac{\eta_1}{\eta_2} y_f \right), t_D \leq \frac{1}{4y_f} \quad (3a.5)$$

For typical water injection test, y_f is small because of small water compressibility, this makes the exponential terms in the solution to be close to one after a short time of injection.

Equation (4.4) and (4.5) can be written as a function of time as follows,

$$P_{wD} = \frac{1}{2} \left[Ei \left(-\frac{1}{F_m 4t_D} \right) - Ei \left(-\frac{y_f}{F_m} \right) + F_m M Ei \left(-\frac{\eta_1}{\eta_2} y_f \right) \right], \quad t_D \geq \frac{1}{4y_f} \quad (3a.6)$$

$$P_{wD} = F_m \frac{M}{2} Ei \left(-\frac{\eta_1}{\eta_2} \frac{1}{4t_D} \right), \quad t_D \leq \frac{1}{4y_f} \quad (3a.7)$$

If the logarithmic approximation is used, Equation (4.6) and (4.7) can be written respectively as:

$$p_{wf} - p_i = \frac{162.6qB\mu_w}{k_w h} \left[\frac{1}{F_m} \log \frac{\alpha t}{r_w^2} + F_m M \log \frac{k_o}{\phi \mu_o c_{t2} \alpha} - 3.23 F_m M \right] \quad (3a.8)$$

And

$$p_{wf} - p_i = \frac{162.6qB\mu_w}{k_w h} F_m M \left[\log \frac{k_o t}{\phi \mu_o c_{t2} r_w^2} - 3.23 \right] \quad (3a.9)$$

Where

$$\alpha = \frac{5.615qB}{\pi h \phi \Delta s_w}$$

3.10 Fall-Off Solution

The assumption of stationary interface is generally acceptable due to the fact that the compressibility of fluids is negligible. Therefore, any volumetric expansion or compression of the fluids is negligible. The first bank is often large at time of shut-in; therefore any volume change expressed in terms of radial distance produces a negligible change in the location of the interface. In addition to the small duration of fall-off test compared to injection time, one can generate a fall-off solution by superimposing the injection solution assuming that the fall-off period corresponds to pressure decay in the radially composite reservoir that is formed at the end of the injection period.

The fall-off solution can be written as:

$$P_{D_{falloff}} = P_D(t_{iD} + \Delta t_D) - P_D(\Delta t_D) \quad (3a.10)$$

The p_D terms on the right side of the above equation represent the injectivity solutions satisfying the governing partial-differential equations and boundary conditions of the fall-off problem.

$$P_{D(falloff)} = \frac{1}{2} \left[\begin{aligned} & Ei\left(-\frac{1}{4F_m(t_{iD} + \Delta t_D)}\right) - Ei\left(-\frac{r_{Df}^2}{4F_m(t_{iD} + \Delta t_D)}\right) + F_m M e^{-\frac{r_{Df}^2}{4(t_{iD} + \Delta t_D)}\left(\frac{1}{F_m} \frac{\eta_1}{\eta_2}\right)} \\ & Ei\left(-\frac{\eta_1}{\eta_2} \frac{r_{Df}^2}{4(t_{iD} + \Delta t_D)}\right) \end{aligned} \right] \\ - \frac{1}{2} \left[\begin{aligned} & Ei\left(-\frac{1}{4F_m \Delta t_D}\right) - Ei\left(-\frac{r_{Df}^2}{4F_m \Delta t_D}\right) + F_m M e^{-\frac{r_{Df}^2}{4\Delta t_D}\left(\frac{1}{F_m} \frac{\eta_1}{\eta_2}\right)} Ei\left(-\frac{\eta_1}{\eta_2} \frac{r_{Df}^2}{4\Delta t_D}\right) \end{aligned} \right] \quad (3a.11)$$

When the radius of investigation is within the water bank and the injection time is generally larger than the fall-off period, Eq. (A.35) of the appendix is simplified to,

$$P_{wD} = -\frac{1}{2} \left[Ei\left(-\frac{1}{4F_m \Delta t_D}\right) - Ei\left(\frac{1}{4F_m(t_{iD} + \Delta t_D)}\right) + Ei\left(-\frac{r_{Df}^2}{4F_m t_{iD}}\right) - F_m M Ei\left(-\frac{\eta_1}{\eta_2} \frac{r_{Df}^2}{4t_{iD}}\right) \right] \quad (3a.12)$$

At later times when the radius of investigation exceeds r_{Df} , Eq. (3a.12) becomes,

$$P_{wD} = -\frac{F_m M}{2} \left[Ei\left(-\frac{\eta_1}{\eta_2} \frac{1}{4\Delta t_D}\right) - Ei\left(-\frac{\eta_1}{\eta_2} \frac{1}{4(t_{iD} + \Delta t_D)}\right) \right] \quad (3a.13)$$

Thus the semilog plot of the dimensionless bottom-hole pressure P_{wD} versus the dimensionless time $\frac{t_{iD} + \Delta t_D}{\Delta t_D}$ should exhibit two straight lines. The first straight line has slope $-\frac{1}{2}$ and defines the mobility of

the water bank and the second line has slope $-\frac{F_m M}{2}$ and corresponds to the mobility of the native reservoir fluid.

If the logarithmic approximation is used, Equations (3a.12) and (3a.13) can be written as

$$p_i - p_{ws} = -\frac{162.6qB\mu}{k_w h} \left[\log\left(\frac{t_i + \Delta t}{\Delta t}\right) + F_m M \log\frac{k_o}{\phi\mu_o c_{i2}\alpha} - 3.23F_m M - \log\frac{k_w}{\phi\mu_w c_{i1}\alpha} + 3.23 \right] \quad (3a.14)$$

And

$$P_i - P_{ws} = -\frac{162.6qB\mu}{k_w h} F_m M \log\left(\frac{t_i + \Delta t}{\Delta t}\right) \quad (3a.15)$$

Equation (3a.14) and (3a.15) can also be written as

$$p_i - p_{ws} = m \left[\log\left(\frac{t_i + \Delta t}{\Delta t}\right) + F_m M \log\frac{k_o}{\phi\mu_o c_{i2}\alpha} - 3.23F_m M - \log\frac{k_w}{\phi\mu_w c_{i1}\alpha} + 3.23 \right] \quad (3a.14b)$$

$$P_i - P_{ws} = mF_m M \log\left(\frac{t_i + \Delta t}{\Delta t}\right) \quad (3a.15b)$$

$$\text{Where } m = \frac{162.6qB_w\mu_w}{K_w h}$$

3.11 Skin Factor

The skin factor S can be determined using Eq. (3a.8),

$$p_{wf} - p_i = \frac{162.6qB_w\mu_w}{k_w h} \left[\frac{1}{F_m} \log \frac{\alpha t}{r_w^2} + F_m M \log \frac{k_o}{\phi\mu_o c_{t2}\alpha} - 3.23F_m M + 0.87S \right] \quad (3a.16)$$

Thus, the skin factor S is given by

$$S = 1.1513 \left[\frac{\Delta P_{1hr} K_w h}{162.6qB_w\mu_w} - \frac{1}{F_m} \log\left(\frac{\alpha t}{r_w^2}\right) - F_m M \left(\log \frac{k_o}{\mu_o \phi c_{t2} \alpha} - 3.23 \right) \right] \quad (3a.17a)$$

Equation (3a.17a) can also be written as

$$S = 1.1513 \left[\frac{\Delta P_{1hr}}{m} - \frac{1}{F_m} \log\left(\frac{\alpha t}{r_w^2}\right) - F_m M \left(\log \frac{k_o}{\mu_o \phi c_{t2} \alpha} - 3.23 \right) \right] \quad (3a.17b)$$

For the fall-off period, the mechanical skin factor is obtained from the conventional semilog plot if the first semilog straight line corresponding to the water bank is present. If only the semilog straight line corresponding to the oil bank is developed, the skin factor can be computed from this line. Therefore, the combination of equation (3a.15b) and (3a.17b) will give,

$$S = 1.1513 \left[F_m M \left(\frac{\Delta P_{1hr}}{F_m \times m \times M} - \log \frac{k_o}{\phi\mu_o c_{t2} r_w^2} + 3.23 \right) + \left(M - \frac{1}{F_m} \right) \log \frac{\alpha t}{r_w^2} \right] \quad (3a.18a)$$

Eq. (3a.18a) can also be written as

$$S = F_m M S' + 1.1513 \left(M - \frac{1}{F_m} \right) \log \frac{\alpha t}{r_w^2} \quad (3a.18b)$$

Where

$$S' = 1.1513 \left[\frac{\Delta P_{1hr}}{F_m \times m \times M} - \log \frac{k_o}{\phi\mu_o c_{t2} r_w^2} + 3.23 \right] \text{ And } \alpha = \frac{5.615q_{inj} B_w}{\pi h \phi \Delta S_w}$$

S' is an apparent skin factor which neglects the presence of the water bank.

3.12 Pressure Derivative Calculations

Pressure derivative provides valuable qualitative information about the heterogeneity of the reservoir because of its sensitivity to small change in pressure. The semilog analysis could not give valid information about the reservoir heterogeneity.

3.12.1 During injection period

The derivative of equation (3a.8) and (3a.9) with respect to the natural logarithm of the dimensionless time t_D yields,

$$\frac{dP_D}{dLnt_D} = \frac{F_m M}{2} \quad (3a.19)$$

And

$$\frac{dP_D}{dLnt_D} = \frac{1}{2} \quad (3a.20)$$

In real parameters, Equations (3a.19) and (3a.20) can be written as,

$$\frac{dP}{dLnt} = t \cdot \frac{dP}{dt} = \frac{70.6q_{inj} B_w \mu_w F_m M}{k_w h} \quad (3a.21)$$

And

$$\frac{dP}{dLnt} = t \cdot \frac{dP}{dt} = \frac{70.6q_{inj} B_w \mu_w}{k_w h} \quad (3a.22)$$

The above equations state that during the infinite acting radial flow periods, the slopes of the plot of $\frac{dp}{dLnt}$ versus t on log-log scale are constant and are equal to $\frac{70.6qB\mu_w F_m M}{k_w h}$ and $\frac{70.6qB\mu_w}{k_w h}$ respectively.

3.12.2 During fall-off period

Taking the derivative of Eq. (3a.14a) and (3a.15a) with respect to the natural logarithm of the dimensionless shut-in time Δt_D when $\Delta t_D \ll t_{iD}$ yield,

$$\frac{dP_D}{dLn(\Delta t_D)} = \frac{1}{2} \quad (3a.23)$$

And

$$\frac{dP_D}{dLn(\Delta t_D)} = \frac{F_m M}{2} \quad (3a.24)$$

In real parameters, Equations (3a.23) and (3a.24) become,

$$\frac{dP}{dLn(\Delta t)} = t. \frac{dP}{d(\Delta t)} = \frac{70.6q_{inj}B_w\mu_w}{k_w h} \quad (3a.25)$$

And

$$\frac{dP}{dLn(\Delta t)} = t. \frac{dP}{d(\Delta t)} = \frac{70.6q_{inj}B_w\mu_w F_m M}{k_w h} \quad (3a.26)$$

The infinite acting radial flow periods are characterized by constant slopes of $\frac{70.6qB\mu_w}{k_w h}$ and

$\frac{70.6qB\mu_w F_m M}{k_w h}$ on a log-log plot of $\frac{dp}{dLn(\Delta t)}$ versus Δt respectively.

3.13 Application of the Derivative Equations to Tiab's Direct Synthesis (TDS) Techniques

The dimensionless pressure p_{wD} , time t_D , and wellbore storage coefficient are expressed as follows:

$$p_D = \left(\frac{kh}{141.2qB\mu} \right) \Delta p \quad (3a.27)$$

$$t_D = \left(\frac{0.0002637k}{\phi\mu c_t r_w^2} \right) t \quad (3a.28)$$

$$c_D = \left(\frac{0.8935}{\phi c_t h r_w^2} \right) c \quad (3a.29)$$

During early time, the pressure curve is characterized by a unit slope line which corresponds to pure wellbore storage effects. This unit slope line is a unique feature of early time for injection and fall-off tests. During these periods, fluid is dumped into the wellbore. In case of constant wellbore storage, Van Everdingen and Agarwal et al studied this early period and developed equations governing the sand face flow rate.

Tiab stated that during pure wellbore storage period, the pressure in the wellbore is directly proportional to the time, i.e.

$$p_D = \frac{t_D}{c_D} \quad (3a.30)$$

The derivative of Eq. (3a.30) with respect to (t_D / c_D) is

$$\left(\frac{t_D}{c_D} \right) p'_D = \frac{t_D}{c_D} \quad (3a.31)$$

Combining Eq. (3a.28) and Eq. (3a.29) will give:

$$\frac{t_D}{c_D} = \frac{2.9513 \times 10^{-4} kh t}{\mu c} \quad (3a.32a)$$

For water zone:

$$\frac{t_D}{c_D} = \frac{2.9513 \times 10^{-4} k_w h t}{\mu_w c} \quad (3a.32b)$$

Substituting Eq. (4.40) and (4.45a) into Eq. (4.43) and solving for the wellbore storage coefficient, this will give

$$c = \frac{qB t}{24 \Delta p} \quad (3a.33)$$

The infinite acting radial flow portion of the pressure derivative is a horizontal line. The equation of this line for a homogeneous reservoir can be written as

$$(p_D)_r = \frac{1}{2} \left[\text{Ln} \left(\frac{t_D}{c_D} \right)_r + 0.80907 + \text{Ln}(c_D e^{2S}) \right] \quad (3a.34)$$

The derivative of Eq. (3a.34) with respect to (t_D / c_D) is given as follows

$$\left[\left(\frac{t_D}{c_D} \right) p_D' \right]_r = 0.5 \quad (3a.35)$$

Taking the derivative of Eq. (3a.27) with respect to (t_D / c_D) , and substituting Eq. (3a.32a), will yield

$$p_D' = \frac{\partial p_D}{\partial (t_D / c_D)} = \frac{kh}{141.2qB\mu} \frac{\partial \Delta p}{\partial (t_D / c_D)} = \frac{kh}{141.2qB\mu} \frac{\partial \Delta p}{\partial t} \frac{\partial t}{\partial (t_D / c_D)} = \frac{kh}{141.2qB\mu} \cdot \frac{c\mu}{2.95 \times 10^{-4} kh} \Delta p'$$

Or

$$p_D' = \frac{24c}{qB} \Delta p' \quad (3a.36)$$

Substituting Eq. (3a.32b) into Eq. (3a.36) gives:

$$\frac{t_D}{c_D} p_D' = \frac{k_w h}{141.2qB\mu_w} (t \Delta p') \quad (3a.37)$$

3.13.1 Pressure injection period

The wellbore storage coefficient that is given by Eq. (3a.33) can also be written as

$$c = \frac{q_{inj} B_w t}{24 \Delta p} \quad (3a.38)$$

Where t and Δp are obtained from the unit slope line of the pressure and pressure derivative curve.

3.13.1.1 First radial flow

From the pressure derivative curve during the first infinite acting radial flow period, the derivative of Equation (3a.9) yields:

$$(t.\Delta p')_{r1} = \frac{70.6qB\mu_w F_m M}{k_w h} \quad (3a.39)$$

Eq. (4.52) provides permeability corresponding to the water zone.

$$k_w = \frac{70.6qB\mu_w F_m}{(t.\Delta p')_{r1} h} \quad (3a.40)$$

Where $(t.\Delta p')_{r1}$ is the value of pressure derivative corresponding to the first infinite acting flow regime. The early-time unit slope line and the early-time infinite acting radial flow line of the pressure derivative intersect at

$$\left[\left(\frac{t_D}{c_D} \right) p_D' \right]_{i1} = 0.5 F_m M \quad (3a.41)$$

$$(p_D)_i = \left(\frac{t_D}{c_D} \right)_{i1} = 0.5 F_m M \quad (3a.42)$$

Where the subscript i stands for intersection; if the unit slope line is the same for pressure and pressure derivative curves at the intersection point, then, we have,

$$(\Delta p)_{i1} = (t\Delta p')_{i1} = (t.\Delta p')_{r1} \quad (3a.43)$$

In real units, the coordinates of this intersection point are,

$$(t.\Delta p')_{i1} = \frac{70.6qB\mu_w F_m M}{k_w h} \quad (3a.44)$$

And

$$t_{i1} = \frac{1695\mu_w c F_m M}{k_w h} \quad (3a.45)$$

Then we can determine from Eq. (3a.45) k_w and c as follows:

$$k_w = \frac{1695\mu_w c F_m}{t_{il} h} \quad (3a.46a)$$

$$c = \frac{k_o h t_{il}}{1695\mu_o F_m} \quad (3a.46b)$$

The coordinates of the 'peaks' for $c_D e^{2S} > 10^2$ were obtained from the second derivative and plotted on a Cartesian graph.

The equation of this line is given by Tiab for single phase production wells,

$$\left[\left(\frac{t_D}{c_D} \right) p_D' \right]_x = 0.36 \left(\frac{t_D}{c_D} \right)_x - 0.42 \quad (3a.47)$$

Combining Equations (3a.32b), (3a.37) and (3a.47), will yield

$$(t\Delta p')_x = \left(0.015 \frac{qB}{c} \right) t_x - \frac{59.30q\mu_w B}{k_w h} \quad (3a.48)$$

$(t\Delta p')_x$ and t_x are the coordinates of the maximum point (peak) of the pressure derivative curve. Combining equation (3a.39), (3a.45) and (3a.48) yield the mobility ratio M as,

$$M = \frac{0.84}{F_m \left(0.36 \frac{t_x}{t_{il}} - \frac{(t\Delta p')_x}{(t\Delta p')_{r1}} \right)} \quad (3a.49)$$

A log-log plot of $\log(c_D e^{2S})$ versus the coordinates of the peaks yielded the following,

$$\log(c_D e^{2S}) = 0.35 \left(\frac{t_D}{c_D} \right)_x^{1.24} \quad (3a.50)$$

$$\log(c_D e^{2S}) = 1.71 \left(\frac{t_D}{c_D} p_D' \right)_x^{1.10} \quad (3a.51)$$

Substituting the combination of Equations (3a.32a), (3a.37), (3a.39) and (3a.45) into Equations (3a.50) and (3a.51) gives:

$$\log(c_D e^{2S}) = 0.1482 \left(\frac{t_x F_m M}{t_{il}} \right)^{1.24} \quad (3a.52)$$

and

$$\log(c_D e^{2S}) = 0.80 \left(\frac{(t \cdot \Delta p')_x F_m M}{(t \cdot \Delta p')_{r1}} \right)^{1.10} \quad (3a.53)$$

Substituting Eq. (3a.29) i.e. C_d into Equations (3a.52) and (3a.53) and then solve for the skin factor, gives respectively,

$$S = 0.1707 \left(\frac{t_x F_m M}{t_{i1}} \right)^{1.24} - 0.5 \text{Ln} \left(\frac{0.8935c}{\phi h c_{i1} r_w^2} \right) \quad (3a.54)$$

And

$$S = 0.9212 \left(\frac{(t \cdot \Delta p')_x F_m M}{(t \cdot \Delta p')_{i1}} \right)^{1.1} - 0.5 \text{Ln} \left(\frac{0.8935c}{\phi h c_{i1} r_w^2} \right) \quad (3a.55)$$

3.13.1.2 Second radial flow

The equation of the second infinite acting radial flow line can be written as,

$$\left[\left(\frac{t_D}{c_D} \right) p_D \right]_{r2} = \frac{1}{2} \quad (3a.56)$$

Combining Equations (3a.56) and (3a.25) and solving for the effective water permeability results into

$$k_o = \frac{70.6 q_{inj} B_o \mu_o M}{h (t \cdot \Delta p')_{r2}} \quad (3a.57)$$

The early time the unit slope line and the later time infinite acting line of the pressure derivative intersect at,

$$\left[\left(\frac{t_D}{c_D} \right) p_D \right]_{i2} = \frac{1}{2} \quad (3a.58)$$

And

$$p_{Di2} = \left(\frac{t_D}{c_D} \right)_{i2} = \frac{1}{2} \quad (3a.59)$$

In real units, Eq. (3a.58) and (3a.59) will give

$$k_o = \frac{70.6 q B \mu_o}{(t \cdot \Delta p')_{i2} h} \quad (3a.60)$$

$$t_{i2} = \frac{1695\mu_o c}{k_o h} \quad (3a.61)$$

Eq. (3a.61) can be used to determine k_o or c .

Another expression is derived for the mobility ratio, M , by dividing Eq. (3a.48) with Eq. (3a.39) and combining with Eq. (3a.61) to yields:

$$M = \frac{1}{F_m} \frac{(t.\Delta p')_{r1}}{(t.\Delta p')_x} \left(0.36 \frac{t_x}{t_{i2}} - 0.84 \right) \quad (3a.62)$$

The later infinite acting radial flow line equation can be written as,

$$p_{Dr2} = 0.5 \left[\frac{1}{F_m} \text{Ln} \frac{\alpha t_{r2}}{r_w^2} + F_m M \left(\text{Ln} \frac{5.9 \times 10^{-4} k_o}{\phi \mu_o c_{i2} \alpha} \right) + 2S \right] \quad (3a.63)$$

By dividing Eq. (4.44) with Eq. (4.37), using the real units and solving for skin factor, gives

$$S = 0.5 \left[\frac{\Delta p_{r2}}{(t.\Delta p')_{r2}} - F_m M \text{Ln} \frac{k_o}{\phi \mu_o c_{i2} \alpha} + 7.43 F_m M - \frac{1}{F_m} \text{Ln} \frac{\alpha t_{r2}}{r_w^2} \right] \quad (3a.64)$$

Where t_{r2} is any convenient time during the second infinite acting radial flow period and (Δp_{r2}) is the corresponding pressure value.

When t is expressed in hours, α can be written as $\alpha = \frac{5.615 q_{inj} B_w}{24 \pi h \phi \Delta s_w}$

3.13.2 During fall-off period

During the pressure fall-off response, the pressure wave passes through the water invaded zone. Thus, pressure response during this flow regime is representative of the invaded zone properties.

3.13.2.1 During first radial flow

Equation of this flow period is given as:

$$\left[\left(\frac{t_D}{c_D} \right) p_D' \right]_{r1} = 0.5 \quad (3a.65a)$$

Expressing Eq. (3a.65a) in oilfield variables and solving for permeability at 100% water saturation during first radial flow will give

$$k_w = \frac{70.6 q_{inj} B_w \mu_w F_m}{h(t.\Delta p')_{r1}} \quad (3a.65b)$$

However, the wellbore storage coefficient is given by Eq. (3a.38). Where t is any shut-in time on the unit slope line and Δp is the corresponding pressure value. The equation of the first infinite acting radial flow line of the pressure derivative during this period is given by Eq.(3a.56) and the effective water permeability is given by Eq.(3a.57), where the pressure derivative corresponds to the first fall-off infinite acting radial flow.

If we divide equation (3a.48) by equation (3a.39), we obtain,

$$\frac{(t.\Delta p')_x}{(t.\Delta p')_{r1}} = \left[2.1246 \times 10^{-4} \left(\frac{k_w h}{\mu_w F_m M} \right) \frac{\Delta t_x}{c} - \frac{0.84}{F_m M} \right] \quad (3a.66)$$

The above equation is used to calculate k_w or c . The skin can also be given as

$$S = 0.1707 \left(\frac{t_x F_m M}{t_{il}} \right)^{1.24} - 0.5 \text{Ln} \left(\frac{0.8935c}{\phi h c_{t1} r_w^2} \right) \quad (3a.67)$$

And

$$S = 0.9212 \left(\frac{(t.\Delta p')_x F_m M}{(t.\Delta p')_{r1}} \right)^{1.1} - 0.5 \text{Ln} \left(\frac{0.8935c}{\phi h c_{t1} r_w^2} \right) \quad (3a.68)$$

3.13.2.2 During second radial flow

At later time during pressure fall-off, the pressure wave is dominated by the uninvaded (Oil) zone properties. The representative equation of this time period in oil field units is

$$P_i - P_{ws} = \frac{162.6qB_w \mu_o}{k_o h} \log \left(\frac{t + \Delta t}{\Delta t} \right) \quad (3a.69a)$$

The derivative of the above equation is

$$\frac{d\Delta P}{dt} \times t = \frac{d\Delta P}{d(\ln t)} = \frac{70.6qB_w \mu_o}{k_o h} \quad (3a.69b)$$

For the second infinite acting radial flow, the effective oil permeability is then calculated using Eq. (3a.69b)

$$k_o = \frac{70.6qB_w \mu_o}{(t.\Delta p')_{rf2} h} \quad (3a.69c)$$

Where pressure derivative $(t.\Delta p')_{rf2}$ refers to second radial (Infinite acting) of the fall-off period. Wellbore storage co-efficient is estimated from the intersection point of the second infinite acting radial line with the early time unit slope line.

$$t_{i,2rf} = \frac{1695\mu_o C}{k_o h} \quad (3a.70a)$$

$$k_o = \frac{1695\mu_o C}{t_{i,2fo} h} \quad (3a.70b)$$

Thus k_o or C can be estimated using above Eq. (3a.70b)

An expression for the mobility ratio M can be derived using Eq. (3a.46b) and Eq. (3a.66) for fall-off, to obtain:

$$M = 5.55 \frac{\Delta t_{i2}}{\Delta t_x} \left[0.5 \frac{(t.\Delta p')_x}{(t.\Delta p')_{rf1}} + \frac{0.42}{F_m} \right] \quad (3a.71)$$

M can also be obtained by substituting Eq. (3a.46b) and Eq. (3a.39) into Eq. (3a.71)

$$M = 133.4 \frac{c}{qB} \frac{(t.\Delta p')_{rf2}}{\Delta t_x} \left[0.5 \frac{(t.\Delta p')_x}{(t.\Delta p')_{rf1}} + \frac{0.42}{F_m} \right] \quad (3a.72)$$

Eq. (3a.49) can also be used to compute, M , which can be given as

$$M = \frac{0.84}{F_m \left(0.36 \frac{\Delta t_x}{\Delta t_{if2}} - \frac{(t.\Delta p')_x}{(t.\Delta p')_{rf2}} \right)} \quad (3a.73)$$

The skin factor S can also be computed using Equations (3a.67) and (3a.68), where t_{i1} for injection is replaced by Δt_{i2} for fall-off as

$$S = 0.1707 \left(\frac{t_x F_m M}{t_{i2fo}} \right)^{1.24} - 0.5 \text{Ln} \left(\frac{0.8935c}{\phi h c_{t1} r_w^2} \right) \quad (3a.74)$$

And

$$S = 0.9212 \left(\frac{(t.\Delta p')_x F_m M}{(t.\Delta p')_{r2fo}} \right)^{1.1} - 0.5 \text{Ln} \left(\frac{0.8935c}{\phi h c_{t1} r_w^2} \right) \quad (3a.75)$$

3.14 Summary of Equations

Pressure Injection (1st Radial Flow)

| Eq. No. | Parameter | Equation |
|---------|-----------|---|
| 3a.39 | k_w | $k_w = \frac{70.6qB\mu_w F_m M}{(t.\Delta p')_{r1} h}$ |
| 3a.44 | k_w | $k_w = \frac{70.6qB\mu_w F_m M}{(t.\Delta p')_{i1} h}$ |
| 3a.45 | k_w | $k_w = \frac{1695\mu_w c F_m M}{t_{i1} h}$ |
| 3a.54 | S | $S = 0.1707 \left(\frac{t_x F_m M}{t_{i1}} \right)^{1.24} - 0.5 \text{Ln} \left(\frac{0.8935c}{\phi h c_{t1} r_w^2} \right)$ |
| 3a.55 | S | $S = 0.9212 \left(\frac{(t.\Delta p')_x F_m M}{(t.\Delta p')_{i1}} \right)^{1.1} - 0.5 \text{Ln} \left(\frac{0.8935c}{\phi h c_{t1} r_w^2} \right)$ |

Pressure Injection (2nd Radial Flow)

| | | |
|-------|-------|---|
| 3a.57 | K_o | $k_o = \frac{70.6q_{inj} B_o \mu_o M}{h(t.\Delta p')_{r2}}$ |
| 3a.61 | K_o | $k_o = \frac{1695\mu_o c}{t_{i2} h}$ |
| 3a.62 | M | $M = \frac{1}{F_m} \frac{(t.\Delta p')_{r1}}{(t.\Delta p')_x} \left(0.36 \frac{t_x}{t_{i2}} - 0.84 \right)$ |
| 3a.64 | S | $S = 0.5 \left[\frac{\Delta p_{r2}}{(t.\Delta p')_{r2}} - F_m M \text{Ln} \frac{k_o}{\phi \mu_o c_{t2} \alpha} + 7.43 F_m M - \frac{1}{F_m} \text{Ln} \frac{\alpha t_{r2}}{r_w^2} \right]$ |

Pressure Fall-off (First Radial)

| | | |
|--------|-------|---|
| 3a.65b | k_w | $k_w = \frac{70.6q_{inj}B_w\mu_wF_m}{h(t.\Delta p')_{r1}}$ |
| 3a.67 | S | $S = 0.1707 \left(\frac{t_x F_m M}{t_{i1}} \right)^{1.24} - 0.5Ln \left(\frac{0.8935c}{\phi h c_{i1} r_w^2} \right)$ |
| 3a.68 | S | $S = 0.9212 \left(\frac{(t.\Delta p')_x F_m M}{(t.\Delta p')_{i1}} \right)^{1.1} - 0.5Ln \left(\frac{0.8935c}{\phi h c_{i1} r_w^2} \right)$ |

Pressure Fall-off (Second Radial)

| | | |
|-------|-------|---|
| 3a.45 | k_o | $k_o = \frac{70.6q_{inj}B_o\mu_o}{h(t.\Delta p')_{r2}}$ |
| 3a.71 | M | $M = 5.55 \frac{\Delta t_{i2}}{\Delta t_x} \left[0.5 \frac{(t.\Delta p')_x}{(t.\Delta p')_{rf1}} + \frac{0.42}{F_m} \right]$ |
| 3a.72 | M | $M = 133.4 \frac{c}{qB} \frac{(t.\Delta p')_{rf2}}{\Delta t_x} \left[0.5 \frac{(t.\Delta p')_x}{(t.\Delta p')_{rf1}} + \frac{0.42}{F_m} \right]$ |
| 3a.73 | M | $M = \frac{0.84}{F_m \left(0.36 \frac{\Delta t_x}{\Delta t_{if2}} - \frac{(t.\Delta p')_x}{(t.\Delta p')_{rf2}} \right)}$ |
| 3a.74 | S | $S = 0.1707 \left(\frac{t_x F_m M}{t_{i2fo}} \right)^{1.24} - 0.5Ln \left(\frac{0.8935c}{\phi h c_{i1} r_w^2} \right)$ |
| 3a.75 | S | $S = S = 0.9212 \left(\frac{(t.\Delta p')_x F_m M}{(t.\Delta p')_{r2fo}} \right)^{1.1} - 0.5Ln \left(\frac{0.8935c}{\phi h c_{i1} r_w^2} \right)$ |

CHAPTER 4

RESULTS AND DISCUSSIONS

4.0 Simulated Pressure Injection Tests

4.1 System Description

Real pressure injection test data with wellbore storage and skin are almost non-existent. Tiab and Abdesselam, (2001), used a numerical model to simulate pressure injection tests so as to compare with the analytical solutions. A commercial reservoir simulator 'Model Black Oil' is used and a regular Cartesian grid system of 41 grid blocks is selected to run these tests.

The data used are from Tamadanet fields and Hassi Messaoud 'Zone II'. The viscosity and compressibility of oil and water is assumed to be constant and independent of pressure. The relative permeability curves for both cases are shown in Figure 4.1 and 4.5. The temperature- and saturation-dependent total mobility F_M can be calculated using the following equation,

$$F_m(S_w, T) = M_t 10^A = \frac{10^{\left(-1.6173 + \frac{247.8}{T_{inj} - 140}\right) \left(\frac{K_{ro}}{\mu_o} + \frac{K_{rw}}{\mu_w}\right) \bar{s}_w}{K_{rw(1-s_{or})}} \quad (4.1)$$

The mobility ratio M is defined by

$$M = \frac{(k_w / \mu_w)_{\bar{s}_w}}{(k_o / \mu_o)_{s_{wi}}} = \frac{\lambda_w}{\lambda_o} \quad (4.2)$$

Where $(k_o / \mu_o)_{s_{wi}}$ is the oil mobility at the initial water saturation condition and $(k_w / \mu_w)_{\bar{s}_w}$ is the water mobility at the average water saturation behind the flood front. \bar{s}_w is obtained from the fractional-flow curves (Figs 5.2 and 5.6). In absence of gravity and capillary pressure, the fractional-flow relationship is given by:

$$f_w = \frac{1}{1 + \frac{k_{ro} \mu_w}{k_{rw} \mu_o}} \quad (4.3)$$

The data generated by the simulator are analyzed using semilog analysis and TDS (isothermal and non-isothermal) techniques.

4.2 Simulated Injection Test (Case-1)

Table 4.1 gives the reservoir, well, and fluid data (Tamadanet field). Figures 4.3 and 4.4 present the semilog and pressure derivative plots of the injection simulated data respectively. From the first semilog straight line,

we can calculate the mobility of water in the flooded zone using $\lambda_w = \frac{162.6q_w B_w}{m_w h}$ and the mobility in the oil zone using the second semilog straight line- $\lambda_o = \frac{162.6q_w B_o}{m_o h}$. These two straight lines are characterized by the two horizontal lines on the derivative plot.

Table 4. 1: Rock and Fluid properties and Well Conditions for Simulated test, Case-1

(Sources: Tiab and Abdesselam, 2001)

| | |
|------------------------------------|--|
| Initial Reservoir Pressure, p_i | 3298.895 psi |
| Initial Water Saturation, S_{wi} | 0.15 |
| Reservoir Thickness, h | 49.2 ft |
| Porosity, ϕ | 0.16 |
| Absolute Permeability, k | 50 md |
| Oil Compressibility, c_o | $3.23 \times 10^{-5} \text{ psi}^{-1}$ |
| Water Compressibility, c_w | $3.2 \times 10^{-6} \text{ psi}^{-1}$ |
| Rock Compressibility, c_r | $3.51 \times 10^{-6} \text{ psi}^{-1}$ |
| Oil Viscosity, μ_o | 0.35 cp |
| Water Viscosity, μ_w | 0.31 cp |
| Wellbore Radius, r_w | 0.29 ft |
| Water FVF, B_w | 1.033 bbl/stb |
| Residual Oil Saturation, S_{or} | 0.25 |
| Injection Temperature, T_{inj} | 289K (60.8F) |
| Injection Rate, q_w | 943.35 bbl/day |
| Oil FVF, B_o | 1.25 bbl/stb |

4.2.1. Conventional Semilog Analysis

From the first semilog straight line, we can determine the permeability and mobility in the water zone

$$K_w = \frac{162.6q_w B_w \mu_w}{m_w h} = \frac{162.6 \times 943.35 \times 1.033 \times 0.31}{124.96 \times 49.2} = 8 \text{ md}$$

$$\lambda_w = \frac{162.6q_w B_w}{m_w h} = \frac{162.6 \times 943.35 \times 1.033}{124.96 \times 49.2} = 25.77 \text{ md / cp}$$

From the second semilog straight line we determine the permeability and mobility in the oil zone:

$$K_o = \frac{162.6q_w B_o \mu_o}{m_o h} = \frac{162.6 \times 943.35 \times 1.25 \times 0.35}{91 \times 49.2} = 14.99 \text{ md}$$

$$\lambda_o = \frac{162.6q_w B_o}{m_o h} = \frac{162.6 \times 943.35 \times 1.25}{91 \times 49.2} = 42.83 \text{ md / cp}$$

The mobility ratio is

$$M = \frac{\lambda_w}{\lambda_o} = \frac{25.77}{42.83} = 0.6$$

$$C_{tw} = (1 - S_{or})C_w + S_{or}C_o + C_f = (1 - 0.25) \times 3.2 \times 10^{-6} + 0.25 \times 3.23 \times 10^{-5} + 3.51 \times 10^{-6} = 1.4 \times 10^{-5}$$

The mechanical skin factor is calculated using Eq.3.30a,

$$S = 1.1513 \left[\frac{\Delta p_{1hr}}{m_w} - \log \frac{\lambda_w}{\phi C_{tw} r_w^2} + 3.23 \right] = 1.1513 \left[\frac{162.5}{124.96} - \log \left(\frac{25.77}{0.16 \times 1.4 \times 10^{-5} \times 0.29^2} \right) + 3.23 \right] = -4.15$$

4.2.2 Tiab's Direct Synthesis Techniques: Isothermal Condition

From the pressure and pressure derivative plots, we read the different characteristic points and are given by,

$$(t.dp')_{rw} = 70 \text{ psi}$$

$$(t.dp')_{ro} = 40 \text{ psi}$$

$$t_{ro} = 244.7 \text{ hrs}$$

$$\Delta p_{ro} = 565 \text{ psi}$$

The permeability and mobility of the water zone is given by:

$$K_w = \frac{70.6q_w B_w \mu_w}{(t.dp')_{rw} h} = \frac{70.6 \times 943.35 \times 1.033 \times 0.31}{70 \times 49.2} = 6.2 \text{ md}$$

$$\lambda_w = \frac{70.6q_w B_w}{(t.dp')_{rw} h} = \frac{70.6 \times 943.35 \times 1.033}{70 \times 49.2} = 20 \text{ md / cp}$$

The permeability and mobility of the oil is given by,

$$K_o = \frac{70.6q_w B_o \mu_o}{(t.dp')_{ro} h} = \frac{70.6 \times 943.35 \times 1.25 \times 0.35}{40 \times 49.2} = 14.81 \text{ md}$$

$$\lambda_o = \frac{70.6q_w B_o}{(t.dp')_{ro} h} = \frac{70.6 \times 943.35 \times 1.25}{40 \times 49.2} = 42.3 \text{ md / cp}$$

The mobility can be estimated as

$$M = \frac{\lambda_w}{\lambda_o} = \frac{20}{42.3} = 0.47$$

The skin factor is obtained using Eq.3.77a:

$$S = 0.5 \left[\frac{\Delta p_{rw}}{(t.\Delta p')_{rw}} - Ln \frac{\lambda_w t_{rw}}{\phi c_{rw} r_w^2} + 7.43 \right] = 0.5 \left[\frac{320}{70} - Ln \left(\frac{20 \times 4.8}{0.16 \times 1.40 \times 10^{-5} \times 0.29^2} \right) + 7.43 \right] = -4.02$$

4.2.3 Tiab's Direct Synthesis Techniques: Non-Isothermal Condition

From the pressure and pressure derivative plots, we read the different characteristic points and are given by,

$$(t.dp')_{rw} = 70 \text{ psi}, \quad T_{inj} = 289 \text{ K}, \quad t_{ro} = 244.7 \text{ hrs}$$

$$(t.dp')_{ro} = 40 \text{ psi}, \quad \Delta p_{ro} = 565 \text{ psi}$$

The temperature- and saturation-dependent total mobility, F_M is calculated as

$$F_m(S_w, T) = M_t 10^A = \frac{10^{\left(-1.6173 + \frac{247.8}{T_{inj} - 140} \right)} \left(\frac{K_{ro}}{\mu_o} + \frac{K_{rw}}{\mu_w} \right)_{S_w}}{K_{rw(1-s_{or})}} = \frac{10^{\left(-1.6173 + \frac{247.8}{289 - 140} \right)} \left(\frac{0.10}{0.35} + \frac{0.14}{0.31} \right)}{0.63} = 1.30$$

The permeability and mobility of water zone is given by,

$$K_w = \frac{70.6q_w B_w \mu_w F_m}{(t.dp')_{rw} h} = \frac{70.6 \times 943.35 \times 1.033 \times 0.31 \times 1.30}{70 \times 49.2} = 8.05 \text{ md}$$

$$\lambda_w = \frac{70.6q_w B_w F_m}{(t.dp')_{rw} h} = \frac{70.6 \times 943.35 \times 1.033 \times 1.3}{70 \times 49.2} = 25.97 \text{ md / cp}$$

The permeability and mobility of the oil is given by,

$$K_o = \frac{70.6q_w B_o \mu_o}{(t.dp')_{ro} h} = \frac{70.6 \times 943.35 \times 1.25 \times 0.35}{40 \times 49.2} = 14.81 \text{ md}$$

$$\lambda_o = \frac{70.6q_w B_o}{(t.dp')_{ro} h} = \frac{70.6 \times 943.35 \times 1.25}{40 \times 49.2} = 42.3 \text{ md / cp}$$

The mobility can be estimated as

$$M = \frac{\lambda_w}{\lambda_o} = \frac{25.97}{42.3} = 0.61$$

The skin factor is obtained using Eq.3.77a:

$$S = 0.5 \left[\frac{\Delta p_{rw}}{(t.\Delta p')_{rw}} - \text{Ln} \frac{\lambda_w t_{rw}}{\phi c_{tw} r_w^2} + 7.43 \right] = 0.5 \left[\frac{320}{70} - \text{Ln} \left(\frac{25.97 \times 4.8}{0.16 \times 1.40 \times 10^{-5} \times 0.29^2} \right) + 7.43 \right] = -4.15$$

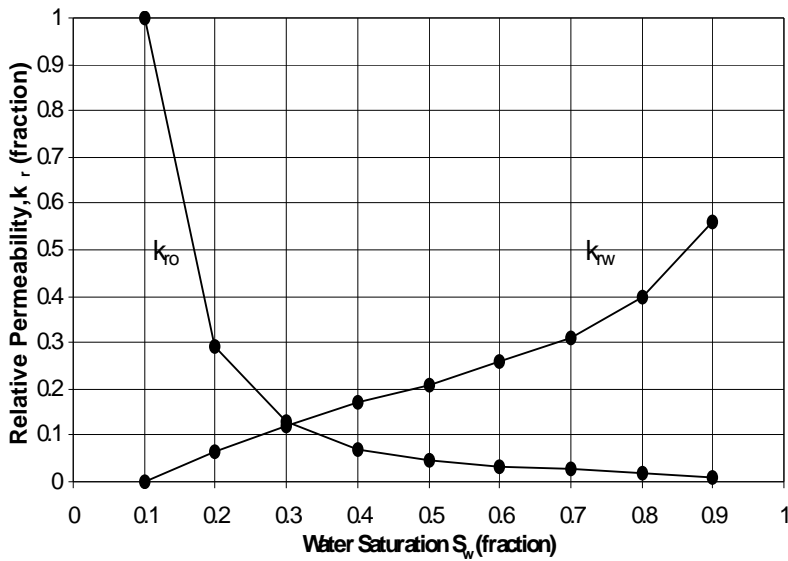


Figure 4.1: Relative Permeability Curves (Case 1)

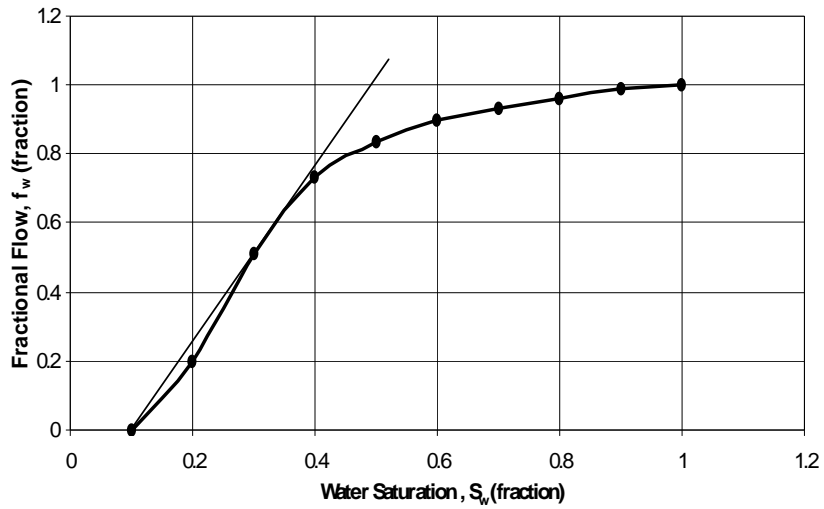


Figure 4.2: Fractional Flow Curve (Case 1)

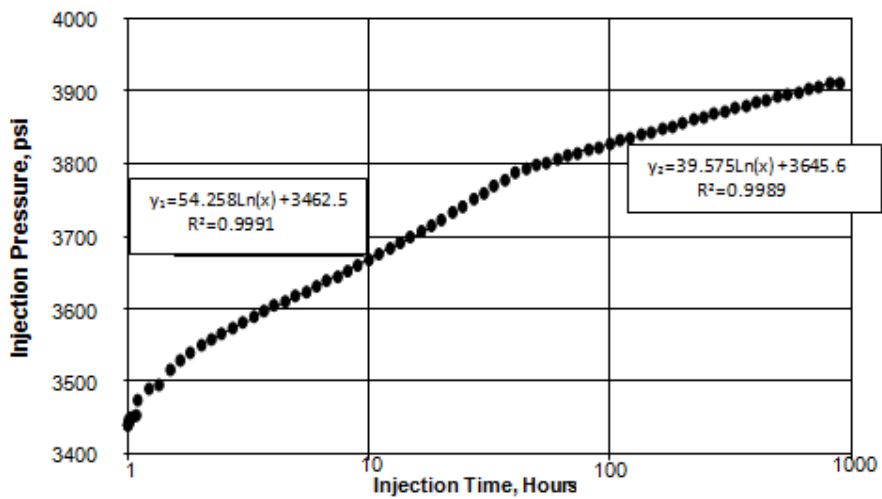
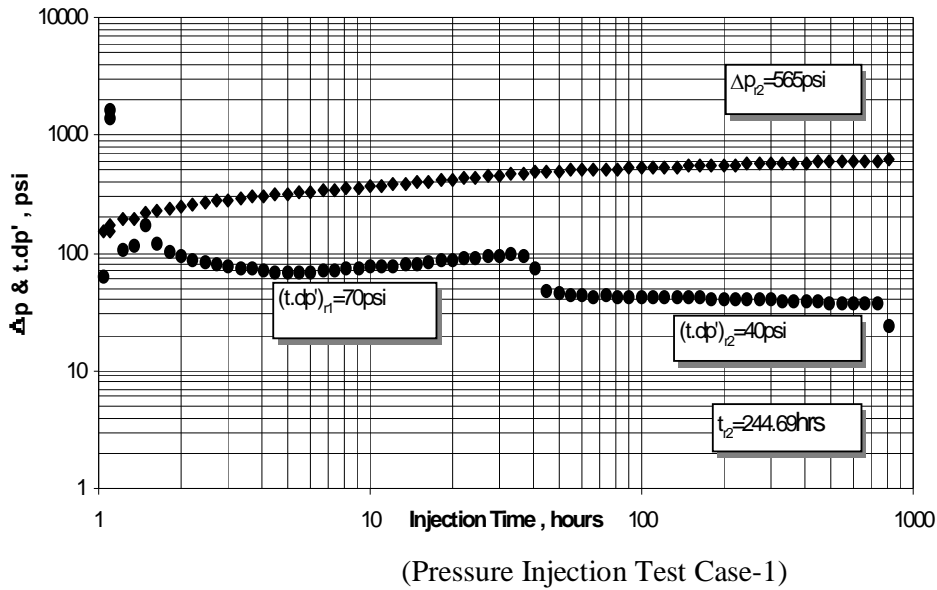


Figure 4. 1: Semilog Plot of Pressure vs. Time (Pressure Injection Test Case-1)

Figure 4.2: Log-log Plots of Simulated Pressure and Pressure Derivative Data



4.3 Simulated Pressure Injection Test (Case-2)

Table 4.2 gives the reservoir and fluid data used in the numerical reservoir simulator (Hassi Messaoud field). Figs.4.7 and 4.8 present the semilog and pressure and pressure derivative plots of the injection simulated data respectively.

Table 4.2: Rock and Fluid properties and Well Conditions for Simulated test, Case-2

(Sources: Tiab and Abdesselam, 2001)

| | |
|------------------------------------|--|
| Initial Reservoir Pressure, p_i | 2133 psi |
| Initial Water Saturation, S_{wi} | 0.15 |
| Reservoir Thickness, h | 49.2 ft |
| Porosity, ϕ | 0.05 |
| Absolute Permeability, k | 4.64 md |
| Oil Compressibility, c_o | $3.16 \times 10^{-5} \text{ psi}^{-1}$ |
| Water Compressibility, c_w | $2.49 \times 10^{-6} \text{ psi}^{-1}$ |
| Rock Compressibility, c_r | $2.8 \times 10^{-6} \text{ psi}^{-1}$ |

| | |
|-----------------------------------|---------------|
| Oil Viscosity, μ_o | 0.5 cp |
| Water Viscosity, μ_w | 0.35 cp |
| Wellbore Radius, r_w | 0.25 ft |
| FVF (B_w) | 1.001 bbl/stb |
| Residual Oil Saturation, S_{or} | 0.34 |
| FVF(Bo) | 1.2 bbl/stb |
| Injection Temperature, T_{inj} | 293K (68F) |
| Injection Rate, q_w | 283 bbl/day |

4.3.1 Conventional Semilog Analysis

From the first semilog straight line, we compute the permeability and mobility of the water zone as

$$K_w = \frac{162.6q_w B_w \mu_w}{m_w h} = \frac{162.6 \times 283 \times 1.001 \times 0.35}{153.12 \times 49.2} = 2.14 \text{ md}$$

$$\lambda_w = \frac{162.6q_w B_w}{m_w h} = \frac{162.6 \times 283 \times 1.001}{153.12 \times 49.2} = 6.1 \text{ md / cp}$$

From the second semilog straight line, we determine the permeability and mobility in the oil zone as

$$K_o = \frac{162.6q_w B_o \mu_o}{m_o h} = \frac{162.6 \times 283 \times 1.2 \times 0.5}{87.78 \times 49.2} = 6.69 \text{ md}$$

$$\lambda_o = \frac{162.6q_w B_o}{m_o h} = \frac{162.6 \times 283 \times 1.2}{87.78 \times 49.2} = 12.79 \text{ md / cp}$$

The mobility ratio is

$$M = \frac{\lambda_w}{\lambda_o} = \frac{6.1}{12.79} = 0.477$$

$$C_{tw} = (1 - s_{or})C_w + S_{or}C_o + C_f = (1 - 0.34) \times 2.49 \times 10^{-6} + 0.34 \times 3.16 \times 10^{-5} + 2.8 \times 10^{-6} = 1.519 \times 10^{-5}$$

The mechanical skin factor is calculated using Eq.3.30:

$$S = 1.1513 \left[\frac{\Delta p_{1hr}}{m_w} - \log \frac{\lambda_w}{\phi c_{tw} r_w^2} + 3.23 \right] = 1.1513 \left[\frac{121.98}{153.12} - \log \left(\frac{6.1}{0.05 \times 1.519 \times 10^{-5} \times 0.25^2} \right) + 3.23 \right] = -4.7$$

4.3.2 Tiab's Direct Synthesis Techniques: Isothermal Condition

From the pressure and pressure derivative plots, we read the different characteristic points and are given by:

$$\begin{aligned} (t.dp')_{rw} &= 248 \text{ psi} \\ (t.dp')_{ro} &= 37.82 \text{ psi} \\ t_{ro} &= 153.6 \text{ hrs} \\ \Delta p_{ro} &= 932.5 \text{ psi} \\ \Delta p_{rw} &= 500 \text{ psi} \end{aligned}$$

The permeability and mobility of the water zone is given by:

$$\begin{aligned} K_w &= \frac{70.6 q_w B_w \mu_w}{(t.dp')_{rw} h} = \frac{70.6 \times 283 \times 1.001 \times 0.35}{248 \times 49.2} = 0.57 \text{ md} \\ \lambda_w &= \frac{70.6 q_w B_w}{(t.dp')_{rw} h} = \frac{70.6 \times 283 \times 1.001}{248 \times 49.2} = 1.64 \text{ md / cp} \end{aligned}$$

The permeability and mobility of the oil is given by:

$$\begin{aligned} K_o &= \frac{70.6 q_w B_o \mu_o}{(t.dp')_{ro} h} = \frac{70.6 \times 283 \times 1.2 \times 0.5}{37.82 \times 49.2} = 6.44 \text{ md} \\ \lambda_o &= \frac{70.6 q_w B_o}{(t.dp')_{ro} h} = \frac{70.6 \times 283 \times 1.2}{37.82 \times 49.2} = 12.9 \text{ md / cp} \end{aligned}$$

The mobility can be estimated as:

$$M = \frac{\lambda_w}{\lambda_o} = \frac{1.64}{12.9} = 0.13$$

The skin factor is obtained using Eq.3.77a:

$$S = 0.5 \left[\frac{\Delta p_{rw}}{(t.\Delta p')_{rw}} - \text{Ln} \frac{\lambda_w t_{rw}}{\phi c_{tw} r_w^2} + 7.43 \right] = 0.5 \left[\frac{500}{248} - \text{Ln} \left(\frac{1.64 \times 1.2}{0.05 \times 1.519 \times 10^{-5} \times 0.25^2} \right) + 7.43 \right] = -4$$

4.3.3 Tiab's Direct Synthesis Techniques: Non-Isothermal Condition

From the pressure and pressure derivative plots, we read the different characteristic points and are given by:

$$\begin{aligned}(t.dp')_{rw} &= 248 \text{ psi} \\ (t.dp')_{ro} &= 37.82 \text{ psi} \\ t_{ro} &= 153.6 \text{ hrs} \\ \Delta p_{ro} &= 932.5 \text{ psi} \\ \Delta p_{rw} &= 500 \text{ psi} \\ T_{inj} &= 293 \text{ K}\end{aligned}$$

The permeability and mobility of the water zone is given by:

$$F_m(S_w, T) = M_t 10^A = \frac{10^{\left(-1.6173 + \frac{247.8}{T_{inj} - 140}\right)} \left(\frac{K_{ro}}{\mu_o} + \frac{K_{rw}}{\mu_w} \right)_{S_w}}{K_{rw(1-s_{or})}} = \frac{10^{\left(-1.6173 + \frac{247.8}{293 - 140}\right)} \left(\frac{0.38}{0.5} + \frac{0.02}{0.35} \right)}{0.22} = 3.734$$

The permeability and mobility of water zone is given by:

$$\begin{aligned}K_w &= \frac{70.6 q_w B_w \mu_w F_m}{(t.dp')_{rw} h} = \frac{70.6 \times 283 \times 1.001 \times 0.35 \times 3.734}{248 \times 49.2} = 2.14 \text{ md} \\ \lambda_w &= \frac{70.6 q_w B_w F_m}{(t.dp')_{rw} h} = \frac{70.6 \times 283 \times 1.001 \times 3.734}{248 \times 49.2} = 6.12 \text{ md / cp}\end{aligned}$$

The permeability and mobility of the oil is given by:

$$\begin{aligned}K_o &= \frac{70.6 q_w B_o \mu_o}{(t.dp')_{ro} h} = \frac{70.6 \times 283 \times 1.2 \times 0.5}{37.82 \times 49.2} = 6.44 \text{ md} \\ \lambda_o &= \frac{70.6 q_w B_o}{(t.dp')_{ro} h} = \frac{70.6 \times 283 \times 1.2}{37.82 \times 49.2} = 12.9 \text{ md / cp}\end{aligned}$$

The mobility can be estimated as:

$$M = \frac{\lambda_w}{\lambda_o} = \frac{6.12}{12.9} = 0.474$$

The skin factor is obtained using Eq.3.77a:

$$S = 0.5 \left[\frac{\Delta p_{rw}}{(t.\Delta p')_{rw}} - Ln \frac{\lambda_w t_{rw}}{\phi c_{tw} r_w^2} + 7.43 \right] = 0.5 \left[\frac{500}{248} - Ln \left(\frac{6.12 \times 1.2}{0.05 \times 1.519 \times 10^{-5} \times 0.25^2} \right) + 7.43 \right] = -4.7$$

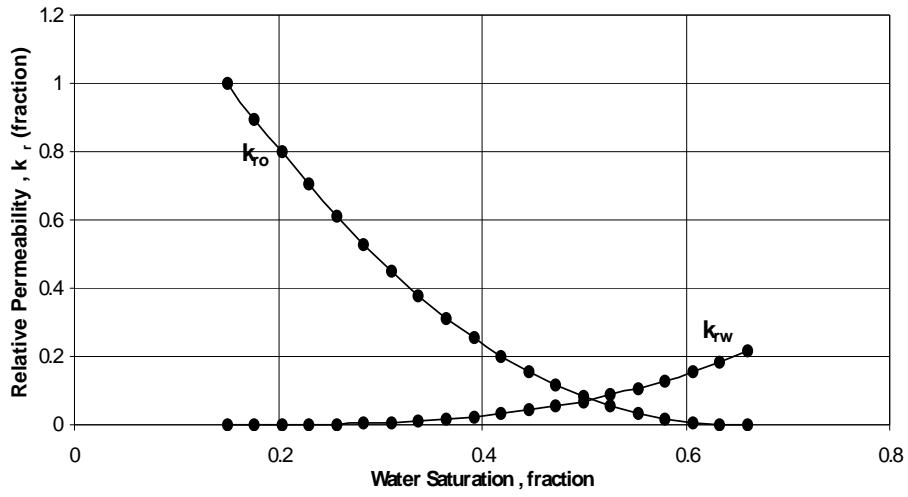


Figure 4. 3: Relative Permeability Curves (Case-2)

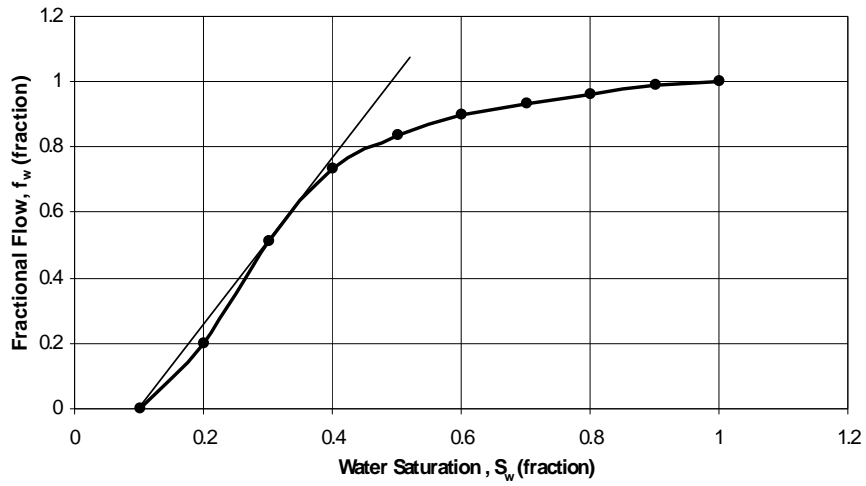


Figure 4.6: Fractional-Flow Curve (Case 2)

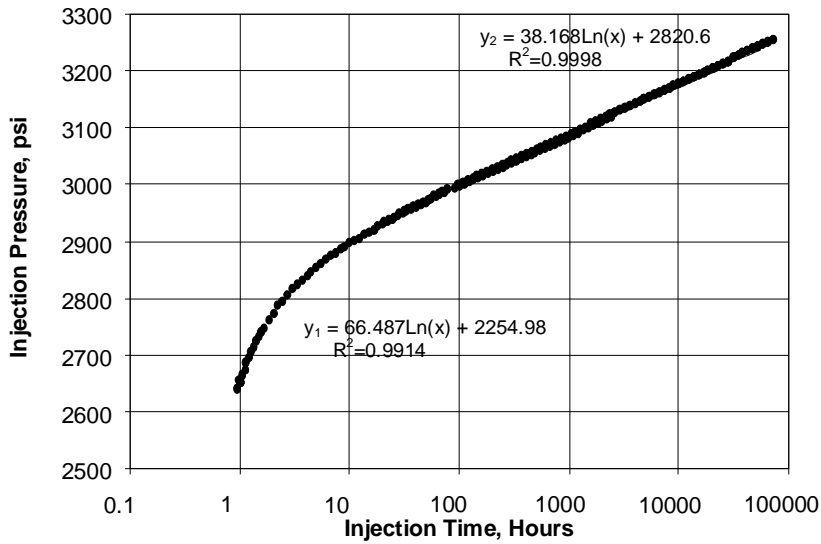


Figure 4.7: Semilog Plot of Simulated Pressure Injection Test Data (Case 2)

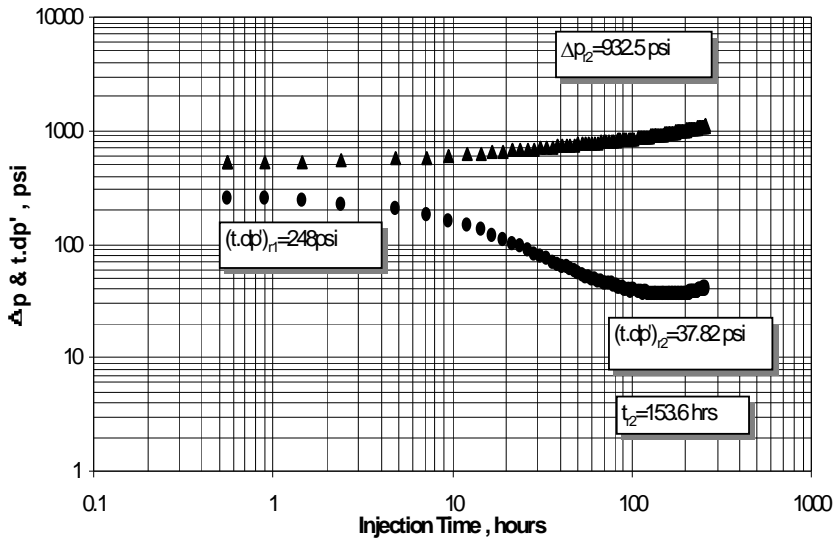


Figure 4. 4: Log-log Plots of Simulated Pressure Injection Test Data (Case-2)

4.4 Numerical Examples of Pressure Fall-off Tests in Water Injection Wells

4.4.1 Conventional method (Field Case-1)

The shut-in bottom-hole pressure as a function of time and the pressure derivative calculation are presented in Table 5.4. Other pertinent reservoir and fluid data are given below.

Table 4.3: Reservoir Rock, Fluid, and Well Data (Pressure Fall-off Test) (Example-1)

(Sources: Tiab and Abdesselam, 2001)

| | |
|--|--|
| Reservoir Thickness, h | 37.73 ft |
| Porosity, ϕ | 0.22 |
| Total Injection Time, t_{inj} | 230 hrs |
| Water FVF, B_w | 1 RB/STB |
| Total System Compressibility, C_{ti} | $5.44 \times 10^{-6} \text{ psi}^{-1}$ |
| Oil Viscosity, μ_o | 3.56 cp |
| Water Viscosity, μ_w | 1 cp |
| Wellbore Radius, r_w | 0.328 ft |
| Oil FVF (B_o) | 1.17 RB,STB |
| Saturation, ΔS_w | 0.24 |
| Injection temperature, T_{inj} | 303K (86F) |
| Injection Rate, q_w | 490.6 bbl/day |

Figure 4.9 shows the semilog plot of pressure data as function of time. The log-log plot of pressure and pressure derivative data Vs. Horner time is shown in Figure 4.10. From the two plots, it is clear that wellbore storage effects dominate early time data. Two straight lines on the semilog plot represent the infinite acting radial flow in the water and oil zones. These two periods are shown on the derivative plot as two horizontal lines.

Using the first semilog straight line, we determine the water zone permeability and mobility as follows,

$$K_w = \frac{162.6q_w B_w \mu_w}{m_w h} = \frac{162.6 \times 490.6 \times 1 \times 1}{163 \times 37.73} = 12.97 \text{ md}$$

$$\lambda_w = \frac{K_w}{\mu_w} = \frac{162.6q_w B_w}{m_w h} = \frac{162.6 \times 490.6 \times 1}{163 \times 37.73} = 12.97 \text{ md / cp}$$

The permeability and mobility of the oil zone is determined using the second semilog straight line as follows:

$$K_o = \frac{162.6q_w B_o \mu_o}{m_o h} = \frac{162.6 \times 490.6 \times 1.17 \times 3.56}{320.67 \times 37.73} = 27.47 \text{ md}$$

$$\lambda_o = \frac{K_o}{\mu_o} = \frac{162.6q_w B_o}{m_o h} = \frac{162.6 \times 490.6 \times 1.17}{320.6 \times 37.73} = 7.72 \text{ md / cp}$$

The skin factor is estimated using the first semilog straight line

$$S = 1.1513 \left[\frac{\Delta p_{1hr}}{m_w} - \log \frac{\lambda_w}{\phi c_{tw} r_w^2} + 3.23 \right]$$

$$S = 1.1513 \left[\frac{438.2}{163} - \log \left(\frac{12.97}{0.22 \times 5.44 \times 10^{-6} \times 0.328^2} \right) + 3.23 \right] = -2.4$$

The position of the flood front is obtained using the material balance equation as,

$$r_f = \left[\frac{5.615q_w B_w t_{inj}}{\pi h \Delta S_w \phi} \right]^{1/2} = \left[\frac{5.615 \times 490.6 \times 1 \times 230}{\pi \times 37.73 \times 0.24 \times 0.22 \times 24} \right]^{1/2} = 64.95 \text{ ft}$$

Where $\Delta S_w = \bar{S}_w - S_{wi}$ and \bar{S}_w denote the average water saturation behind the front.

Table 4. 4: Pressure and Pressure Derivative Data (Example-1)

| $\Delta t, \text{hrs.}$ | $(ti+\Delta t/\Delta t)$ | p_{ws}, psi | dp', psi | t^*dp', psi |
|-------------------------|--------------------------|----------------------|-------------------|----------------------|
| 0 | | 2683.20 | | |
| 0.02174 | 10580.58 | 2626.78 | 56.42 | |
| 0.03043 | 7559.33 | 2608.65 | 74.55 | 60.66 |
| 0.03913 | 5878.84 | 2592.11 | 91.08 | 71.76 |
| 0.04348 | 5290.79 | 2584.28 | 98.92 | 76.55 |
| 0.06533 | 3521.59 | 2550.20 | 133.00 | 93.62 |
| 0.08696 | 2645.89 | 2521.92 | 161.28 | 105.96 |
| 0.13 | 1770.23 | 2477.10 | 206.10 | 118.23 |

| | | | | |
|--------|---------|---------|--------|--------|
| 0.174 | 1322.84 | 2443.02 | 240.18 | 121.53 |
| 0.217 | 1060.91 | 2416.18 | 267.01 | 123.76 |
| 0.304 | 757.58 | 2376.01 | 307.19 | 118.36 |
| 0.348 | 661.92 | 2360.49 | 322.71 | 115.28 |
| 0.391 | 589.24 | 2347.15 | 336.05 | 114.16 |
| 0.4345 | 530.34 | 2335.25 | 347.94 | 113.24 |
| 0.652 | 353.76 | 2292.47 | 390.73 | 106.38 |
| 0.869 | 265.67 | 2264.33 | 418.87 | 99.77 |
| 1.304 | 177.38 | 2227.34 | 455.85 | 92.61 |
| 1.739 | 133.26 | 2202.54 | 480.65 | 86.39 |
| 2.174 | 106.80 | 2184.12 | 499.07 | 83.98 |
| 3.043 | 76.58 | 2157.00 | 526.20 | 81.48 |
| 3.913 | 59.78 | 2137.57 | 545.63 | 79.59 |
| 4.348 | 53.90 | 2129.15 | 554.04 | 80.37 |
| 6.522 | 36.27 | 2098.26 | 584.94 | 79.42 |
| 8.695 | 27.45 | 2076.21 | 606.98 | 80.09 |
| 13.04 | 18.64 | 2044.31 | 638.89 | 82.89 |
| 17.39 | 14.23 | 2020.96 | 662.24 | 83.49 |
| 21.74 | 11.58 | 2002.54 | 680.66 | 86.16 |
| 30.43 | 8.56 | 1972.80 | 710.39 | 93.41 |
| 39.13 | 6.88 | 1949.16 | 734.04 | 94.59 |
| 43.48 | 6.29 | 1939.30 | 743.90 | 95.69 |
| 65.22 | 4.53 | 1898.69 | 784.51 | 106.17 |

| | | | | |
|--------|------|---------|---------|--------|
| 86.96 | 3.64 | 1868.52 | 814.68 | 110.81 |
| 130.43 | 2.76 | 1822.98 | 860.22 | 118.14 |
| 173.91 | 2.32 | 1789.77 | 893.43 | 119.79 |
| 217.39 | 2.06 | 1763.08 | 920.12 | 123.76 |
| 304.35 | 1.76 | 1721.31 | 961.89 | 174.89 |
| 391.3 | 1.59 | 1663.15 | 1020.05 | 13.29 |
| 434.78 | 1.53 | 1675.48 | 1007.72 | 49.20 |

4.4.2 Tiab's Direct Synthesis Techniques: Isothermal Condition

From the pressure derivative plot, the following characteristic points are read.

$$\begin{aligned} \Delta t_x &= 0.22 \text{ hr} & (t.\Delta p')_x &= 124 \text{ psi} \\ (t.\Delta p')_{r1} &= 80 \text{ psi} & (t.\Delta p')_{r2} &= 120 \text{ psi} \\ \Delta t_{i1} &= 0.035 \text{ hr} & \Delta t_{i2} &= 0.054 \text{ hr} \end{aligned}$$

Wellbore storage coefficient is determined using the unit slope line equation.

$$c = \frac{q_w B_w \Delta t}{24 \Delta p} = \frac{490.6 \times 1 \times 0.039}{24 \times 91} = 0.0088 \text{ RB} / \text{psi}$$

The permeability and mobility of the water zone is estimated as follows

$$K_w = \frac{70.6 q_w B_w \mu_w}{(t.\Delta p')_{rw} h} = \frac{70.6 \times 490.6 \times 1 \times 1}{80 \times 37.73} = 11.48 \text{ md}$$

$$\lambda_w = \frac{70.6 q_w B_w}{(t.\Delta p')_{rw} h} = \frac{70.6 \times 490.6 \times 1}{80 \times 37.73} = 11.48 \text{ md} / \text{cp}$$

λ_w can also be computed using Eq.(3.59a)

$$\lambda_w = \frac{1695c}{\Delta t_{i1} h} = \frac{1695 \times 0.0088}{0.035 \times 37.73} = 11.3 \text{ md} / \text{cp}$$

Equation (3.61) is used to estimate the wellbore storage coefficient,

$$C = \frac{0.015q_w B_w \Delta t_x}{(t.\Delta p')_x + \frac{59.3q_w B_w}{\lambda_w h}} = \frac{0.015 \times 490.6 \times 1 \times 0.22}{124 + \frac{59.3 \times 490.6 \times 1}{11.3 \times 37.73}} = 0.0084 RB / psi$$

Eq. (3.79) can also be used to estimate the mobility of the water zone.

$$\begin{aligned} \lambda_w &= 9416.2 \frac{c}{h \Delta t_x} \left[0.5 \frac{(t.\Delta p')_x}{(t.\Delta p')_{rw}} + 0.42 \right] \\ &= 9416.2 \frac{0.0084}{37.73 \times 0.22} \left[0.5 \frac{124}{80} + 0.42 \right] = 11.39 md / cp \end{aligned}$$

Using the following equation, the mobility of oil zone is determined as,

$$\begin{aligned} K_o &= \frac{70.6q_w B_o \mu_o}{(t.\Delta p')_{ro} h} = \frac{70.6 \times 490.6 \times 1.17 \times 3.56}{120 \times 37.73} = 31.86 md \\ \lambda_o &= \frac{70.6q_w B_o}{(t.\Delta p')_{ro} h} = \frac{70.6 \times 490.6 \times 1.17}{120 \times 37.73} = 7.65 md / cp \end{aligned}$$

The mobility ratio M is computed using Eq. (3.83)

$$M = 5.55 \frac{\Delta t_{i2}}{\Delta t_x} \left[0.5 \times \frac{(t.\Delta p')_x}{(t.\Delta p')_{r1}} + 0.42 \right] = 5.55 \frac{0.054}{0.22} \left[0.5 \frac{124}{80} + 0.42 \right] = 1.63$$

Using Eq. (3.84), one gets the mobility ratio,

$$M = \frac{0.84}{0.36 \frac{\Delta t_x}{\Delta t_{i2}} - \frac{(t.\Delta p')_x}{(t.\Delta p')_{r2}}} = \frac{0.84}{0.36 \times \frac{0.22}{0.054} - \frac{124}{120}} = 1.94$$

The skin factor is computed using either Eq.(3.85) or Eq.(3.86)

$$\begin{aligned} S &= 0.171 \left(\frac{\Delta t_x}{\Delta t_{i1}} \right)^{1.24} - 0.5 \text{Ln} \left(\frac{0.8935c}{\phi h c_{i1} r_w^2} \right) \\ S &= 0.171 \left(\frac{0.22}{0.035} \right)^{1.24} - 0.5 \text{Ln} \left(\frac{0.8935 \times 0.0088}{0.22 \times 5.44 \times 10^{-6} \times 37.73 \times 0.328^2} \right) = -2 \end{aligned}$$

Using Eq. (3.86)

$$S = 0.921 \left[\frac{(t.\Delta p')_x}{(t.\Delta p')_{r1}} \right]^{1.1} - 0.5 \text{Ln} \left(\frac{0.8935c}{\phi h c_{r1} r_w^2} \right)$$

$$S = 0.921 \left(\frac{124}{80} \right)^{1.1} - 0.5 \text{Ln} \left(\frac{0.8935 \times 0.0088}{0.22 \times 37.73 \times 5.44 \times 10^{-6} \times 0.328^2} \right) = -2.2$$

Using Eq. (3.85) the skin factor is,

$$S = 0.17 \left[\left(\frac{\Delta t_x}{\Delta t_{i2fo}} \right) M \right]^{1.24} - 0.5 \text{Ln} \left(\frac{0.8935c}{\phi h c_{r1} r_w^2} \right)$$

$$S = 0.17 \left[\frac{124}{120} \times 1.63 \right]^{1.24} - 0.5 \text{Ln} \left(\frac{0.8935 \times 0.0088}{0.22 \times 37.73 \times 5.44 \times 10^{-6} \times 0.328^2} \right) = -2.1$$

4.4.3 Tiab's Direct Synthesis Techniques: Non-Isothermal Condition

From the pressure derivative plot, the following characteristic points are read.

$$\begin{aligned} \Delta t_x &= 0.22 \text{ hr} & (t.\Delta p')_x &= 124 \text{ psi} \\ (t.\Delta p')_{r1} &= 80 \text{ psi} & (t.\Delta p')_{r2} &= 120 \text{ psi} \\ \Delta t_{i1} &= 0.035 \text{ hr} & \Delta t_{i2} &= 0.054 \text{ hr} \end{aligned}$$

Wellbore storage coefficient is determined using the unit slope line equation.

$$C = \frac{q_w B_w \Delta t}{24 \Delta p} = \frac{490.6 \times 1 \times 0.039}{24 \times 91} = 0.0088 \text{ RB} / \text{psi}$$

$$F_m(S_w, T) = M_t 10^A = \frac{10^{\left(-1.6173 + \frac{247.8}{T_{mj} - 140} \right) \left(\frac{K_{ro}}{\mu_o} + \frac{K_{rw}}{\mu_w} \right)_{\bar{s}_w}}}{K_{rw(1-\bar{s}_{or})}} = \frac{10^{\left(-1.6173 + \frac{247.8}{303-140} \right) \left(\frac{0.41}{3.56} + \frac{0.21}{1} \right)}}{0.23} = 1.13$$

The permeability and mobility of the water zone is estimated as follows

$$K_w = \frac{70.6 q_w B_w \mu_w F_m}{(t.\Delta p')_{rw} h} = \frac{70.6 \times 490.6 \times 1 \times 1 \times 1.13}{80 \times 37.73} = 12.97 \text{ md}$$

$$\lambda_w = \frac{70.6 q_w B_w F_m}{(t.\Delta p')_{rw} h} = \frac{70.6 \times 490.6 \times 1 \times 1.05}{80 \times 37.73} = 12.97 \text{ md} / \text{cp}$$

Equation (3a.48) can also be used to estimate the wellbore storage coefficient,

$$C = \frac{0.015q_w B_w \Delta t_x}{(t.\Delta p')_x + \frac{59.3q_w B_w}{\lambda_w h}} = \frac{0.015 \times 490.6 \times 1 \times 0.22}{124 + \frac{59.3 \times 490.6 \times 1}{12.97 \times 37.73}} = 0.0088 RB / psi$$

λ_w can also be computed using Eq. (3a.45)

$$\lambda_w = \frac{1695cF_m}{\Delta t_{i1}h} = \frac{1695 \times 0.0088 \times 1.13}{0.035 \times 37.73} = 12.8 md / cp$$

Eq. (3a.66) can also be used to estimate the mobility of the water zone

$$\lambda_w = 9416.2 \frac{c \times F_m}{h \Delta t_x} \left[0.5 \frac{(t.\Delta p')_x}{(t.\Delta p')_{rw}} + \frac{0.42}{F_m} \right] = 9416.2 \frac{0.0088 \times 1.13}{37.73 \times 0.22} \left[0.5 \frac{124}{80} + \frac{0.42}{1.13} \right] = 12.94 md / cp$$

Using the following equation, the mobility of oil zone is determined as,

$$K_o = \frac{70.6q_w B_o \mu_o}{(t.\Delta p')_{ro} h} = \frac{70.6 \times 490.6 \times 1.17 \times 3.56}{120 \times 37.73} = 31.86 md$$

$$\lambda_o = \frac{70.6q_w B_o}{(t.\Delta p')_{ro} h} = \frac{70.6 \times 490.6 \times 1.17}{120 \times 37.73} = 7.65 md / cp$$

The mobility ratio M is computed using Eq. (3a.71)

$$M = 5.55 \frac{\Delta t_{i2}}{\Delta t_x} \left[0.5 \times \frac{(t.\Delta p')_x}{(t.\Delta p')_{r1}} + \frac{0.42}{F_m} \right] = 5.55 \frac{0.054}{0.22} \left[0.5 \frac{124}{80} + \frac{0.42}{1.13} \right] = 1.56$$

Using Eq. (3a.73), one gets the mobility ratio

$$M = \frac{0.84}{F_m \left(0.36 \frac{\Delta t_x}{\Delta t_{i2}} - \frac{(t.\Delta p')_x}{(t.\Delta p')_{r2}} \right)} = \frac{0.84}{1.13 \left(0.36 \times \frac{0.22}{0.054} - \frac{124}{120} \right)} = 1.65$$

The skin factor is computed using either Eq.(3a.74) or Eq.(3a.75)

$$S = 0.1707 \left(\frac{\Delta t_x F_m M}{t_{i1}} \right)^{1.24} - 0.5 Ln \left(\frac{0.8935c}{\phi h c_{i1} r_w^2} \right)$$

$$S = 0.1707 \left(\frac{0.22 \times 1.13 \times 1.56}{0.035} \right)^{1.24} - 0.5 Ln \left(\frac{0.8935 \times 0.0088}{0.22 \times 5.44 \times 10^{-6} \times 37.73 \times 0.328^2} \right) = -2.34$$

Using Eq. (3a.75)

$$S = 0.9212 \left[\frac{(t \cdot \Delta p')_x F_m M}{(t \cdot \Delta p')_{r1}} \right]^{1.1} - 0.5 \text{Ln} \left(\frac{0.8935c}{\phi h c_{r1} r_w^2} \right)$$

$$S = 0.9212 \left(\frac{124 \times 1.13 \times 1.56}{80} \right)^{1.1} - 0.5 \text{Ln} \left(\frac{0.8935 \times 0.0088}{0.22 \times 37.73 \times 5.44 \times 10^{-6} \times 0.328^2} \right) = -2.36$$

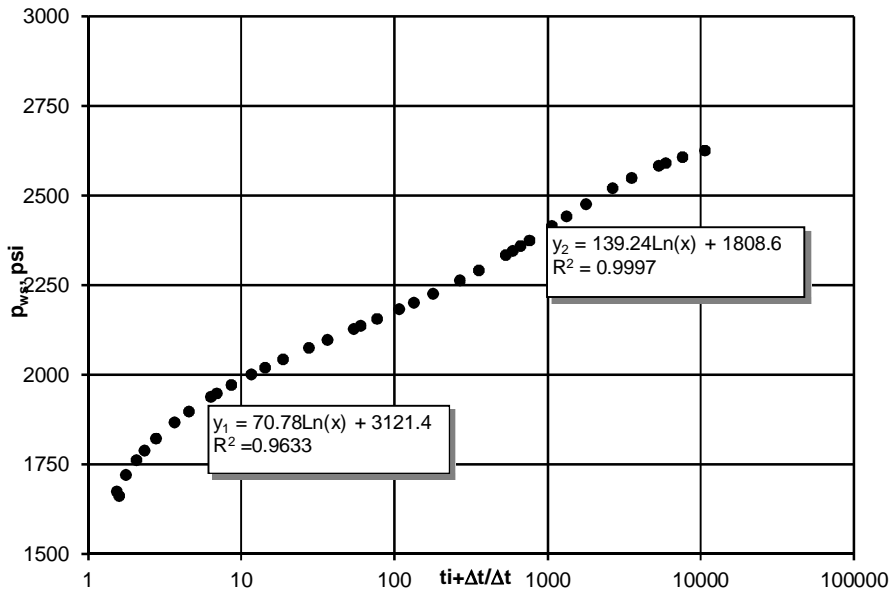


Figure 4.5: Semilog Plot of Pressure Fall-off Data (Example1)

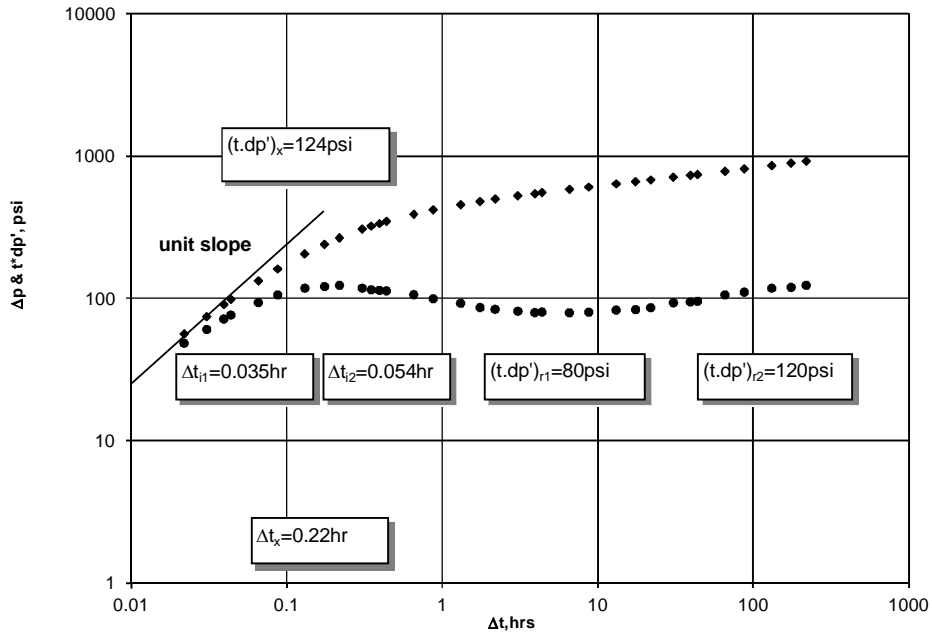


Figure 4.6: Pressure and Pressure Derivative Plot Pressure Fall-off Data (Example-1)

Table 4.5: Final Results (Example-1)

| Equation No. | Parameter | Value |
|--------------|---------------------|--------|
| Eq.43a.65b | k_w , md | 12.97 |
| Eq.3a.45 | k_w , md | 12.80 |
| Eq.4.3a.44 | k_w , md | 12.94 |
| Eq.3a.69c | λ_o , md/cp | 8.95 |
| Eq.3a.58 | M | 1.56 |
| Eq.3a.73 | M | 1.65 |
| Eq.3a.74 | S | -2.34 |
| Eq.3a.75 | S | -2.4 |
| Eq.3a.38 | C, bbl/psi | 0.0088 |
| Eq.3a.48 | C, bbl/psi | 0.0088 |

Table 4. 6: Comparison of Results (Example-1)

| Parameter | Conventional analysis | TDS-Isothermal | TDS-Non Isothermal | Kong and Lu |
|---------------------------|-----------------------|----------------|--------------------|-------------|
| k_w, md | 12.97 | 11.48 | 12.97 | 12.64 |
| $\lambda_o, \text{md/cp}$ | 7.65 | 7.65 | 7.65 | 7.28 |
| S | -2.4 | -2 | -2.4 | -2.36 |
| M | 1.48 | 1.9 | 1.56 | 2 |
| $c, \text{ bbl/psi}$ | 0.0088 | 0.0088 | 0.0088 | 0.0071 |

4.5 Field Example-2

Table 4.8 gives the bottom-hole pressure as a function of time and pressure derivative calculation. Other reservoir and fluid data are given in Table 4.7

Table 4.7: Reservoir Rock, Fluid, and Well Data (Pressure Fall-off Test) (Example-2)

(Sources: Tiab and Abdesselam, 2001)

| | |
|--|--|
| Reservoir Thickness, h | 28.54 ft |
| Porosity, ϕ | 0.18 |
| Total Injection Time, t_{inj} | 1200 hrs |
| Water FVF, B_w | 1 RB/STB |
| Total System Compressibility, C_{ti} | $3.68 \times 10^{-6} \text{ psi}^{-1}$ |
| Oil Viscosity, μ_o | 2.2 cp |
| Water Viscosity, μ_w | 1 cp |
| Wellbore Radius, r_w | 0.328 ft |
| Oil FVF (B_o) | 1.2 RB/STB |

| | |
|----------------------------------|---------------|
| Saturation, ΔS_w | 0.4 |
| Injection Temperature, T_{inj} | 308K (95F) |
| Injection Rate, q_w | 830.3 bbl/day |

4.5.1 Conventional Analysis

Fig 4.11 is the semilog plot of pressure fall-off test against Horner time $\frac{t_{inj} + \Delta t}{\Delta t}$. Figure 4.12 shows the log-log plots of pressure and pressure derivative data versus shut-in time Δt . As it can be seen on the two plots, the early data is dominated by wellbore storage effects indicated by a unit slope line on the log-log plots of pressure and pressure derivative data. Two semilog straight lines defining the infinite acting radial flow periods in both water bank and the uninvaded oil zone are identified on the semilog plot. These two periods are shown on the derivative plot as two horizontal lines separated by a transition zone.

Using the slope of the first semilog straight line, we can estimate the permeability and mobility of the water bank as:

$$K_w = \frac{162.6q_w B_w \mu_w}{m_w h} = \frac{162.6 \times 830.3 \times 1 \times 1}{182.79 \times 28.54} = 25.88 \text{ md}$$

$$\lambda_w = \frac{162.6q_w B_w}{m_w h} = \frac{162.6 \times 830.3 \times 1}{182.79 \times 28.54} = 25.88 \text{ md / cp}$$

The permeability and mobility of the oil zone is determined using the slope of the second semilog straight line:

$$K_o = \frac{162.6q_w B_o \mu_o}{m_o h} = \frac{162.6 \times 830.3 \times 1.2 \times 2.2}{669.8 \times 28.54} = 18.64 \text{ md}$$

$$\lambda_o = \frac{162.6q_w B_o}{m_o h} = \frac{162.6 \times 830.3 \times 1.2}{669 \times 28.54} = 8.47 \text{ md / cp}$$

The skin factor is computed using the first semilog straight line,

$$S = 1.1513 \left[\frac{\Delta p_{1hr}}{m_w} - \log \left(\frac{\lambda_w}{\phi c_{t1} r_w^2} \right) + 3.23 \right]$$

$$S = 1.1513 \left[\frac{715.83}{228.65} - \log \left(\frac{20.7}{0.18 \times 3.68 \times 10^{-6} \times 0.328^2} \right) + 3.23 \right] = -2.42$$

The radius to the flood front is given by:

$$r_f = \left[\frac{5.615q_w B_w t_{inj}}{24 \times \pi h \phi \Delta S_w} \right]^{1/2} = \left[\frac{5.615 \times 830.3 \times 1 \times 1200}{24 \times \pi \times 28.54 \times 0.18 \times 0.4} \right]^{1/2} = 190 \text{ ft}$$

Table 4. 8: Pressure and Pressure Derivative Data (Example-2)

| t, hrs | t+Δt/Δt | P _{ws} , psi | Δp, psi | t*dp', psi |
|--------|-------------|-----------------------|---------|------------|
| 0 | | 3190.829 | | |
| 0.025 | 48001 | 3111.204 | 79.625 | |
| 0.035 | 34286.71429 | 3100.181 | 90.648 | 59.139 |
| 0.045 | 26667.66667 | 3077.410 | 113.419 | 100.294 |
| 0.05 | 24001 | 3066.387 | 124.442 | 109.020 |
| 0.075 | 16001 | 3014.899 | 175.930 | 146.416 |
| 0.1 | 12001 | 2968.777 | 222.052 | 175.399 |
| 0.15 | 8001 | 2890.166 | 300.663 | 214.511 |
| 0.2 | 6001 | 2825.770 | 365.059 | 235.251 |
| 0.25 | 4801 | 2772.541 | 418.288 | 257.079 |
| 0.35 | 3429.571429 | 2676.961 | 513.868 | 204.237 |
| 0.4 | 3001 | 2657.091 | 533.738 | 189.709 |
| 0.45 | 2667.666667 | 2629.534 | 561.295 | 228.434 |
| 0.5 | 2401 | 2606.327 | 584.502 | 220.941 |
| 0.75 | 1601 | 2523.656 | 667.173 | 196.018 |
| 1 | 1201 | 2475.649 | 715.180 | 164.666 |
| 1.5 | 801 | 2420.679 | 770.150 | 130.316 |
| 2 | 601 | 2388.771 | 802.058 | 107.328 |

| | | | | |
|-----|--------|----------|----------|---------|
| 2.5 | 481 | 2367.015 | 823.814 | 99.109 |
| 3.5 | 343.85 | 2335.107 | 855.722 | 98.988 |
| 4.5 | 267.66 | 2310.451 | 880.378 | 97.900 |
| 5 | 241 | 2300.298 | 890.531 | 98.626 |
| 7.5 | 161 | 2258.237 | 932.592 | 110.954 |
| 10 | 121 | 2226.329 | 964.500 | 118.931 |
| 15 | 81 | 2175.566 | 1015.264 | 132.709 |
| 20 | 61 | 2137.856 | 1052.973 | 139.236 |
| 25 | 49 | 2105.947 | 1084.882 | 148.785 |
| 35 | 35.285 | 2055.039 | 1135.790 | 160.412 |
| 45 | 27.666 | 2014.284 | 1176.545 | 185.576 |
| 50 | 25 | 1993.543 | 1197.286 | 197.106 |
| 75 | 17 | 1920.734 | 1270.095 | 192.973 |
| 100 | 13 | 1864.895 | 1325.934 | 204.793 |
| 150 | 9 | 1781.063 | 1409.766 | 222.995 |
| 200 | 7 | 1716.231 | 1474.598 | 230.900 |
| 250 | 5.8 | 1665.613 | 1525.216 | 235.324 |
| 350 | 4.428 | 1585.697 | 1605.132 | 245.948 |
| 450 | 3.666 | 1525.071 | 1665.758 | 251.930 |
| 500 | 3.4 | 1498.239 | 1692.590 | 464.604 |

4.5.2 Tiab's Direct Synthesis Techniques: Isothermal Condition

From the pressure derivative plot the characteristic points are read

$$(t.\Delta p')_{r1} = 100 \text{ psi}, \quad (t.\Delta p')_x = 255 \text{ psi}, \quad \Delta t_x = 0.27 \text{ hr}, \\ \Delta t_{i2} = 0.11 \text{ hr}, \quad (t.\Delta p')_{r2} = 280 \text{ psi}, \quad \Delta t_{i1} = 0.04 \text{ hr},$$

The permeability and mobility of the water zone is estimated as follows

$$K_w = \frac{70.6q_w B_w \mu_w}{(t.\Delta p')_{rw} h} = \frac{70.6 \times 830.3 \times 1 \times 1}{100 \times 28.54} = 20.54 \text{ md}$$

$$\lambda_w = \frac{70.6q_w B_w}{(t.\Delta p')_{rw} h} = \frac{70.6 \times 830.3 \times 1}{100 \times 28.54} = 20.54 \text{ md} / \text{cp}$$

The wellbore storage coefficient is computed using the unit slope line,

$$C = \frac{0.015q_w B_w \Delta t_x}{(t.\Delta p')_x + \frac{59.3q_w B_w}{\lambda_w h}} = \frac{0.015 \times 830.3 \times 1 \times 0.25}{257 + \frac{59.3 \times 830.3 \times 1}{20.54 \times 28.54}} = 0.0091 \text{ RB} / \text{psi}$$

Eq. (3.79) can also be used to estimate the mobility of the water zone.

$$\lambda_w = 9416.2 \frac{c}{h \Delta t_x} \left[0.5 \frac{(t.\Delta p')_x}{(t.\Delta p')_{rw}} + 0.42 \right] \\ = 9416.2 \frac{0.0091}{28.54 \times 0.25} \left[0.5 \frac{257}{100} + 0.42 \right] = 20.48 \text{ md} / \text{cp}$$

Using the following equation, the mobility of oil zone is determined as,

$$K_o = \frac{70.6q_w B_o \mu_o}{(t.\Delta p')_{ro} h} = \frac{70.6 \times 830.3 \times 1.2 \times 2.2}{280 \times 28.54} = 19.37 \text{ md}$$

$$\lambda_o = \frac{70.6q_w B_o}{(t.\Delta p')_{ro} h} = \frac{70.6 \times 830.3 \times 1.2}{280 \times 28.54} = 8.8 \text{ md} / \text{cp}$$

The mobility ratio M is computed using Eq. (3.83)

$$M = 5.55 \frac{\Delta t_{i2}}{\Delta t_x} \left[0.5 \times \frac{(t.\Delta p')_x}{(t.\Delta p')_{r1}} + 0.42 \right] = 5.55 \frac{0.11}{0.27} \left[0.5 \frac{255}{100} + 0.42 \right] = 3.83$$

Using Eq. (3.85), one gets the mobility ratio,

$$M = 133.4 \frac{c}{qB} \frac{(t.\Delta p')_{rf2}}{\Delta t_x} \left[0.5 \frac{(t.\Delta p')_x}{(t.\Delta p')_{rf1}} + 0.42 \right] = 133.4 \times \frac{0.0091}{830.3 \times 1} \times \frac{280}{0.27} \left[0.5 \times \frac{255}{100} + 0.42 \right] = 3.62$$

The skin factor is computed using either Eq. (3.85)

$$S = 0.171 \left(\frac{\Delta t_x}{\Delta t_{i1}} M \right)^{1.24} - 0.5 \text{Ln} \left(\frac{0.8935c}{\phi h c_{i1} r_w^2} \right)$$

$$S = 0.171 \left(\frac{0.27 \times 3.83}{0.11} \right)^{1.24} - 0.5 \text{Ln} \left(\frac{0.8935 \times 0.0091}{0.18 \times 28.54 \times 3.68 \times 10^{-6} \times 0.328^2} \right) = -1.39$$

4.5.3 Tiab's Direct Synthesis Techniques: Non-Isothermal Condition

From the pressure derivative plot the characteristic points are read:

$$\Delta t_x = 0.27 \text{ hr} \quad (t.\Delta p')_x = 255 \text{ psi}$$

$$(t.\Delta p')_{r1} = 100 \text{ psi} \quad (t.\Delta p')_{r2} = 280 \text{ psi}$$

$$\Delta t_{i1} = 0.04 \text{ hr}$$

$$\Delta t_{i2} = 0.11 \text{ hr}$$

$$F_m(S_w, T) = M_i 10^A = \frac{10^{\left(-1.6173 + \frac{247.8}{T_{mj} - 140}\right)} \left(\frac{K_{ro}}{\mu_o} + \frac{K_{rw}}{\mu_w} \right)_{\bar{s}_w}}{K_{rw(1-s_{or})}} = \frac{10^{\left(-1.6173 + \frac{247.8}{308 - 140}\right)} \left(\frac{0.45}{2.2} + \frac{0.25}{1} \right)}{0.26} = 1.26$$

The permeability and mobility of the water zone is estimated as follows:

$$K_w = \frac{70.6 q_w B_w \mu_w F_m}{(t.\Delta p')_{rw} h} = \frac{70.6 \times 830.3 \times 1 \times 1 \times 1.26}{100 \times 28.54} = 25.88 \text{ md}$$

$$\lambda_w = \frac{70.6 q_w B_w F_m}{(t.\Delta p')_{rw} h} = \frac{70.6 \times 830.3 \times 1 \times 1.26}{100 \times 28.54} = 25.88 \text{ md / cp}$$

Equation (3a.48) can also be used to estimate the wellbore storage coefficient,

$$C = \frac{0.015 q_w B_w \Delta t_x}{(t.\Delta p')_x + \frac{59.3 q_w B_w}{\lambda_w h}} = \frac{0.015 \times 830.3 \times 1 \times 0.27}{255 + \frac{59.3 \times 830.3 \times 1}{25.88 \times 28.54}} = 0.01 \text{ RB / psi}$$

Eq. (3a.66) can also be used to estimate the mobility of the water zone

$$\lambda_w = 9416.2 \frac{c \times F_m}{h \Delta t_x} \left[0.5 \frac{(t.\Delta p')_x}{(t.\Delta p')_{rw}} + \frac{0.42}{F_m} \right] = 9416.2 \frac{0.01 \times 1.26}{28.54 \times 0.27} \left[0.5 \frac{255}{100} + \frac{0.42}{1.26} \right] = 25.76 \text{ md / cp}$$

Using the following equation, the mobility of oil zone is determined as:

$$K_o = \frac{70.6 q_w B_o \mu_o}{(t.\Delta p')_{ro} h} = \frac{70.6 \times 830.3 \times 1.2 \times 2.2}{280 \times 28.54} = 19.37 \text{ md}$$

$$\lambda_o = \frac{70.6q_w B_o}{(t.\Delta p')_{ro} h} = \frac{70.6 \times 490.6 \times 1.17}{120 \times 37.73} = 8.8 \text{ md / cp}$$

The mobility ratio M is computed using Eq. (3a.71)

$$M = 5.55 \frac{\Delta t_{i2}}{\Delta t_x} \left[0.5 \times \frac{(t.\Delta p')_x}{(t.\Delta p')_{r1}} + \frac{0.42}{F_m} \right] = 5.55 \frac{0.11}{0.27} \left[0.5 \frac{255}{100} + \frac{0.42}{1.26} \right] = 3.64$$

Using Eq. (3a.72), one gets the mobility ratio as

$$M = 133.4 \frac{c}{qB} \frac{(t.\Delta p')_{rf2}}{\Delta t_x} \left[0.5 \frac{(t.\Delta p')_x}{(t.\Delta p')_{rf1}} + \frac{0.42}{F_m} \right] = 133.4 \times \frac{0.01}{830.3 \times 1} \times \frac{280}{0.27} \left[0.5 \times \frac{255}{100} + \frac{0.42}{1.26} \right] = 3.68$$

The skin factor is computed using either Eq. (3a.74) or Eq. (3a.75)

$$S = 0.1707 \left(\frac{\Delta t_x F_m}{t_{i1}} \right)^{1.24} - 0.5 \text{Ln} \left(\frac{0.8935c}{\phi h c_{t1} r_w^2} \right)$$

$$S = 0.1707 \left(\frac{0.27 \times 1.26}{0.04} \right)^{1.24} - 0.5 \text{Ln} \left(\frac{0.8935 \times 0.01}{0.18 \times 3.68 \times 10^{-6} \times 28.54 \times 0.328^2} \right) = -2.43$$

$$S = 0.9212 \left[\frac{(t.\Delta p')_x F_m}{(t.\Delta p')_{r1}} \right]^{1.1} - 0.5 \text{Ln} \left(\frac{0.8935c}{\phi h c_{t1} r_w^2} \right)$$

$$S = 0.9212 \left(\frac{255 \times 1.26}{100} \right)^{1.1} - 0.5 \text{Ln} \left(\frac{0.8935 \times 0.01}{0.18 \times 3.68 \times 10^{-6} \times 28.54 \times 0.328^2} \right) = -2.41$$

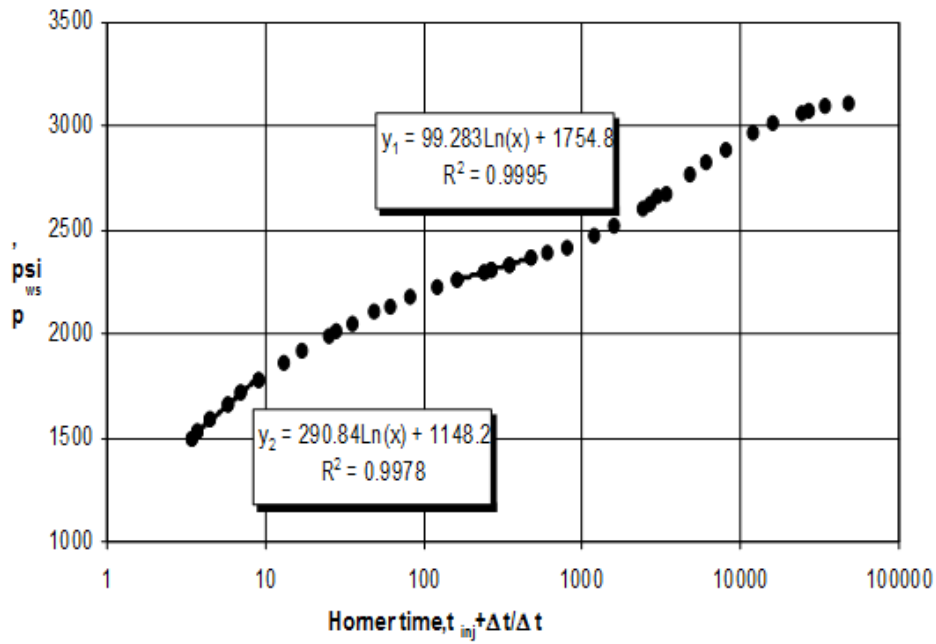


Figure 4.7: Plot of Pressure Vs Horner time-Semilog Fall-off Data (Example-2)

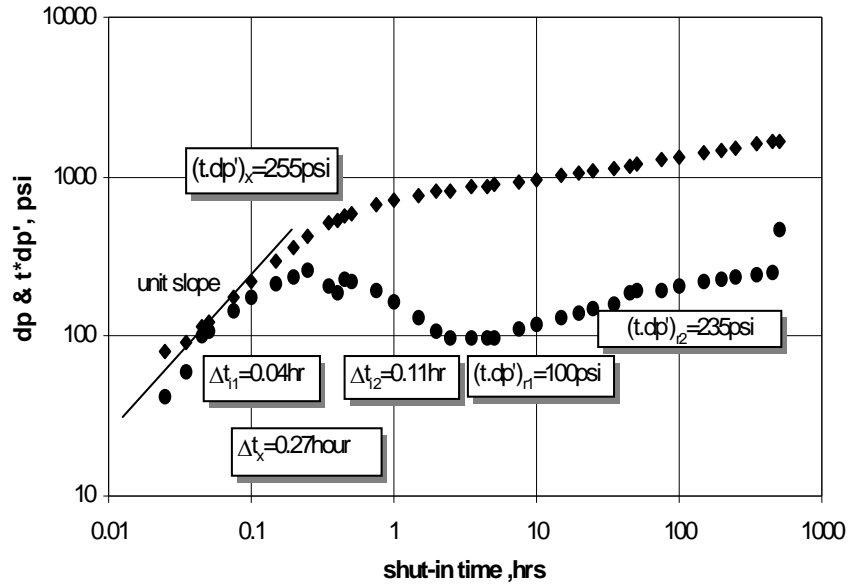


Figure 4.8: Pressure and Pressure Derivative Plots (Example-2)

Table 4.9: Final Results (Example-2)

| Equation No. | Parameter | Value |
|--------------|---------------------|-------|
| Eq.3a.65b | k_w , md | 25.88 |
| Eq.3a.45 | k_w , md | 25.76 |
| Eq.3a.69c | λ_o , md/cp | 8.8 |
| Eq.3a.58 | M | 3.64 |
| Eq.3a.73 | M | 3.68 |
| Eq.3a.74 | S | -1.77 |
| Eq.3a.75 | S | -1.76 |
| Eq.3a.48 | C , bbl/psi | 0.010 |

Table 4.10: Comparison of Results (Example-2)

| Parameter | Conventional analysis | TDS-Isothermal | TDS-Non Isothermal | Kong and Lu |
|---------------------|-----------------------|----------------|--------------------|-------------|
| k_w , md | 25.88 | 20.54 | 25.88 | 25.73 |
| λ_o , md/cp | 8.47 | 8.8 | 8.8 | 8.8 |
| S | -2.42 | -1.39 | -2.43 | -2.40 |
| M | 3.78 | 3.83 | 3.68 | 3.68 |
| c , bbl/psi | 0.0096 | 0.0091 | 0.010 | 0.010 |

CHAPTER 5

CONCLUSION AND SUMMARY

5.1 Summary

Analytical solutions that take into account the effect of temperature- and saturation-gradient during pressure injectivity and fall-off test was developed. Pressure derivative was introduced to these solutions for both the injectivity and fall-off tests. This was done to improve the definition of the analysis plots and therefore providing valuable qualitative information about the reservoir heterogeneity. The pressure derivative was applied to Tiab's Direct Synthesis (TDS) techniques and new equations for determining the different reservoir parameters from the injection and fall-off data were obtained. A new factor F_M which accounts for the effect of temperature- and saturation-gradient was introduced into the TDS techniques. This further increased the accuracy of the techniques when compared to other methods used.

5.2 Conclusion

The conclusions drawn from this study are:

1. The TDS technique was successfully extended to injection and fall-off tests during Non-isothermal condition. The equations was tested by their application to field data and compared to the results obtained by isothermal condition and conventional analysis. The results obtained by using the TDS technique were in good conformity with those obtained using conventional analysis.
2. An analytical solution obtained showed two different flow regimes representing water (invaded) and oil (uninvaded) zones in injection and pressure fall-off test. The injection data when plotted on a semilog scale exhibited two linear sections corresponding to the pressure transience through the water zone and the oil zone. Also, for the fall-off tests, if the test is run long enough, the derivative plot of fall-off test data would show two flat regions that reflect the characteristics of both the invaded and un-invaded zones.
3. If Non-isothermal pressure transients are ignored, the skin value can be grossly overestimated or underestimated. There is need to account for both temperature and saturation effects associated with cold-water injection so as to analyze injection and fall-off tests accurately.
4. Changes in slope caused by Non-isothermal pressure transients may be incorrectly interpreted as reservoir boundaries. Fall-off tests should, however, be run at early stages of waterflooding to characterize the process effectively.
5. The TDS technique presented is applicable to a wide range of injection and fall-off problems; it can be applied directly to determine different reservoir parameters from an injection or fall-off test.

Nomenclature

B = formation volume factor, RB/STB

B_w = water formation volume factor, RB/STB

B_o = oil formation volume factor, RB/STB

c_f = formation compressibility, psi^{-1}

c_o = oil compressibility, psi^{-1}

c_t = total system compressibility, psi^{-1}

c = wellbore storage coefficient, bbl/psi.

F_m = Temperature- and saturation- dependent total mobility, dimensionless

$E_1(x)$ = exponential integral, $\int_x^\infty e^{-u}$

f_w = fractional flow of water.

h = formation thickness, ft.

k = absolute reservoir permeability, md.

k_{ro} = oil relative permeability.

k_{rw} = water relative permeability.

$k_{rw(1-s_{or})}$ = end point water relative permeability

λ = Mobility

M = mobility ratio.

m = slope from the semilog plot.

p = pressure, psi.

p_D = dimensionless pressure

p_{wD} = dimensionless wellbore pressure,

p_{wf} = flowing bottom-hole pressure, psi.

p_{ws} = wellbore pressure during the shut in, psi.

q_i = water injection rate, STB/D.

r = radius, ft.

r_D = dimensionless radius.

r_f = radius to the flood front, ft.

r_w = wellbore radius, ft.

S = skin factor.

S_o = oil saturation, fraction

S_{or} = residual oil saturation, fraction

S_w = water saturation, fraction

T_{inj} = Injection temperature, K

t = time, hours.

t_D = dimensionless time.

t_i = injection time, hours.

Δp = pressure difference, psi.

$\Delta p'$ = pressure derivative, psi.

Δt = shut-in time, hours.

y = Boltzmann transformation variable.

y_f = Boltzmann transformation variable evaluated at $r = r_f$.

α = characteristic injection constant.

η = diffusivity equation, $k / \phi \mu c_t$.

μ_o = oil viscosity, cp.

μ_w = water viscosity, cp.

ϕ = porosity, fraction.

Subscripts

a = apparent

D = dimensionless

f = front

i = injection

o = oil

r = relative

t = total

w = water

1 = Invaded zone

2 = Uninvaded zone

Superscripts

⁻ = average

' = first derivative

" = second derivative

REFERENCES

- Abbaszadeh, M., and Kamal, M.M., (1989): "Pressure-Transient Testing of Water-Injection Wells," *SPEFE* (Feb. 1989) 115-124.
- Ahmed, T. (2006): "Reservoir Engineering Handbook", Third edition, Elsevier, Gulf Professional Publishing, New York.
- Barkve, T. (1989): "Non-isothermal Effects in Water-Injection Well Tests," *SPEFE* (June 1989) 281-286
- Benson, S.M., and Bodvarsson, G.S., (1986): "Nonisothermal Effects During Injection and Fall-off Tests," *SPEFE* (Feb. 1986) 53-63.
- Bixel, H.C., and van Poolen, H.K., (1967): "Pressure Drawdown and Buildup in the Presence of Radial Discontinuities," *SPEJ* (Sept. 1967) 301-309.
- Bodvarsson, G.S., and Tsang, C.F., (1980): "Thermal Effects in the Analysis of Fractured Reservoirs," *Proc. Third Invitational Well Testing Symposium, Berkeley, CA* (1980) 110-19.
- Bratvold, R.B. (1989): "An Analytical Study of Reservoir Pressure Response Following Cold Water Injection," PhD dissertation, Stanford U., Stanford, CA (March 1989).
- Bratvold, R.B., and Horn, R.N., (1990): "Analysis of Pressure-Falloff Test Following Cold-Water Injection," *SPEFE* (Sept. 1990) 293-302.
- Bratvold, R.B., and Larsen, L., (1989): "Effects of Linear Boundaries on Pressure-Transient Injection and Falloff Data," paper SPE 19830, presented at the 1989 SPE Annual Technical Conference and Exhibition, San Antonio, Oct. 8-11.
- Buckley, S.E., and Leverett, M.E., (1942): "Mechanism of Fluid Displacement in Sands," *Trans., AIME* (1942) 146, 107-16.
- Dake, L.P. (1978): "Fundamentals of Reservoir Engineering," Elsevier, Amsterdam-London-New York-Tokyo.
- Earlougher, R.C. (1977): "Advances in Well Test Analysis," *SPE Monograph, Vol. 5, SPE AIME, Dallas*, (1977).
- Escobar, F.H., Ascencio, J.M., and Real, D.F., (2013): "Injection and Fall-Off tests Transient Analysis of Non-Newtonian Fluids," *ARNP Journal of Engineering and Applied Sciences* (Sep. 2013) Vol. 8, No 9.
- Fayers, F.J. (1962): "Some Theoretical Results Concerning the Displacement of a Viscous Oil by a Hot Fluid in a Porous Medium, Part I," *Fluid Mech.* (1962) 1365-76.

- Garg, S.K., and Pritchett, J.W., (1981): "Cold Water Injection into Two Phase Geothermal Reservoirs," *Proc., Seventh Workshop on Geothermal Reservoir Engineering*, Stanford U., Palo Alto. CA (1981) 175-78
- Hazebroek, P., Rainbow, H., and Matthews, C.S., (1958): "Pressure Fall-Off in Water Injection Wells." *Trans., AIME* (1958) 213, 250-260.
- Hovdan, M. (1986): "Water Injection-Incompressible Analytical Solution with Temperature Effects," technical report MH-1186, Statoil, Stavanger, Norway (Sept. 1986).
- Karakas, M., Saneie, S., and Yortsos, Y., (1986): "Displacement of a Viscous Oil by the Combined Injection of Hot Water and Chemical Additive," *SPE* (July 1986) 391-402; *Trans., AIME*, 282.
- Kazemi, H., Merrill, L.S., and Jargon, J.R., (1972): "Problems in Interpretation of Pressure Fall Off Tests in Reservoirs With and Without Fluid Banks," *JPT* (Sept. 1972) 1147-56.
- Kazemi, H. (1966): "Locating a Burning Front by Pressure Transient Measurements," *Trans., AIME* (Feb. 1966) 227-232.
- Kong, X.Y., and Lu, D.T., (1991): "Pressure Falloff Analysis of Water Injection Wells," SPE 23419, April 1991.
- Larkin, B.K. (1963): "Solutions to the Diffusion Equation for a Region Bounded by a Circular Discontinuity," *SPEJ* (June 1963) 113-15; *Trans., AIME*. 228.
- Lee, J. W. (1982): "Well Testing," SPE Textbook series, Vol. 1, SPE AIME, New York, (1982)
- Merrill, L.S., Jr. Kazemi, H., and Gogarty, W.B., (1974): "Pressure Falloff Analysis in Reservoir with Fluid Banks." *JPT* (July 1974) 809-18; *Trans... AIME*. 257.
- Micheal, M. L. (2002): " Application of Water Injection/Falloff Tests for Reservoir Appraisal: New Analytical Solution Method for Two-Phase Variable Rate Problems," paper SPE 77532, presented at SPE Annual Technical Conference and Exhibition, San Antonio, Sep. 29-Oct. 2, 2002.
- Nyhus, E. (1987): "Modelling of Thermal Injection and Falloff Tests," technical report, Rogaland Research Inst., Stavanger, Norway (Oct. 1987) 299
- Odeh, A.S. (1969): "Flow Test Analysis for a Well with Radial Discontinuity," *JPT* (Feb. 1969) 207-210; *Trans. • AIME*. 249.
- O'Sullivan, M.I., and Pruess, K., (1980): "Analysis of Injection Testing of Geothermal Reservoirs," *Trans. Geothermal Resources Council* (1980) 4, 401-04.
- Onyekonwu, M.O., Ramey, H.J., and Brigham, W.E., (1984): "Interpretation of Simulated Falloff Tests," Stanford University, SPE 12746, April 1984.
- Raj, B., Thompson, L.G., and Reynolds, A.C., (1998): "Injection/ Falloff Testing in Heterogeneous Reservoirs," *SPE*, December 1998.
- Ramakrishnan, T.S., and Kuchuk, F.J, (1994): "Testing Injection Wells with Rate and Pressure Data," *SPEFE*, sept. 1994.

- Ramey, H.I. Jr. (1970): "Approximate Solutions for Unsteady Liquid Flow in a Composite Reservoir," J. Cdn. Pet. Tech. (March 1970) 32-37.
- Reldar, B. B., and Roland, N.H., (1990): "Analysis of Pressure-Falloff Tests Following Cold-Water Injection," SPEFE, (Sept. 1990) 293-302.
- Satman, A., et al. (1980): "An Analytical Study of Transient Flow in Systems with Radial Discontinuities," paper SPE 9399 presented at the 1980 SPE Annual Technical Conference and Exhibition. Dallas. Sept. 21-24.
- Sosa, A., Raghavan, R., and Limon, T.J., (1981): "Effect of Relative Permeability and Mobility Ratio on Pressure Fall-off Behavior," *JPT* (June 1981) 1125-35.
- Tiab, D. (1993): "Analysis of Pressure and Pressure Derivative without Type-Curve Matching - 1. Skin and Wellbore Storage," *Journal of Petroleum Science and Engr.*, Vol. 12, No. 3 (Jan. 1993) 171-181.
- Tiab, D., and Abdesselam, H., (2001): "Interpretation of Pressure Injectivity and Falloff Tests Using Tiab's Direct Synthesis Technique," MSc Thesis, University of Oklahoma, Norman, Oklahoma (2001).
- Tiab, D., and Engler, T., (1995): "Analysis of Pressure And Pressure Derivative Without Type Curve Matching in Naturally Fractured Reservoirs," *Journal of Petroleum Science and Engineering*, June 1995.
- Tiab, D., and Kumar, A., (1980): "Application of the P_D' Function to Interference Analysis," *JPT*, August 1980.
- Tsang, Y.W., and Tsang, C.F. (1978): "An Analytic Study of Geothermal Reservoir Pressure Response to Cold Water Reinjection," Proc. Fourth Workshop on Geothermal Reservoir Engineering, Stanford U., Palo Alto, CA (1978) 322-31.
- Van Poolen, H.K. (1965): "Transient Tests Find Fire Front in an In-Situ Combustion Project." *Oil and Gas J.* (1965) 78-80.
- Woodward, O.K. and Thambynayagam, R.K.M., (1983): "Pressure Buildup and Falloff Analysis of Water-Injection Tests," paper SPE 12344 available from SPE Book Order Dept., Richardson, TX (1983).
- Yeh, N. S. and Agarwal, R.G., (1989): "Pressure Transient Analysis of Injection Wells in Reservoirs with Multiple Fluid Banks," paper SPE 19775 presented at the 1989 SPE Annual Technical Conference and Exhibition, San Antonio, Texas.

Appendix

Injection Solution

We derived the injection solution in an infinite reservoir with the transform approach assuming that the reservoir consists of two different regions separated by a moving discontinuity in fluid saturation as outlined in Fig 4.1. The model is described to consist of a reservoir that is assumed to be cylindrical with the well located at the center. The reservoir is assumed to be of uniform and constant porosity, permeability, heat capacity, thermal conductivity and infinite of constant thickness. The fluids have a negligible compressibility and injected at a constant rate. Gravity slumping of cold-water front is neglected and the viscosities are assumed to be functions of temperature only. The well has a finite radius and fully penetrates the entire formation thickness. Piston-like displacement of oil and water is assumed as the reservoir is completely saturated with oil and water.

For an infinite system with a line source well, we have;

Governing Equations

The invaded zone

$$F_m \frac{\partial^2 P_{D1}}{\partial r_D^2} + F_m \frac{1}{r_D} \frac{\partial P_{D1}}{\partial r_D} = \frac{\partial P_{D1}}{\partial t_D}, \quad 0 < r_D < r_{Df} \quad (\text{A.1})$$

The uninvaded zone

$$\frac{\partial^2 P_{D2}}{\partial r_D^2} + \frac{1}{r_D} \frac{\partial P_{D2}}{\partial r_D} = \frac{\eta_1}{\eta_2} \frac{\partial P_{D2}}{\partial t_D}, \quad r_{Df} < r_D < \infty \quad (\text{A.2})$$

Where

$$P_D(t_D, r_D) = \frac{2\pi k_w h}{q\mu_w B_w} \Delta P$$

$$t_D = \frac{k_w t}{\phi\mu_w c_{t1} r_w^2}$$

$$r_D = \frac{r}{r_w}$$

$$\eta_1 = \frac{k_w}{\phi\mu_w c_{t1}}$$

$$\eta_2 = \frac{k_o}{\phi\mu_o c_{t2}}$$

Initial conditions:

$$P_{D1} = P_{D2} = 0, \quad t_D = 0 \quad (\text{A.3})$$

$$r_{Df} = 0, \quad t_D = 0 \quad (\text{A.4})$$

Boundary conditions:

$$\lim_{r_D \rightarrow 0} r_D \left(\frac{\partial P_{D1}}{\partial r_D} \right) = -1 \quad (\text{A.5})$$

$$\lim_{r_D \rightarrow \infty} P_{D2} = 0 \quad (\text{A.6})$$

Moving boundary conditions:

$$P_{D1} = P_{D2}, \quad r_D = r_{Df} \quad (\text{A.7})$$

$$F_m \frac{\partial P_{D1}}{\partial r_D} = \frac{1}{M} \frac{\partial P_{D2}}{\partial r_D}, \quad r_D = r_{Df} \quad (\text{A.8})$$

$$\text{And } F_m(S_w, T) = M_t 10^A = \frac{10^{(-1.6173 + \frac{247.8}{T_{inj} - 140})} \left(\frac{K_{ro}}{\mu_o} + \frac{K_{rw}}{\mu_w} \right)}{K_{rw(1-s_{or})}} \quad (\text{A.9})$$

Where η_1, η_2 are the hydraulic diffusivities of the invaded and uninvaded zones respectively. All other variables and parameters are dimensionless, P_{D1} and P_{D2} are the pressures in the invaded and uninvaded regions respectively, r_{Df} is the position of the moving interface between the two regions and F_m represent temperature- and saturation-dependent total mobility. From the Buckley-Leverett theory, we know that the saturation profile is defined by the frontal advance equation given as:

$$\left[r_D \left(\frac{dr_D}{dt_D} \right) \right]_{s_w} = \varepsilon f' \quad (\text{A.10})$$

Where, $\varepsilon = \frac{qBc_{11}\mu_w}{2\pi hk_w}$ and $f' = \frac{df}{ds_w}$ denote the slope of the fractional-flow curve.

By integrating Eq. (A.10), we obtain,

$$r_D^2 = 2\varepsilon f' t_D \quad (\text{A.11})$$

By transforming the problem from independent variables r_D and t_D to the Boltzmann variable $y = \frac{r_D^2}{4t_D}$,

we fix the moving interface and transform the moving-boundary problem into a composite problem in one variable.

If we substitute y by its expression, equation (A.1) and (A.2) becomes

$$F_m y \frac{d^2 P_{D1}}{dy^2} + (F_m + y) \frac{dP_{D1}}{dy} = 0 \quad (\text{A.12})$$

$$y \frac{d^2 P_{D2}}{dy^2} + \left(1 + \frac{\eta_1}{\eta_2} y\right) \frac{dP_{D2}}{dy} = 0 \quad (\text{A.13})$$

With

$$\lim_{y \rightarrow 0} y \left(\frac{dP_{D1}}{dy} \right) = -\frac{1}{2} \quad (\text{A14})$$

$$\lim_{y \rightarrow \infty} P_{D2} = 0 \quad (\text{A15})$$

$$P_{D1} = P_{D2}, \quad y = y_f \quad (\text{A16})$$

$$F_m M \frac{dP_{D1}}{dy} = \frac{dP_{D2}}{dy}, \quad y = y_f \quad (\text{A17})$$

Where

$$y_f = \frac{r_{Df}^2}{4t_D}$$

By applying separation of variables to Eq. (A.12), we get

$$\frac{P_{D1}''}{P_{D1}'} = -\frac{(F_m + y)}{yF_m}, \quad (\text{A.18})$$

$$\text{where } P_{D1}'' = \frac{d^2 P_{D1}}{dy^2} \text{ and } P_{D1}' = \frac{dP_{D1}}{dy}$$

By integrating equation (A.18), we have

$$P_{D1}' = c_1 \frac{e^{-\frac{y}{F_m}}}{y} \quad (\text{A.19a})$$

Where c_1 is the constant of integration.

From the boundary condition (A.14), we can obtain $c_1 = -\frac{1}{2}$ and Eq. (A.19a) becomes,

$$P_{D1}' = -\frac{1}{2} \frac{e^{-\frac{y}{F_m}}}{y} \quad (\text{A.19b})$$

Integration of Eq. (A.19b) yields,

$$P_{D1} = -\frac{1}{2} \int_{y_f}^y \frac{e^{-\frac{y}{F_m}}}{y} dy + c_2 \quad (\text{A.20a})$$

Eq. (A.20a) can be re-written as follows,

$$P_{D1} = -\frac{1}{2} \left[\int_{y_f}^{\infty} \frac{e^{-\frac{y}{Fm}}}{y} dy - \int_y^{\infty} \frac{e^{-\frac{y}{Fm}}}{y} dy \right] + c_2 \quad (\text{A.20b})$$

$$P_{D1} = -\frac{1}{2} \left[E_i\left(-\frac{y}{Fm}\right) - E_i\left(-\frac{y_f}{Fm}\right) \right] + c_2 \quad (\text{A.20c})$$

Applying the

same approach to Eq. (A.13), we get

$$P_{D2}' = c_3 \frac{e^{-\frac{\eta_1 y}{\eta_2}}}{y} \quad (\text{A.21})$$

Applying the boundary condition (A.8) on Eq. (A.21), we have

$$F_m \frac{M}{2} \frac{e^{-\frac{y_f}{Fm}}}{y_f} = c_3 \frac{e^{-\frac{\eta_1 y_f}{\eta_2}}}{y_f}$$

which yields $c_3 = F_m \frac{M}{2} e^{-y_f \left(\frac{1}{Fm} - \frac{\eta_1}{\eta_2}\right)}$ and Eq.(A.21) becomes,

$$P_{D2}' = F_m \frac{M}{2} e^{-y_f \left(\frac{1}{Fm} - \frac{\eta_1}{\eta_2}\right)} \cdot \frac{e^{-\frac{\eta_1 y}{\eta_2}}}{y} \quad (\text{A.22})$$

Integration of Eq. (A.22) gives,

$$P_{D2} = F_m \frac{M}{2} e^{-y_f \left(\frac{1}{Fm} - \frac{\eta_1}{\eta_2}\right)} E_i\left(-\frac{\eta_1}{\eta_2} y\right) + c_4 \quad (\text{A.23})$$

From the boundary condition (A.14), we determine $c_4 = 0$, and Eq. (A.23) becomes,

$$P_{D2} = F_m \frac{M}{2} e^{-y_f \left(\frac{1}{Fm} - \frac{\eta_1}{\eta_2}\right)} E_i\left(-\frac{\eta_1}{\eta_2} y\right) \quad (\text{A.24})$$

From the boundary condition (A.16), the constant C_2 will be

$$c_2 = -F_m \frac{M}{2} e^{-y_f \left(\frac{1}{Fm} - \frac{\eta_1}{\eta_2}\right)} E_i\left(-\frac{\eta_1}{\eta_2} y_f\right) \quad (\text{A.25})$$

and Eq.(A.20c) becomes:

$$P_{D1} = \frac{1}{2} \left[E_i\left(-\frac{y}{Fm}\right) - E_i\left(-\frac{y_f}{Fm}\right) \right] + F_m \frac{M}{2} e^{-y_f \left(\frac{y}{Fm} - \frac{\eta_1}{\eta_2}\right)} E_i\left(-\frac{\eta_1}{\eta_2} y_f\right), \quad 0 < r_D < r_{Df} \quad (\text{A.26})$$

To obtain the wellbore pressure in an infinite system, Eq. (A.24) and (A.26) at $r_i=1$ will be:

$$P_{wD} = \frac{1}{2} \left[Ei \left(-\frac{y}{F_m} \right) - Ei \left(-\frac{y_f}{F_m} \right) + F_m M \exp \left(-y_f \left(\frac{1}{F_m} - \frac{\eta_1}{\eta_2} \right) \right) Ei \left(-\frac{\eta_1}{\eta_2} y \right) \right], t_D \geq \frac{1}{4y_f} \quad (\text{A.27})$$

$$P_{wD} = F_m \frac{M}{2} \exp \left[-y_f \left(\frac{1}{F_m} - \frac{\eta_1}{\eta_2} \right) \right] Ei \left(-\frac{\eta_1}{\eta_2} y_f \right), t_D \leq \frac{1}{4y_f} \quad (\text{A.28})$$

For typical water injection test, y_f is small because of small water compressibility, this makes the exponential terms in the solution close to one after short time of injection.

The above equations can be written in function of time as follows,

$$P_{wD} = \frac{1}{2} \left[Ei \left(-\frac{1}{F_m 4t_D} \right) - Ei \left(-\frac{y_f}{F_m} \right) + F_m M Ei \left(-\frac{\eta_1}{\eta_2} y_f \right) \right], t_D \geq \frac{1}{4y_f} \quad (\text{A.29})$$

$$P_{wD} = F_m \frac{M}{2} Ei \left(-\frac{\eta_1}{\eta_2} \frac{1}{4t_D} \right), t_D \leq \frac{1}{4y_f} \quad (\text{A.30})$$

Thus, for injection period the semilog plot of the wellbore dimensionless pressure P_{wD} versus the dimensionless time t_D should exhibit two straight lines. The first straight line corresponds to the mobility of the uninvaded reservoir fluid with a slope of $\frac{F_m M}{2}$. The second line has a slope of $\frac{1}{2}$ and corresponds to the mobility in the completely flooded region where $S_w = 1 - S_{or}$.

If the logarithmic approximation is used, Equation (A.29) and (A.30) can be written respectively as:

$$p_{wf} - p_i = \frac{162.6qB\mu_w}{k_w h} \left[\frac{1}{F_m} \log \frac{\alpha t}{r_w^2} + F_m M \log \frac{k_o}{\phi \mu_o c_{t2} \alpha} - 3.23 F_m M \right] \quad (\text{A.31})$$

And

$$p_{wf} - p_i = \frac{162.6qB\mu_w}{k_w h} F_m M \left[\log \frac{k_o t}{\phi \mu_o c_{t2} r_w^2} - 3.23 \right] \quad (\text{A.32})$$

Where

$$\alpha = \frac{5.615qB}{\pi h \phi \Delta s_w}$$

Fall-off Solution

The assumption of stationary interface is generally acceptable due to the fact that the compressibility of fluids is negligible. Therefore, any volumetric expansion or compression of the fluids is negligible. The first bank is often large at time of shut-in; therefore any volume change expressed in terms of radial distance produces a negligible change in the location of the interface. In addition to the small duration of fall-off test

compared to injection time, one can generate a fall-off solution by superimposing the injection solution assuming that the fall-off period corresponds to pressure decay in the radially composite reservoir that is formed at the end of the injection period.

The fall-off solution is given by

$$P_{D\text{ falloff}} = P_D(t_{iD} + \Delta t_D) - P_D(\Delta t_D) \quad (\text{A.33})$$

The p_D terms on the right side of the above equation represent the injectivity solutions satisfying the governing partial-differential equations and boundary conditions of the fall-off problem.

$$P_{D(\text{falloff})} = \frac{1}{2} \left[\begin{aligned} & Ei\left(-\frac{1}{4F_m(t_{iD} + \Delta t_D)}\right) - Ei\left(-\frac{r_{Df}^2}{4F_m(t_{iD} + \Delta t_D)}\right) + F_m M e^{-\frac{r_{Df}^2}{4(t_{iD} + \Delta t_D)}\left(\frac{1}{F_m} - \frac{\eta_1}{\eta_2}\right)} \\ & Ei\left(-\frac{\eta_1}{\eta_2} \frac{r_{Df}^2}{4(t_{iD} + \Delta t_D)}\right) \end{aligned} \right] - \frac{1}{2} \left[\begin{aligned} & Ei\left(-\frac{1}{4F_m \Delta t_D}\right) - Ei\left(-\frac{r_{Df}^2}{4F_m \Delta t_D}\right) + F_m M e^{-\frac{r_{Df}^2}{4\Delta t_D}\left(\frac{1}{F_m} - \frac{\eta_1}{\eta_2}\right)} Ei\left(-\frac{\eta_1}{\eta_2} \frac{r_{Df}^2}{4\Delta t_D}\right) \end{aligned} \right] \quad (\text{A.34})$$

The above equation can be simplified to

$$P_{D\text{falloff}} = -\frac{M}{2} \left[\begin{aligned} & Ln\left(\frac{t + \Delta t}{\Delta t}\right) + Ln\left(\frac{k_o \Delta t}{r_f^2 \phi \mu_o c_{t2}}\right) + F_m \exp\left(-\frac{r_f^2 \phi \mu_w c_{t1}}{4(0.0002637k_w \Delta t)}\left(\frac{1}{F_m} - \frac{\eta_1}{\eta_2}\right)\right) \\ & \times Ei\left(-\frac{r_f^2 \phi \mu_o c_{t2}}{4F_m(0.0002637k_o \Delta t)}\right) \end{aligned} \right] + \frac{1}{2} \left[\begin{aligned} & Ln\left(\frac{k_w \Delta t}{\phi \mu_w c_{t1} r_f^2}\right) - 0.80907 - Ei\left(-\frac{r_f^2 \phi \mu_w c_{t1}}{4F_m(0.0002637k_w \Delta t)}\right) \end{aligned} \right] \quad (\text{A.35})$$

Substituting Eq. (A.21) into Eq. (A.25) yields the pressure at the well ($r_D = 1$) when the radius of investigation is within the water bank and the injection time is generally larger than the fall-off period. Thus Eq. (A.33) is simplified to,

$$P_{Dw} = -\frac{1}{2} \left[Ei\left(-\frac{1}{4F_m \Delta t_D}\right) - Ei\left(-\frac{1}{4F_m(t_{iD} + \Delta t_D)}\right) + Ei\left(-\frac{r_{Df}^2}{4F_m t_{iD}}\right) - F_m M Ei\left(-\frac{\eta_1}{\eta_2} \frac{r_{Df}^2}{4t_{iD}}\right) \right] \quad (\text{A.36})$$

At later times when the radius of investigation exceeds r_{Df} , Eq. (A.36) becomes,

$$P_{Dw} = -\frac{F_m M}{2} \left[Ei\left(-\frac{\eta_1}{\eta_2} \frac{1}{4\Delta t_D}\right) - Ei\left(-\frac{\eta_1}{\eta_2} \frac{1}{4(t_{iD} + \Delta t_D)}\right) \right] \quad (\text{A.37})$$

Thus the semilog plot of the dimensionless bottom-hole pressure P_{wD} versus the dimensionless time $\frac{t_{iD} + \Delta t_D}{\Delta t_D}$ should exhibit two straight lines. The first straight line has slope $-\frac{1}{2}$ and defines the mobility of the water bank and the second line has slope $-\frac{F_m M}{2}$ and corresponds to the mobility of the native reservoir fluid.

If the logarithmic approximation is used, the above equations can be written as

$$p_i - p_{ws} = -\frac{162.6qB\mu}{k_w h} \left[\log\left(\frac{t_i + \Delta t}{\Delta t}\right) + F_m M \log\frac{k_o}{\phi\mu_o c_{i2}\alpha} - 3.23F_m M - \log\frac{k_w}{\phi\mu_w c_{i1}\alpha} + 3.23 \right] \quad (\text{A.38})$$

And

$$P_i - P_{ws} = -\frac{162.6qB\mu}{k_w h} F_m M \log\left(\frac{t_i + \Delta t}{\Delta t}\right) \quad (\text{A.39a})$$

Equations (A.38) and (A.39) can also be written as

$$p_i - p_{ws} = m \left[\log\left(\frac{t_i + \Delta t}{\Delta t}\right) + F_m M \log\frac{k_o}{\phi\mu_o c_{i2}\alpha} - 3.23F_m M - \log\frac{k_w}{\phi\mu_w c_{i1}\alpha} + 3.23 \right] \quad (\text{A.38b})$$

$$P_i - P_{ws} = m F_m M \log\left(\frac{t_i + \Delta t}{\Delta t}\right) \quad (\text{A.39b})$$

Where $m = \frac{162.6qB_w\mu_w}{K_w h}$